

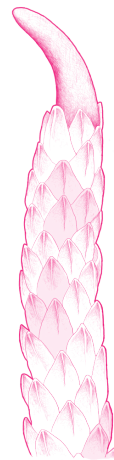
# Chapter 5

## Intricate mixtures: Diving inside the venoms

**Ariadna Rodríguez-Vargas, Andres Pereañez, Camila Figueredo-Salinas, Juan Carlos Vega-Garzon, Adrian Marcelo Franco-Vasquez, Teddy Angarita-Sierra**

**Abstract:** Since snake venoms have evolved to subdue or immobilize their prey and to favor their digestive processes and deter predators, snake venom toxins exhibit high specificities for precise functional and metabolic targets. For instance, metalloproteinases act mainly by altering endothelial junctions, phospholipases A<sub>2</sub> injure skeletal muscle tissues, and three-finger toxins affect transmission at neuromuscular synaptic junctions. Therefore, snakebite envenoming can be characterized according to the occurring hemocytotoxic, myotoxic, and neurotoxic pathophysiological processes. Currently, hypotheses about toxic action mechanisms and potencies of the individual components of the venom remain open, as do hypotheses about the main drivers in the composition variability of snake venoms. These are fundamental topics because they play a main role in the outcome of the snakebite envenomation. This chapter addresses a comprehensive review about the complex composition of snake venoms, detailing the biochemical and functional nature of the toxins while highlighting their activity during snakebite envenomation.

**Keywords:** Snake venoms, toxins, envenomation, functional activity, 3D models.



Citation: Rodríguez-Vargas A; Pereañez A; Figueredo-Salinas C; Vega-Garzon, JC; Franco-Vasquez, AM; Angarita-Sierra T. Chapter 5. Intricate mixtures: Diving inside the venoms. In Book: *Bites, venoms, and venomous snakes of Colombia*; Angarita-Sierra, T., Ruiz-Gomez, FJ, Eds.; Instituto Nacional de Salud: Bogota D.C., Colombia, 2024; pp. 201–274. doi:10.33610/848004dipgzd



Copyright: © 2024 by the authors. Open access publication under the terms and conditions of the Creative Commons Attribution (CC BY-NC-ND 4.0) license (<http://creativecommons.org/licenses/by/4.0/>).

Illustrations by:  
Oscar A. Ramírez Ruiz

## 1. On snake venom basics

### 1.1 Venom delivery systems

Snakes are known for their remarkable traits, including their adaptations for overpowering their prey, such as constriction or envenomation. Particularly, venom delivery systems have received great attention due to their sophisticated specialization, evolutionary pathways, and ecological convergences [1–3]. The delivery mechanisms of toxins have been mainly studied in highly venomous families such as Elapidae (e.g., coral snakes, cobras) and Viperidae (e.g., pitvipers, vipers), and most recently in Colubridae (e.g., grass snakes, racer snakes), the largest family of snakes in the world [1].

The venomous apparatus of snakes belonging to the Viperidae, Elapidae, and Colubridae families, almost like any other system that requires similar efficiency, depends on four basic tools for its performance. First, venom must be produced and stored in a reservoir. Then, it needs to be transported to the intended site for discharge. Afterwards, a mechanism is required to release the venom towards a specific organism, minimizing the risk of loss. The fourth component involved is related to the mechanisms surrounding the reservoir, responsible for emptying it and initiating the flow of venom through the system, from the initial storage site to the target [4].

Specifically, the venomous glands and accessory glands, the connecting ducts, the fangs, and the striated muscles that surround the glands represent the global venomous apparatus. The first three components present in pairs, one on each side of the head, towards the temporal region and ending in the maxillary region. The muscle fibers cover a slightly wider area of the head of the snake and are part of the compression system for ejecting the venom. The snake's biting and venom dispensing mechanisms involve the digastric, pterygoid, anterior temporal, and posterior temporal muscle groups that are located on each side of the head [5].

The venomous apparatus of snakes is characterized by its fangs that are always located on the maxilla of the upper jaw and never on any other tooth-bearing bone [6]. Among fanged snakes, the structure and position of the fangs allow the recognition of three types of dental architecture (Figure 1): short front fangs with enclosed venom-conducting canals and a visible suture line connecting the orifices (proteroglyphous: Elapidae and Atractaspididae like coral snakes or African asp snake; Figure 1C); enlarged and tubular front fangs with enclosed venom-conducting ducts and a smooth surface between the orifices (solenoglyphous: Viperidae like rattlesnakes or bushmasters; Figure 1D); and enlarged, solid grooved fangs located at the posterior end of the maxilla (opisthoglyphous: rear fangs of false water cobras; Figure 1B) exhibited by numerous lineages of colubrids (the grooves can be present on anterior, posterior, lingual or labial sides of the fang). The frontal position of the fangs in proteroglyphous and solenoglyphous structures differs not only in fang structure but also in the high level of kinematic freedom of the maxillary bone in solenoglyphous species. This flexibility allows them to position the fangs almost parallel to the roof of the mouth when closed and to rotate them

over 120 degrees along the anteroposterior axis, orienting them directly toward the target [4].

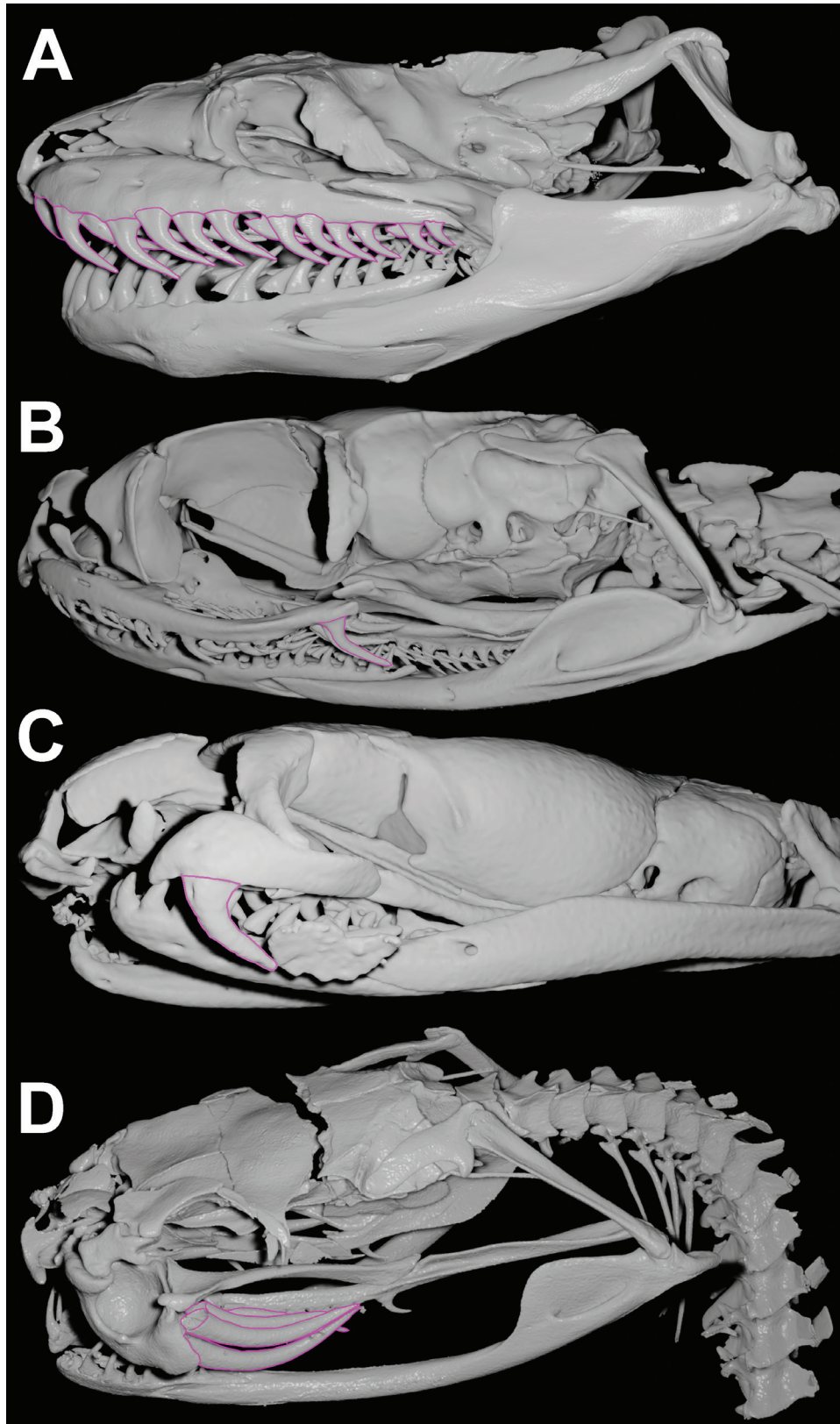


**Figure 1.** Types of types of dental architecture in snakes. (A) Aglyphus (Green anaconda *Eunectes murinus* UF 84822). (B) Opisthoglyphus (Coastal House Snake *Thamnodynastes pallidus*: UMMZ 246849). (C) Proteroglyphus (coral snake *Micrurus nigrocinctus* UMMZ 131984). (D) Solenglyphus (South American rattlesnake *Crotalus durissus*: UMMZ 119571). All images were retrieved and accessed on 5/08/2023 from Morphosource under CC BY-NC-ND 4.0 licence.

The evolutionary origin of fangs, as well as other elements of the venomous apparatus has been the subject of controversy and involves several underlying forces that have driven fang diversification [2]. Despite the unresolved evolutionary questions, most studies agree that the front-fangs exhibited in the Viperidae and Elapidae both independently derived from rear-fang snakes, reflecting convergent evolution [4]. The evolution of the venom delivery system has been frequently associated with dietary and ecological specializations. For instance, among venomous snakes, two predominant predatory strategies exist: rear-fanged snakes and elapids usually exhibit a bite-and-hold strategy, while most vipers and *Atractaspis* use a bite-and-release strategy, particularly for larger prey [2,7]. Thus, the lengthening of the fang suggests that it has been driven by the strike behavior rather than by increased stress (stretching force) associated with structural changes in the venomous apparatus [2].

The venomous apparatus rapidly discharges venom into the prey to ensure a food source or as a form of defense against predators, since snakes move slowly and have a lower metabolism [5]. There are two general mechanisms of venom delivery. The first exhibited in viperid and elapid snakes, is a high-pressure system in which a pulse of venom is delivered quickly by a sudden pressure surge. The second type of venom delivery system is found in rear-fanged colubrids, where the release of oral secretions is more protracted [1]. In this low-pressure system, venom delivery is caused by the mechanical force obtained when the fangs penetrate the prey. In the high-pressure system, the direct action of the jaw muscles on the venom gland generates a pressure that causes quick delivery of venom. The high-pressure system establishes a tight seal between the duct and fang, ensuring that pressure is maintained throughout the conduction channel and driving the venom into the prey. The low-pressure system lacks this tight seal, resulting in a lower pressure of venom flow [1].

Snakes from the Colubridae family possess a different “venomous” apparatus (see Chapter 4). The Duvernoy’s gland, which is homologous to the venomous gland and located in a similar position, lacks a large lumen reservoir and compression muscles around it. This system uses relatively lower pressures than the one mentioned above, and releases secretion slowly into the oral epithelium adjacent to the teeth that may have grooves but not hollows such as the fangs [1,2,7,8]. The Duvernoy’s gland structure varies greatly among species of Colubridae, with all the transitions between the absence of the gland to the presence of a purely serous well-differentiated Duvernoy’s gland [3]. Similarly, Duvernoy’s secretions exhibit a significant degree of compound variability, producing toxins of an enzymatic digestive or pancreatic origin, as well as phospholipases, phosphodiesterases, and proteases [3] (see Chapter 4).

Initial research on snake venoms focused on their toxic properties and oral secretions. It is evident that the components of venoms, including those of the Duvernoy’s glands, have multiple biological functions, and

even biotechnological purposes [5] (see Chapters 4 and 10). The venomous systems of elapids and vipers differ in size and morphology, but they all share a similar basic design of composition and function.

## 1.2. Venom definition

To define venom accurately, we refer to a statement of Arbuckle et al. [10], defining venom as “a biological substance produced by an organism that contains molecules (toxins) that interfere with physiological or biochemical processes in another organism. The venomous organism has evolved this substance to provide benefits to itself once introduced into the other organism. The venom is produced and stored in a specialized structure and actively transferred to another organism through an injury caused by a specialized delivery system”.

In a biological context, the term “toxic” refers to the lethal property of a chemical expressed as the median lethal dose ( $LD_{50}$ ) or absolute lethal dose ( $LD_{100}$ ), usually identified and characterized under defined laboratory conditions. The term “venomous” refers to the function or biological role of the secretion of a substance produced by an animal that is used for defense or the procurement of another animal as prey [6]. The observation of the animal in its natural habitat is usually the basis for concluding whether a secretion is used as venom. The two terms rest on different concepts so more is at issue than mere semantics [3].

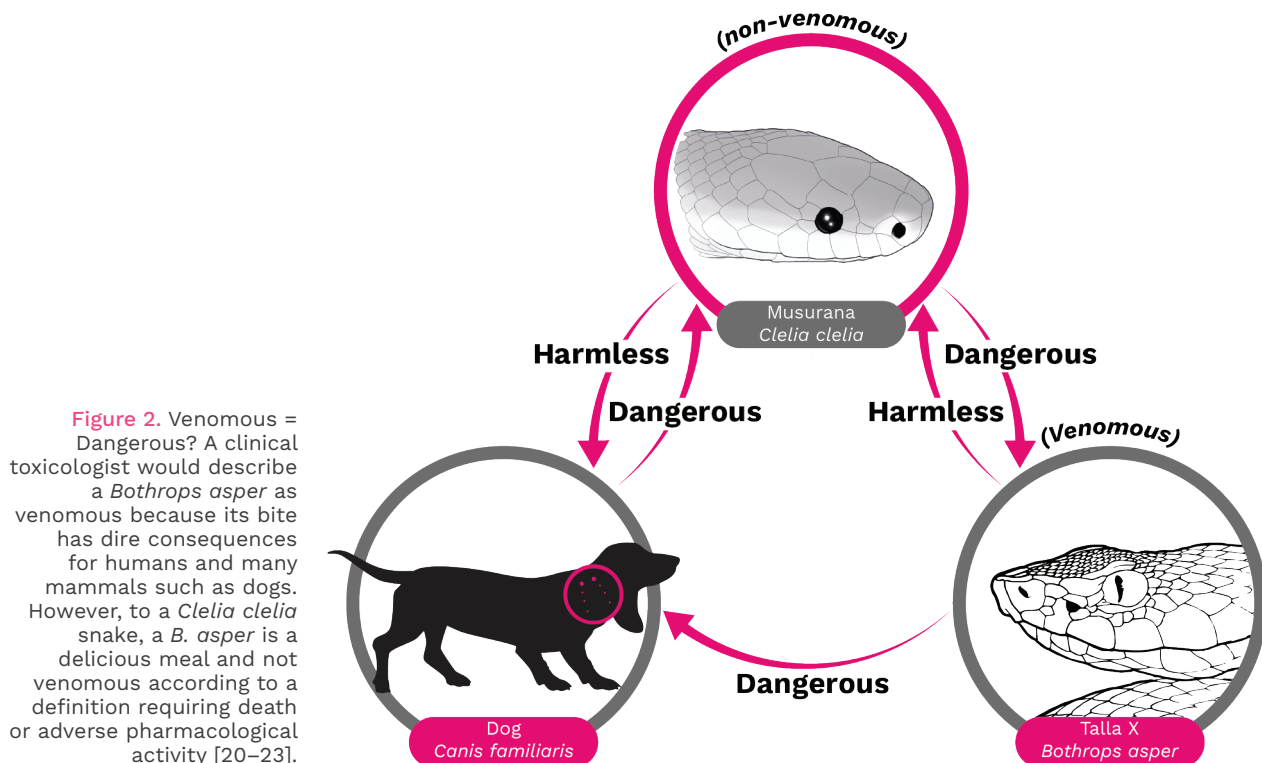
Venoms are mixtures of proteins, enzymes, peptides, ions, carbohydrates, and traces of other molecules produced in glands and secreted through specialized systems to subdue prey and digest, or deter predators (e.g., snake, scorpion, or spider venoms, among others). In contrast, poisons are substances that are concentrated in the bodies of certain organisms or anatomical regions of those organisms. They can cause adverse effects in other organisms that handle or consume them (e.g., lionfish spines or skin of poisons frogs found in the family Dendrobatidae). Toxins are substances produced by living organisms that can disrupt the normal homeostasis of other organisms that are exposed to them [10].

Both venoms and poisons are composed of toxins, and toxinology is the study of these substances. Toxinology is a sub-area of toxicology that is responsible for studying molecules produced by living organisms. These molecules are either distributed as venoms or allocated as poisons in the tissues of animals, plants, fungi, and bacteria; and they may cause damage to the target organism [4,11].

Venomous is an ecological trait that behaves as an intermediary in the interactions between two or more organisms. However, it is important to know that the term “venomous” does not necessarily mean “dangerous” (Figure 2). The level of danger depends on the susceptibility of the target organism to the venom, as well as the amount of venom that is injected. In some cases, such as with a dry bite (a bite without venom inoculation) [12], the venom may not even reach the organism. Venom is a common trait among medically

important snakes that are typically found in Elapidae and Viperidae snake families [13]. However, some non-venomous species, such as certain rear fanged colubrids [19] (see Chapter 4), have been known to cause mild envenoming or even life-threatening symptoms with their secretions.

The composition and activity of snake venoms evolved in parallel with the physiology of their prey and, in some cases, their natural predators. Although it was previously believed that humans have not exerted significant defensive selective pressure on snake venoms, and that envenoming was considered collateral damage in the chemical weapons race between venomous snakes and their prey [15], recent research suggests that the venom and delivery mechanism of spitting cobras (e.g., *Hemachatus haemachatus*, *Naja sumatra*) evolved to cope with hominins and mammals 2.5 million years ago. The venom was directed to produce severe pain in the hominins that posed a possible threat to them [18]. Thus, there are several dimensions of snake venom evolution that remain unexplored and require further research.



### 1.3. Interspecific and intraspecific variation

Snake venoms exhibit significant variation in composition and biological activity, both within and between species, as well as at higher taxonomic levels. This variation is considered adaptive because it enables the snake to have prey readily available or to deter predators [15]. Venom variability has significant implications for both primary venom research and snakebite management, including the selection of antivenoms, specimens and species for antivenom production to address snakebite pathophysiology [15,19,20].

Snake venom exhibits variability in multiple dimensions (see Chapter 3) including: interfamily, intergenera, interspecies, and intraspecies variations, as well as geographical variation between individual specimens, across individual ontogeny, seasonal changes, diet, habitat, and sexual dimorphism [21].

At the taxonomic family level, the venoms of elapids and vipers differ. Certain families of toxins have been recruited into each venom and are found exclusively in the venoms of one lineage and not the other [22]. Similarly, there are differences in venom compositions between genera within each family and between species within each genus. The therapeutic approach should be based on the understanding that antivenoms have been developed based on families, genera, species, and regions [15] (see Chapter 6).

Recently, it has been recognized that venom varies within species, including regional variations, as well as variations between ages and sizes (see Chapter 3). Venom is an ecological trait that evolves dynamically. Composition of a snake's venom is also influenced by the variety of its diet. Juvenile specimens tend to consume different prey than adults of the same species, exhibiting different feeding and behavioral strategies. For instance, juveniles may be nocturnal while adults are more diurnal. As a result, juveniles may employ a bite and hold strategy, while adults may bite and release [15].

Regional variation may be related to ecological differences between populations and to neutral evolution that is present in venomous systems and works in association with positive selection [23]. This suggests that for a trait to evolve rapidly, there must be significant heritable diversity within populations. This supports the hypothesis that variations would occur among the venoms of adult members of a single population [15].

The molecular-level documentation on the dynamism of the evolution of venom is well-established. Transcriptomic and proteomic analyses of *Bothrops atrox* venom reveal that transcription and translation mechanisms facilitate a venom's phenotypic variation. The evidence reveals that venoms contain two types of proteins: conserved core function proteins, which are essential for proper functioning and adaptive proteins, which are less conserved, vary in expression, and can be personalized in their function [19]. These observations suggest that the genetic mechanisms controlling venom variability extend beyond the selection of gene copies or mutations in structural genes. They also include the selection of mechanisms that control gene expression, contributing to the plasticity of venomous snake phenotypes [19].

Venom variability occurs due to evolutionary trends of venomous snakes and the specialization of some of its toxins. For instance, the venoms of both the Elapidae and the Viperidae are dominated by two or three families of proteins: phospholipases A<sub>2</sub> (PLA<sub>2</sub>) and three-finger toxin (3FTX) for elapids, and metalloproteinases (SVMP), PLA<sub>2</sub>, and serine proteinases (SVSP) for vipers. On average, these protein families make up 83% and 67% of the venom proteome for elapids and vipers, respectively [24].

Snake venoms from the Elapidae are mainly neurotoxic, while those from the Viperidae family induce coagulopathies, bleeding, and local tissue damage [25,26]. This is due to the prevalence of 3FTx and PLA<sub>2</sub> proteins in elapid venom that can cause myasthenia gravis-like weakness [27]. This weakness can affect any muscle and if the neuromuscular blockade involves the muscles of respiration, it can lead to death [26,27]. On the other hand, viperid venom has mainly hemotoxic and myotoxic effects. The agents identified in viper's venom include thrombin-like proteinases that lead to coagulopathy [28], hyaluronidases that alter extracellular matrices, phospholipases A<sub>2</sub> that cause local inflammation and pain [29], and metalloproteinases that contribute to hemorrhage [30,31]. The result is local tissue destruction worsened by coagulopathy [26].

There is variation in venom profiles between species within the same genus [32–34]. For instance, the venoms of two species of viperids from the *Bothriechis* genus, *B. lateralis* and *B. schlegelii* that have been compared using proteomics show that the venoms of these two species contain bradykinin-enhancing peptides (BPP) and PLA<sub>2</sub> proteins, serine proteinases, L-amino acid oxidases (LAO), cysteine-rich secretory proteins (CRISP) and Zn<sup>2+</sup>-dependent metalloproteinases (SVMP). However, each species has a different relative abundance of each protein family. Additionally, each venom contains distinct components. For instance, *B. lateralis* includes vascular endothelial growth factor (VEGF) and C-type lectin-like molecules, while *B. schlegelii* has Kasal-type protease inhibitors [35].

The venom proteins of both *Bothriechis* species are less than 10% similar, indicating a significant divergence in venom composition. Despite both species adapting to arboreal habits, the biochemical characteristics of their venom are likely related to the characteristics of their consumed prey [32,35]. The composition of venoms can provide clues to rationalize the various signs of envenoming caused by *B. schlegelii* and *B. lateralis* [35].

There is also variation in the profile of snake venom between individuals of the same species, with intraspecific differences found in geographical locations [28,36,37]. For instance, the composition and toxicological profile of the venom of the rattlesnake *Crotalus simus* in Mexico were analyzed at the subspecies level. The venoms of the subspecies *C. s. simus*, *C. s. culminatus*, and *C. s. tzabcan* differ in the expression of the neurotoxic complex “crotoxin”. *Crotalus s. simus* has the highest concentration of crotoxin followed by *C. s. tzabcan*, while the venom of *C. s. culminatus* is almost devoid of this neurotoxic PLA<sub>2</sub>. Proteomic analysis closely correlates with toxicological profiles. For instance, *C. s. simus* venom contains high amounts of crotoxin and serine proteinases, while *C. s. culminatus* venom has higher amounts of metalloproteinases and crotoxin. This suggests that the geographical variation in venom composition may reflect natural selection to feed on local prey [38]. The rising occurrence of crotoxin in populations of *Crotalus* is sufficient reason to caution the necessity of developing an antivenom that can neutralize this toxin [36].

There is variation in venom composition between young and adult snake species due to differences in diet [39]. Typically, young pit vipers feed on ectothermic animals while adults feed primarily on small mammals [38,40,41]. Consequently, studies focused on the ontogeny of these animals for some species are described [42,43]. Ontogenetic studies on *Bothrops* venoms obtained from adults and newborns revealed different plasma coagulation activities. The research identified two distinct venom profiles: young individuals with little PLA<sub>2</sub> K-49 myotoxin and more proteases, while adults showed a lot of PLA<sub>2</sub> K-49 but fewer proteases [30,50]. Newborn venom is less inflammatory, less hemorrhagic, but more myotoxic and procoagulant compared to adult venom. On the other hand, adult venom exhibits more hemorrhagic activity *in vivo* than young individuals [45–47].

It has been established that certain venom profiles should vary between sexes and adapt to specific prey species [38,41,48,49]. In contrast, electrophoresis analysis of the venoms of 30 offspring from a single litter of *Bitis gabonica* (Gaboon viper) revealed individual variations, but no significant differences based on sex were noted [49]. In Colombian snakes, the relationships between venom variability and life history traits represent an underexplored field that requires greater research efforts.

The venom's action and proportionate mix of actions are determined, at least in part, by the type of prey sought by a population of snakes [20,50]. For instance, it is important to note that CRISP toxins are abundant in colubrid venoms from reptile-feeding species like *Telescopus dhara* (Arabian cat snake) and *Trimorphodon biscutatus* (Western lyre snake). The toxic hypothermic effect of this toxin is useful for slowing down the movement of ectothermic prey (“cold blood”) [51]. The source of variation in snake venom profiles is an exciting and unresolved research field that requires a multidisciplinary approach and significant effort to unveil the mechanisms that generate the intricate mixtures of snake venoms.

## 2. On venom essentials

### 2.1. Snake venom metalloproteinases

Snake venom metalloproteinases (SVMPs) cause hemorrhage in the microvasculature of their prey, which contribute to the prey's immobilization, as observed in snakebite accidents. Additionally, SVMPs induce myotoxicity, edema, dermonecrosis, blister formation, and coagulation disorders [52,53].

The venom mixture contains various toxins, including SVMPs, which can break down proteins into smaller polypeptides or amino acids. SVMPs are a type of zinc-dependent endopeptidase that belongs to the ADAMs/Adamalysin/reprolysins subfamily that is part of the metzincins family [54,55]. Metzincins are metalloproteinases that have globular catalytic domains. Many of these domains are multidomain and contain a consensus zinc-binding amino acid sequence, HEXXHXXGXX, and a  $\beta$ -1-4 turn that has a highly conserved methionine residue (Met-turn). This residue forms a hydrophobic base for the zinc cofactor and the three histidine residues

involved in catalysis [56]. Therefore, these toxins are composed of five domains or functional and/or structural units. First, a signal peptide which is a short peptide (~ 16-32 amino acids) that prompts a cell to translocate the protein, then SVMPs that can contain pro-domain, metalloproteinase, disintegrin, and rich in cysteine [56].

Nevertheless, toxins in venom secretion-mature proteins can be in different combinations of the last three domains and are classified into three types, based on their molecular mass and domain composition. Type P-I SVMPs have a molecular mass between 20 and 30 kDa and exhibit only a metalloproteinase domain. Type P-II SVMPs have a molecular mass between 30 and 60 kDa and contain both metalloproteinase and disintegrin domains. Type P-III SVMPs have a molecular mass between 60 and 100 kDa and are rich in cysteine domains in addition to metalloproteinase and disintegrin domains [54,57,58]. The last subclass is determined based on post-translational modifications, such as proteolytic processing between the proteinase, disintegrin domains (class P-IIIb), dimerization (P-IIIc), protein addition type C-type lectins (P-IIId), and the initially described canonical P-IIIs known as P-IIIA [54,58].

The metalloproteinase domain structure, the most characteristic domain in SVMPs, is formed by five  $\beta$ -sheets, four  $\alpha$ -helices and a short  $\alpha$ -helix in the N-terminal. The  $\beta$ 1,  $\beta$ 2,  $\beta$ 3 and  $\beta$ 5-sheets are parallel to each other, while the  $\beta$ 4-sheet is anti-parallel to the other  $\beta$ -sheets. The domain is divided into two parts (M and S sub-domains) by the substrate binding cleft [65]. Within this cleft,  $Zn^{2+}$  is coordinated by the N $\epsilon$ 2 atom of histidine residues located at positions 142, 152, and 156, as well as catalytic water molecules.

Below the active site lies the side chain of a highly conserved methionine residue that forms a hydrophobic base for the zinc cofactor and constitutes the Met-turn, a highly conserved characteristic within the metzincins family [59]. Additionally, these enzymes require a  $Ca^{2+}$  ion to stabilize their structure, and the location of this cation is structurally opposite the substrate binding cleft [58,59]. The active site of the metalloproteinase domain includes a glutamate residue (Glu143) that is involved in initiating the catalytic cycle by deprotonating the catalytic water (Figure 3).

After deprotonating the water (denotation of a hydrogen cation), the resulting hydroxyl group acts as a nucleophile and attacks the carbonyl of the peptide bond which is then hydrolyzed. An oxyanion subsequently is formed and stabilized by the  $Zn^{2+}$  cofactor. Finally, the dislocated electrons on the oxygen return to their original bond, and the reaction products are released with the help of new water molecules [60].

SVMPs have a substrate binding cleft that plays a crucial role in binding and stabilizing the substrate for further catalytic reaction. Additionally, the catalytic residues and zinc coordination also contribute to the reaction. The cleft contains subsites, including S1, S2, S3, S1', S2' and S3' that interact with the substrate side chains. The enzyme's active site serves as a center,

with S1 to S3 located from the active site to the N-terminal, and S1' to S3' is located from the active site to the C-terminal. The peptide bond to be hydrolyzed is located in the center of the active site, and the substrate has complementary sites as follows: P1 to P3 sites interact with S1 to S3 subsites on the enzyme and P1' to P3' sites interact with S1' to S3' subsites on the enzyme. This nomenclature allows for an exact description of the interaction between the enzyme and substrate or inhibitors [60,61] (Figure 4).

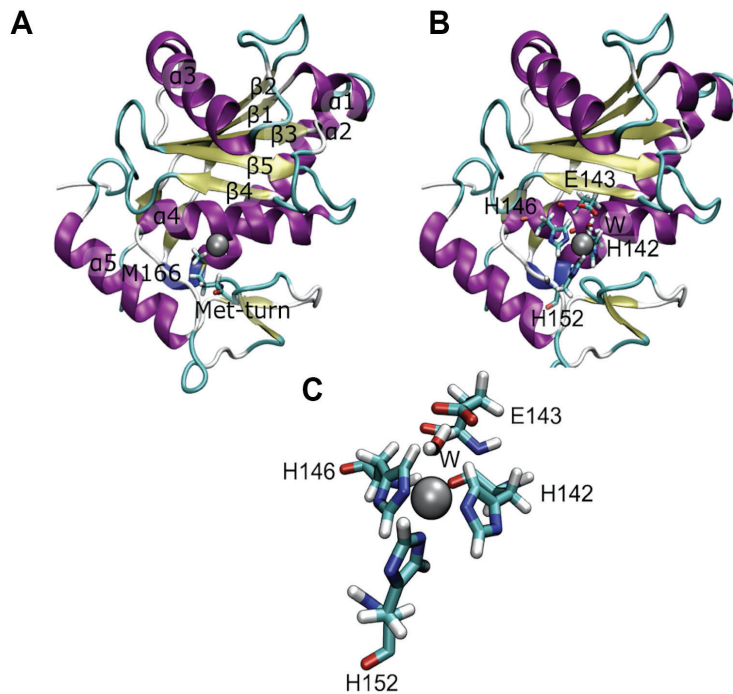


**Figure 3.** Structure of a P-I SVMP: (A) The figure displays the arrangement of secondary structure, including Met166 and the Met-turn. (B) Shows the position of the zinc ion (gray sphere), its coordination, and the catalytic residues. (C) Depicts the active site of the enzyme. The figure was prepared from the structure with PDB code 2W15 using VMD (Visual molecular dynamics). Figure made by by Lina María Preciado Rojo.

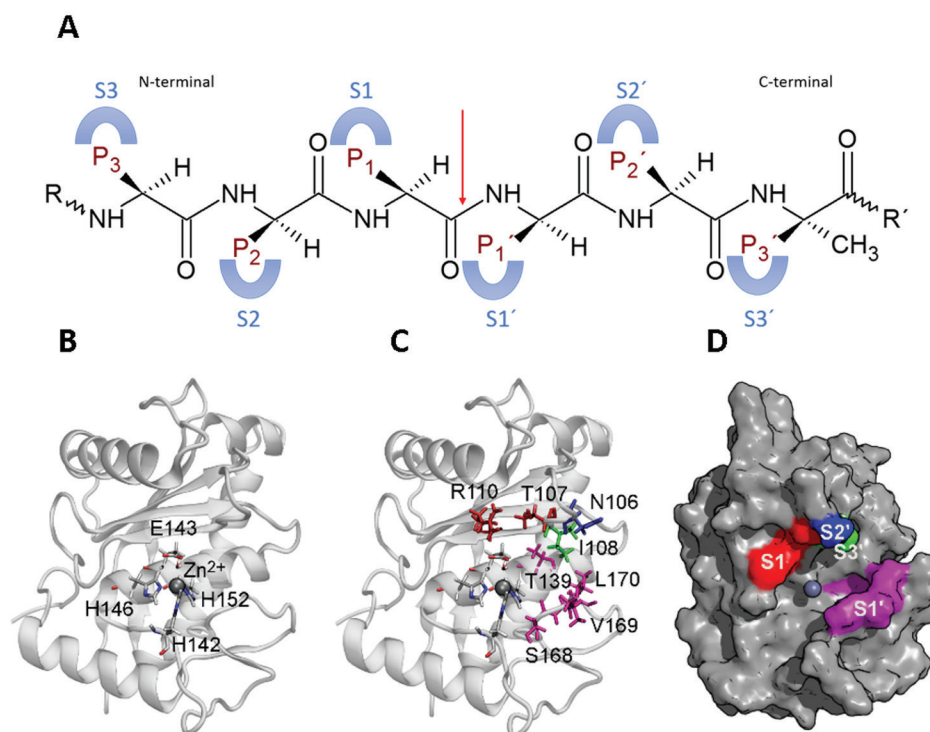


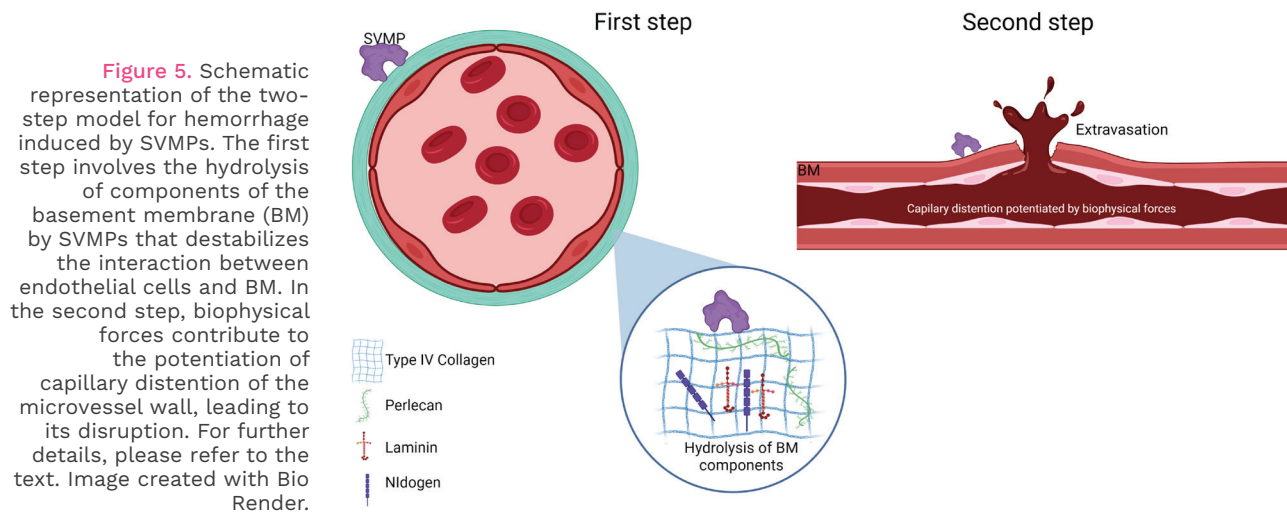
**Figure 4.** Subsites of a P-I SVMP. (A) Schematic representations of subsites in the enzyme and their interaction with sites in the substrate. The red arrow points out the peptide bond to be hydrolyzed. (B) Active site of the enzyme and the catalytic residues. (C) Side chain of the residues involved in the subsites in the enzyme by a color key. Red: S1, blue: S2', light green: S3', and purple: S1'. (D) Surface of the enzyme and the location of the subsites with the same color key as C. The figure was prepared from the structure with PDB code 2W15 using VMD (Visual molecular dynamics). Figure made by by Lina María Preciado Rojo.

## 2.2. Biological effects induced by SVMPs

### Hemorrhage

This activity can be either local or systemic and is catalytic-dependent. A two-steps hypothesis has been proposed to explain how these toxins induce hemorrhage [52]. Initially, SVMPs hydrolyze the substrate at the basement membrane (BM), such as type IV collagen, laminin, nidogen, and perlecan. This cleavage weakens the mechanical stability of the BM and increases the distensibility of the micro vessel wall. Furthermore, SVMPs can degrade other proteins, including those involved in binding BM to the extracellular matrix of muscles, such as non-fibrillar collagens VI, XII, XIV, XV, XVI, and XIX, as well as fibrillar collagen type V [53,62,63].

In the second step, hemodynamic forces act on the microvasculature including shear stress and hydrostatic pressure on the micro vessel wall. These forces potentiate the distention of the wall, leading to its disruption and the extravasation of red blood cells [58] (Figure 5).



There are two types of hemorrhage, per rhexis and per diapedesis. Per rhexis is characteristic of the capillary microvasculature. In this case, extravasation occurs through gaps formed in the vessel wall, as described above. Additionally, the thickness of the endothelial cell is decreased, making the capillary wall weaker [52,53,64]. Although hemorrhage induced by SVMPs is primarily caused by the per rhexis mode, per diapedesis mechanism is observed in venules where erythrocytes escape through widened intercellular junctions instead of in gaps in endothelial cells [65].

Additionally, SVMPs induce apoptosis (a cell death mechanism) of endothelial cells [66–70]. In certain cases, the levels of anti-apoptotic proteins from the BCL-2 family remain unaffected, while in other cases the levels of BCL-XL, another anti-apoptotic protein are decreased [67,70]. In addition, caspase 3 and 8 activation has been observed [67,70]. These proteases participate in the intracellular signaling cascade that leads to cell apoptosis. SVMPs can increase the expression levels of several matrix

metalloproteinases (MMPs) [71], which can increase their hemorrhagic effect by degrading the extracellular matrix and a further weakness of bone marrow derived endothelial cells interaction.

There is a clear difference in the potency of SVMPs inducing hemorrhage. Specifically, P-III and P-II SVMPs are more hemorrhagic than P-I SVMPs. The molecular mechanism underlying this phenomenon has not yet been fully elucidated, but some hypotheses provide insights into this topic. Firstly, P-II and P-III SVMPs contain disintegrin, cysteine-rich domains, and in some cases, a C-type lectin domain (P-III). These domains can direct toxins to specific targets in the microvasculature, concentrating them in the areas where they can cause the most harm [58,61].

For instance, the disintegrin domain can direct to integrins expressed on the cell membrane of endothelial cells [72]. Therefore, P-II and P-III SVMPs exhibit a co-localization pattern with type IV collagen on the vessel wall. In contrast, P-I SVMPs, which lack additional domains, are widely distributed in the extracellular matrix and are not concentrated in the vessels [73,74].

Furthermore, studies have shown that the plasma proteinase inhibitor  $\alpha_2$ -macroglobulin inhibits the proteolytic and hemorrhagic activities of several P-I SVMPs, but it does not have inhibitory capacity against P-II and P-III SVMPs [75–77]. The structural basis for these differences is still unknown. However, one hypothesis is that the additional domains found in P-II and P-III create obstacles for the binding of  $\alpha_2$ -macroglobulin, resulting in failure to recognize. This discovery may also explain the ability of P-II and P-III SVMPs to cause systemic hemorrhage, as they are not impeded by  $\alpha_2$ -macroglobulin once they enter the systemic circulation, whereas P-I SVMPs are rapidly inhibited by this protease inhibitor [53].

Another important aspect related to SVMPs is that P-I SVMPs differ significantly in their ability to induce hemorrhage [78–80]. Although they have similar proteolytic activity towards several substrates *in vitro*, some of these enzymes cause hemorrhage while others do not [63,79,80]. Significant differences were observed between hemorrhagic and non-hemorrhagic SVMPs in their ability to hydrolyze BM components *in vivo*. The P-I SVMP toxin BaP1 hydrolyzes type IV collagen and perlecan to a higher extent than the non-hemorrhagic P-I SVMP leucurulysin-A. Proteomic analysis of exudates collected from muscle tissue injected with these SVMPs also revealed differences in the types of extracellular matrix components present [63].

Nevertheless, the detailed structural determinants of hemorrhagic activity of P-I SVMPs remain largely unknown. Therefore, the possibility to predict the hemorrhagic potential of SVMPs based on structure or sequence analysis remains uncertain. However, a recent hypothesis suggests that differences in the dynamics of a loop located near the catalytic site may explain the variable hemorrhagic activity [82].

Another important finding was the differences in the electrostatic surfaces between these types of proteins [83]. Bioinformatic tools have re-

cently been used to predict the interaction of hemorrhagic P-I or non-hemorrhagic P-I SVMPs with their natural substrates such as type IV collagen, perlecan and laminin domains [84]. Hemorrhagic P-I SVMPs can form catalytic complexes with their substrates, while non-hemorrhagic P-I SVMPs cannot. Additionally, non-hemorrhagic P-I SVMPs may have a greater volume area of the substrate binding cleft than hemorrhagic P-I SVMPs. Despite all the results described, more studies are needed to clarify the hemorrhagic activity among types of P-I SVMPs.

### ***Myonecrosis and impairment muscle regeneration***

The inoculation of snake venom metalloproteinases (SVMPs) results in necrotic muscle damage (myonecrosis) that is caused by hemorrhage induced by the same toxins. Bleeding affects the blood supply to the affected tissue, leading to ischemia. Ischemia may cause hypoxia and muscle cell damage [30,80,85]. This effect can contribute to the myotoxic activity induced by other snake venom toxins, mainly phospholipases A<sub>2</sub>s (PLA<sub>2</sub>s).

The process of muscle regeneration after an injury requires three conditions: intact blood supply, restitution of neuromuscular junction, and intact BM [86]. Additionally, a synchronized interplay among several inflammatory substances and cells is involved. SVMPs affect two of these requirements by degrading the components of BM, resulting in a weakening of the microvasculature wall and extravasation of vessel content. Smooth muscle necrosis in the wall of intramuscular arteries caused by SVMPs can affect muscle regeneration by decreasing the blood supply, [87,88]. Oxygen and nutrients to the affected tissue decrease, and the muscle regeneration process is affected [85].

### ***Blister formation and skin death (dermonecrosis)***

Blister formation induced by SVMPs is caused by their catalytic activity against the BM components located at the dermal-epidermal junction [71,89,90]. The SVMPs hydrolyze collagen type IV, laminin, and nidogen, among other proteins, in the blister fluids [89,90]. Following this hydrolysis, the epidermis separates from the dermis, resulting in the formation of a blister which accumulates mainly plasma fluid, favored by the inflammatory process, as well as fibrinogen and fibrin that are degraded by various SVMPs. Dermonecrosis may occur when cells detached and then die, and subsequently an inefficient regenerative process takes place, either with or without scar formation [96]. However, further studies are needed to obtain more insight into this issue.

### ***Edema and inflammation***

A hypothesis was that the edema-forming activity of SVMPs might be initially related to the extravasation of blood vessels contents into the interstitial space. However, this hypothesis was partially refuted when injections of sub-hemorrhagic doses of SVMPs provoked edema, suggesting that this effect is independent of extravasation and is induced by multi-component events [86], this defines a second mechanism of edema formation mediated by proinflammatory activity. First, leukocyte infiltration occurs in the affected organ. Then, mast cell degranulation and histamine

release occur that can also lead to macrophage activation [71,91–93]. Similarly, SVMPs stimulate the release of IL-1 and IL-6, leading to an increased tumor necrosis factor (TNF) mRNA level, resulting in the overexpression of this protein responsible for inflammation processes [71,93,95].

### 2.3. Snake venom phospholipases A<sub>2</sub>

Venomous snakes employ phospholipases A<sub>2</sub> (PLA<sub>2</sub>s), found in their venoms to cause myonecrosis (death of muscle cells), neurotoxicity (paralysis of breathing muscles), inflammation, pain, and disruption of normal coagulation. All these effects contribute to the immobilization of the prey and can be observed in cases of snakebite envenomation.

#### General aspects: classification, catalyzed reaction, and overall structure

There are sixteen groups of PLA<sub>2</sub>s (IA, IB, IIA, IIB, IIC, IID, IIE, IIF, III, V, IX, X, XIA, XIB, XII, XIV) that are classified based on their sequence, molecular mass, origin, disulfide position, calcium requirement, and other characteristics [95]. The PLA<sub>2</sub>s can hydrolyze the ester bond from the sn-2 position from glycerophospholipids, producing a fatty acid and a lysophospholipid (Figure 6).

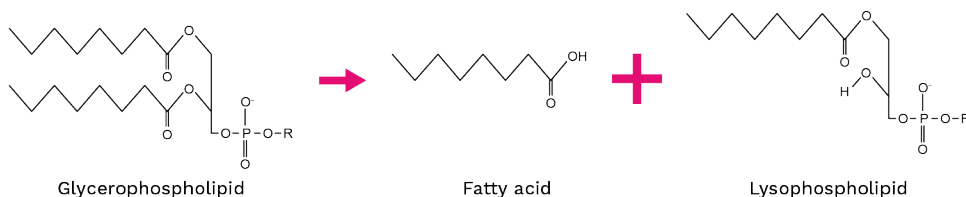


Figure 6. Catalyzed reaction by PLA<sub>2</sub>s.

The PLA<sub>2</sub> enzyme family is present in a wide variety of organisms, including animals, plants, fungi, and bacteria. However, among the sixteen types of PLA<sub>2</sub>, those found in snake venoms belong to groups IA, IIA, and IIB [102]. Group IA PLA<sub>2</sub>s are present in the venoms of the Elapidae that in the Americas is represented by the coralsnakes (*Micrurus* spp.). These PLA<sub>2</sub>s typically have a molecular mass around 13–15 kDa and exhibit seven disulfide bridges, one of which is exclusive to this group and is located between 11 and 77 cysteines.

Group IIA PLA<sub>2</sub>s are found in the venoms of the Viperidae, such as *Crotalus*, *Lachesis*, *Bothrops*, and *Porthidium* snakes. The molecular mass of group IIA PLA<sub>2</sub>s is like that of group IA PLA<sub>2</sub>s, also present in Viperidae venoms, both groups with seven disulfide bridges. The exclusive disulfide bridge in group IIA PLA<sub>2</sub>s is located between 50 and 137 cysteines. Group IIA comprise another set of snake venom PLA<sub>2</sub>s, including an enzyme also isolated from the venom of Russell's viper (*Daboia russellii*) from Asia (India, Pakistan, Nepal, Sri Lanka, Bangladesh, and Bhutan). A unique characteristic of this protein is that it has one less disulfide bridge than PLA<sub>2</sub>s mentioned above [95,96].

Elapid and viperid PLA<sub>2</sub>s have human counterparts. For instance, pancreatic PLA<sub>2</sub> group IB is homologous to the enzymes of group IA. Synovial

PLA<sub>2</sub> belongs to group IIA and has a structure like snake venom proteins in the same group. However, it is well known that human PLA<sub>2</sub>s do not cause the harmful effects observed in snake venoms. These effects include pre and/or post-synaptic neurotoxicity, local and/or systemic myotoxicity, anticoagulation, cardiotoxicity, modulation of platelet aggregation, hemolytic, edema, hypotensive activities, and direct damage to organs such as the kidney, lung, and liver [97].

Snake venom PLA<sub>2</sub>s are classified as basic or acidic proteins based on their isoelectric point. Most PLA<sub>2</sub> are basic. Though acidic PLA<sub>2</sub>s are known to have catalytic activity, they are generally devoid of biological effects. However, in some cases, they show myotoxic and edema-forming activities [98,99]. The acidic proteins have also been identified in Colombian venoms, including species such as *Porthidium nasutum*, *P. lansbergii*, and *Bothrops asper* [100–102].

To explain the variety of effects and differences in the susceptibility among various tissues, a model was proposed that deals with “target sites” on the surface of cells or target tissues [103]. The model suggests that specific “pharmacological sites” responsible for inducing each activity are recognized in these areas that are found in the three-dimensional structure of PLA<sub>2</sub>s. The model proposes that pharmacological sites may or may not overlap with the active site. The pharmacological effects induced by PLA<sub>2</sub>s are determined by the high affinity between the target molecule and the pharmacological site. This is assumed to be due to the ubiquitous presence of phospholipids in cell membranes. It is unlikely that these are the target molecules that the model affirms. In contrast, it is plausible that receptors are glycoproteins or other proteins that are differentially expressed [103].

PLA<sub>2</sub>s from snake venoms are calcium (Ca<sup>2+</sup>) dependent enzymes that structurally consist of three  $\alpha$ -helices, two antiparallel  $\beta$ -sheets, and a calcium-binding loop (Figure 7). These proteins have a variable length, ranging from 119 to 134 amino acids. The hydrophobic channel involved in driving the substrate towards the active side is defined by residues located in two of the  $\alpha$ -helices ( $\alpha$ -helix two, residues 37-57, and  $\alpha$ -helix three, residues 90-109, respectively), in addition to the N-terminal helix ( $\alpha$ -helix one) and the residues Leu2, Val3, Phe5, His6, Ile9, Trp19, Val31, Lys69, Ala102, and Ala103. The active site is formed by His48, Asp49, Tyr52, and Asp99. Then, the calcium-binding loop coordinates the calcium required for catalysis and is formed by Tyr28, Gly30, Gly32, and Asp49 [104] (Figure 7).

The PLA<sub>2</sub>s catalyze reactions that can result in chemical incoherence due to the enzymes being water-soluble, while their substrate is amphipathic (a region of the molecule is hydro soluble, and the other is liposoluble). To overcome this issue, PLA<sub>2</sub>s have an interfacial binding surface (i-face), that mediates their adsorption at the lipid-water interface outside the cell membrane [104] (Figure 8A).

For a catalytic reaction to occur at the interface, a series of events must take place. These include the phospholipid exiting the membrane

and reaching the active site of PLA<sub>2</sub>. The phospholipid passes through a hydrophobic channel via a diffusion process that requires no energy. After locating the substrate in the enzyme's active site, the phospholipid must be anchored to reduce decrease the degrees of freedom of the ester bond at the sn-2 position. This fixation is accomplished by the amino acid at position 69 (Lys or Tyr) through a hydrogen bond usually with the phosphate of the sn-3 position [104] (Figure 8B).

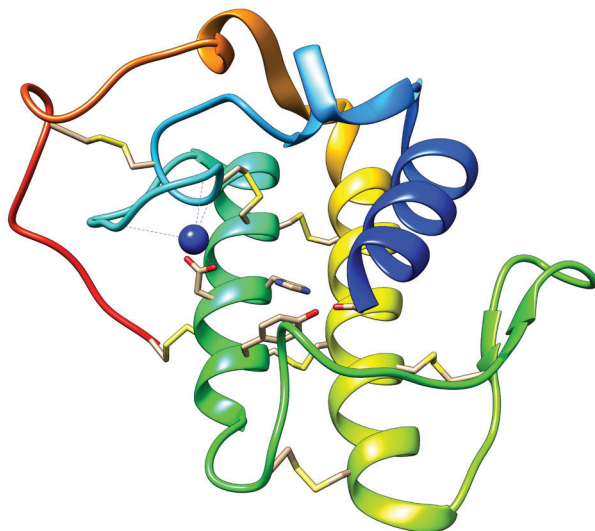


**Figure 7.** Overall structure of snake venom PLA<sub>2</sub>s. The alpha-helices one, two and three are shown in blue, green, and yellow. The calcium-binding loop is shown in cyan (blue-green), and Ca<sup>2+</sup> ion is represented as a blue sphere. The disulfide bridges are presented as yellow sticks. Moreover, catalytic residues are also shown in sticks (His48, Asp49, Tyr52 and Asp99) (Figure was prepared from the structure with PDB code 2QOG, chain B).

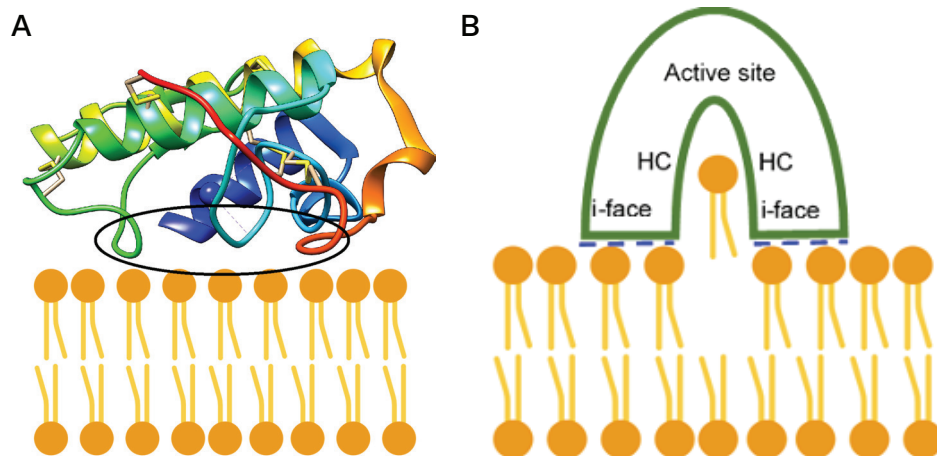


**Figure 8.** (A) Schematic representation of i-face. The black circle indicates the regions involved in membrane recognition and enzyme adsorption onto the lipid-water interface. (B) Schematic representation of the driving of glycerophospholipid to the active site through the hydrophobic channel (HC). The blue dash lines represent hydrophobic and electrostatic interactions between the amino acids of the enzyme and glycerophospholipids. The glycerophospholipids were extracted from Bio Render.

Following the recognition of the substrate and its displacement through the hydrophobic channel, the catalytic cycle begins. His48 is protonated by extracting a hydrogen ion from water, generating a hydroxyl group (OH<sup>-</sup>) that acts as a nucleophile. The OH<sup>-</sup> then attacks the sn-2 ester bond, leading to the formation of an oxyanion that is stabilized by the Ca<sup>2+</sup> ion. Finally, the dislocated electrons on oxygen return to their original bond, and the reaction products are released [104,105].

Snake venom PLA<sub>2</sub>s require catalytic activity to induce most of their biological effects. However, since 1984 [106], a sub-group of these toxins

have been discovered that have substituted their catalytic residue Asp49 for other amino acids (mainly Lys, but including Gln, Ser, and Arg). This replacement renders the new proteins enzymatically inactive, and they are known as PLA<sub>2</sub>-homologues or PLA<sub>2</sub>-like myotoxins. Although they cannot hydrolyze membrane glycerophospholipids, they can cause myotoxicity and edema [22,107].

### **Biological effects induced by snake venoms PLA<sub>2</sub>s**

#### *Myotoxicity*

Snake venom PLA<sub>2</sub>s may induce myonecrosis through myotoxicity. Although the molecular events are not fully understood, there is a detailed description of the cellular processes that involve the damage of these toxins to muscle cells. Firstly, the myotoxin is suggested as binding to the target cell. Some authors have identified a protein from rabbit muscle named type-M receptors [108]. The receptor has a molecular mass of 180 kDa and contains tandem repeats of regions with homologies to carbohydrate recognition domains (CDR).

A recent report suggests that nucleolin, a nuclear protein also expressed in the cell membrane, can interact with and mediate the internalization of a Lys49 PLA<sub>2</sub> [109]. Subsequently, PLA<sub>2</sub>s disrupt the muscle membrane. Asp49 PLA<sub>2</sub> catalyzes this process, while PLA<sub>2</sub>-homologues destabilize the protein through hydrophobic and electrostatic interactions with glycerophospholipids.

Fernandes et al. [110] proposed that these toxins have an oligomeric state that may be allosterically activated by a small molecule, probably a fatty acid. The protein is then docked in the membrane at a specific site called the Membrane Docking Site (MDoS). Finally, PLA<sub>2</sub>s provoked the destabilization of membrane glycerophospholipids through the action of the Membrane Disrupting Site (MDiS) [111]. These events induce changes in the selectivity and permeability of the muscle membrane, leading to massive calcium influx and cellular depolarization. Additionally, creatine kinase (CK), lactic dehydrogenase (LDH), and other molecules are released that are used as markers of myotoxicity.

The elevated concentration of calcium ions in the cytoplasm of muscle cells leads to hypercontraction of the sarcomere, resulting in mechanical damage. Calcium ions also induce an overload of mitochondria, leading to damage in the electron transport chain and ATP synthesis. Additionally, calcium can activate cytosolic PLA<sub>2</sub>s that can increase intracellular damage, particularly in membrane organelles; and it can also stimulate the proteolytic action of calpains, triggering cytoskeletal disorganization. Finally, snake venom PLA<sub>2</sub>s can be internalized, leading to increased internal damage. These events ultimately result in cell death by necrosis (Figure 9), which is a significant factor in snakebite envenoming by viperids, including those in Colombia (see Chapter 9) [111,112].

Systemic myotoxicity is another known biological effect of some snakebites, noted in Colombia in the case of rattlesnake accidents involving

*Crotalus durissus* (see Chapter 9) [113]. Although the molecular determinants for this effect are currently unknown, it is suggested that the toxin might bind to low-affinity sites in the injected area and then be distributed to other anatomical regions of the body. This distribution can induce myotoxicity through the events described above [119]. Snake venom PLA<sub>2</sub>s can cause myotoxic activity leading to rhabdomyolysis that can affect renal function by blocking glomerular filtration due to excess myoglobin in the blood. This can ultimately result in Acute Kidney Failure (AKI) [114,115].

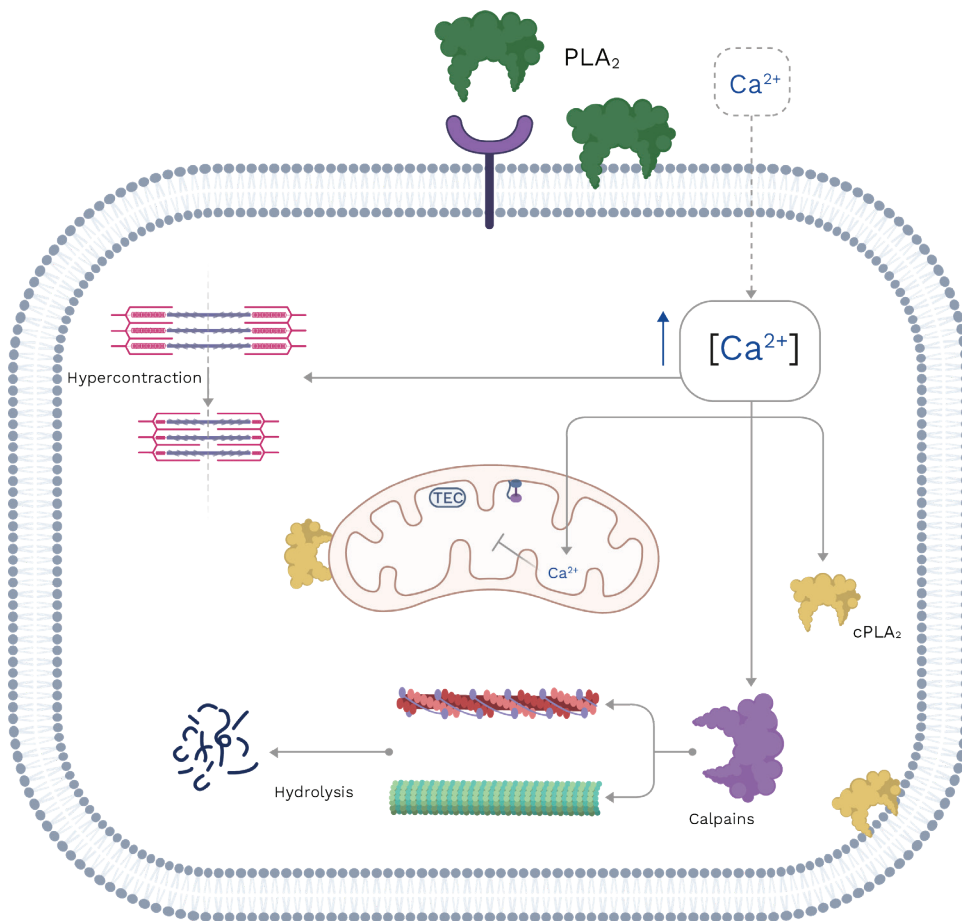


**Figure 9.** Schematic representation of the cellular events that occur during myotoxicity induced by snake venom PLA<sub>2</sub>s. TEC: transport electron chain; cPLA<sub>2</sub>: cytosolic PLA<sub>2</sub>s. The muscle cell membrane is disrupted by catalytic or non-catalytic mechanisms of PLA<sub>2</sub>s, leading to a massive influx of Ca<sup>2+</sup>. This results in hypercontraction of the sarcomere, activation of calpain, and cPLA<sub>2</sub>, all of which contribute to increased damage. For more details, see the text. Image created with BioRender and edited by Oscar A. Ramirez Ruiz.

### Edema

Intramuscular injection of snake venom PLA<sub>2</sub>s induces inflammation, characterized by increased vascular permeability, edema formation, leukocyte recruitment to affected tissues, and the release of inflammatory mediators [116]. However, it should be noted that the mechanisms by which these toxins induce this effect have not been entirely elucidated. Asp49 PLA<sub>2</sub>s can generate arachidonic acid that serves as the starting point for producing eicosanoids that amplify the inflammatory response. In contrast, PLA<sub>2</sub>-homologues induce edema and degranulation of mast cells in a catalytic-independent manner. It is evident that enzymatic activity is not strictly necessary to cause these effects. A variety of endogenous molecules including histamine, 5-hydroxytryptamine, bradykinin, tachykinins, arachidonic acid metabolites, pro-inflammatory cytokines,

and nitric oxide (NO) have been implicated in venom PLA<sub>2</sub>-inflammatory activity [116,117]. Other structural characteristics of PLA<sub>2</sub>s are also involved inducing inflammation. However, further studies are necessary to elucidate these molecular regions [116,117].

#### *Neurotoxicity*

Presynaptic neurotoxicity or  $\beta$ -neurotoxicity is another relevant effect observed in some snakebites. For instance, these are inflicted by South American rattlesnakes (*Crotalus durissus*) and coral snakes (*Micrurus* species; see Chapter 9) [113]. The toxins responsible for this effect are named  $\beta$ -neurotoxins, and their structures possess one, two, three and up to five subunits that can interact either by covalent or non-covalent bonds. One of their subunits is a catalytically active PLA<sub>2</sub> [118]. Toxicity arises from the inhibition of acetylcholine (ACh) release, leading to a flaccid paralysis of respiratory muscles, including the diaphragm. The inhibition of ACh release occurs in three steps: first, there is a slight, transient inhibition of ACh release that is related to the binding of PLA<sub>2</sub> to the presynaptic membrane; second, there is a significant increase in ACh release; finally, there is a sustained inhibition of ACh release [112,119,120].

Cellular events involved in presynaptic neurotoxicity induced by snake venom PLA<sub>2</sub>s include the binding of the toxin to a target cell (motoneuron). Although the precise identification of the receptor has not yet been performed, Lambeau et al. [121] found a high-affinity protein in the rat brain named N-type due to its neuronal origin. These receptors may be located near the region where ACh is released. After binding, PLA<sub>2</sub> hydrolyzes glycerophospholipids at the presynaptic membrane, leading to an accumulation of fatty acids and lysophospholipids [119,122].

The presynaptic membrane's outer layer has a high concentration of lysophospholipids that induce a curvature and promote synaptic vesicle membrane fusion while inhibiting endocytosis. An experiment that added mixtures of fatty acids and lysophospholipids on neuromuscular junctions supported this observation. The effects were similar to those induced by neurotoxic PLA<sub>2</sub>s [123]. The destabilization of the neuron membrane induces an influx of Ca<sup>2+</sup> ions which can activate endogenous PLA<sub>2</sub>s and calpains. This activation can cause internal membrane degradation and cytoskeleton disorganization. Additionally, the high concentration of calcium in the cytosol can destabilize mitochondria and disrupt their biochemical processes [124]. Finally, the toxin is internalized by neurons.

However, the mechanism by which  $\beta$ -neurotoxins are transported into nerve cells remains unknown. These toxins could be internalized through pores generated after presynaptic membrane hydrolysis, or proteins could use endocytosis of synaptic vesicles as a vehicle to enter nerve cells [125]. Once PLA<sub>2</sub> enters the neuron, it binds to certain proteins such as calmodulin, protein disulfide isomerase, and proteins named 14-3-3; but the specific implications for the toxin's mode of action are unclear. Similarly, calmodulin stabilizes the PLA<sub>2</sub>'s ability to hydrolyze glycerophospholipids.

phospholipids [126]. Additionally, proteins 14-3-3 play an important role in directing PLA<sub>2</sub> to synaptic vesicles to carry out their catalytic activity and subsequently inhibit vesicle endocytosis [127]. Ultimately, these events contribute to the failure of the neuromuscular junction, resulting in the inhibition of Ach release and subsequent flaccid paralysis [118–121,128,129] (see Figure 10).

Crotoxin (CTX) is a β-neurotoxin derived from *Crotalus durissus*, the South American rattlesnake [138]. It consists of a basic PLA<sub>2</sub> subunit known as CB and an acidic subunit called crotopotin (subunit A or CA). The latter acts as a chaperon, guiding the CB subunit to target cells (motoneurons) and preventing the binding of the PLA<sub>2</sub> to non-specific sites [131,132]. Additionally, CA increases the neurotoxic activity of CB but decreases its enzymatic activity [133,134]. Therefore, the crotoxin complex is responsible for the neurotoxicity observed in envenomation by Colombian rattlesnake. Other toxins found in Colombia, classified as β-neurotoxins include the PLA<sub>2</sub>s isolated from the venoms of the coral snakes *Micrurus mipartitus* and *M. dumerilii* [135].

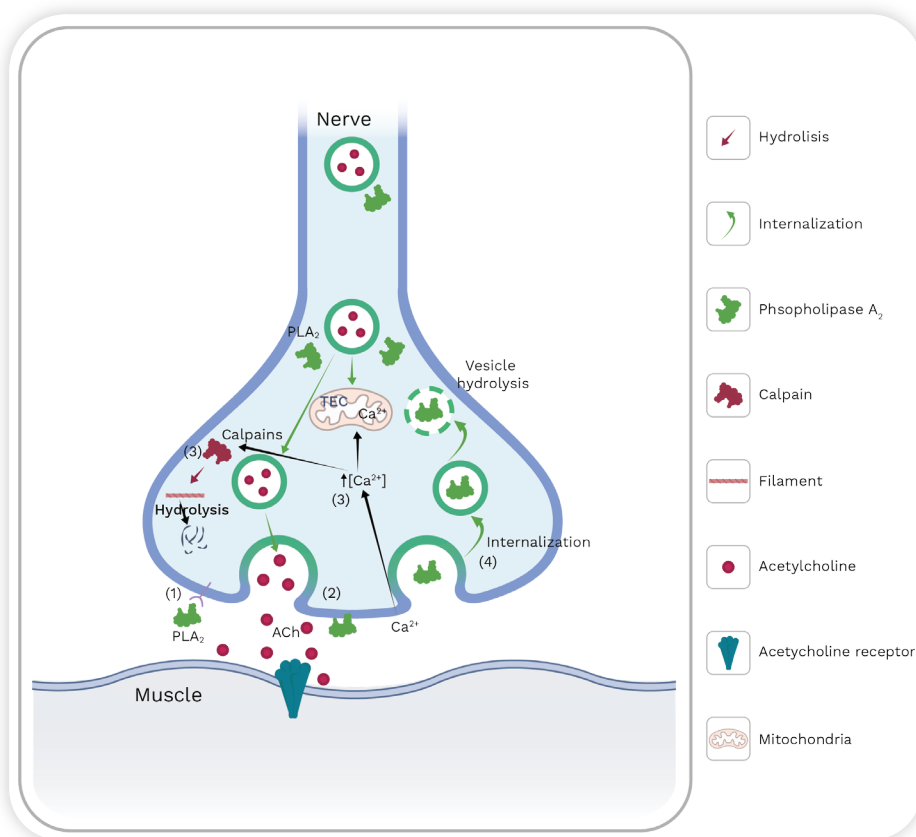


**Figure 10.** Schematic representation of the cellular events that occur during neurotoxicity induced by snake venom PLA<sub>2</sub>s. TEC: transport electron chain. PLA<sub>2</sub>s can enter presynaptic vesicles and hydrolyze them (step 1 and 2). Membrane destabilization can provoke a massive influx of calcium (step 3) that can activate calcium-dependent enzymes, such as calpains that promote cytoskeleton hydrolysis. PLA<sub>2</sub>s are internalized into the nerve terminal to perpetuate the damage (step 4). For more details see the text. Image created with BioRender and edited by Oscar A. Ramirez Ruiz.

### Anticoagulant activity

Based on their anticoagulant potency, PLA<sub>2</sub> enzymes are classified into strong, weak, and non-anticoagulant enzymes. Strongly anticoagulant PLA<sub>2</sub> enzymes inhibit blood coagulation at low concentrations (<2 μg/mL),

while weakly anticoagulant PLA<sub>2</sub> enzymes show effects between 3 and 10 µg/ml. Some venom PLA<sub>2</sub> enzymes do not significantly prolong clotting times, even at 15 µg/ml; and they are, therefore, classified as non-anticoagulant enzymes [138].

Early studies on PLA<sub>2</sub> suggest that catalytic activity is necessary for its anticoagulant effects [137]. However, recent studies propose that strong anticoagulant PLA<sub>2</sub>s act through both enzymatic and non-enzymatic mechanisms, the latter being mediated by an “anticoagulant site”. Kini et al. [138] proposed the position of this site in the three-dimensional structure of PLA<sub>2</sub>s. They suggest that in strong anticoagulant PLA<sub>2</sub>s, the region between the 53 and 76 residues is positively charged, whereas PLA<sub>2</sub>s with weak or non-anticoagulant activity have a predominance of negative or neutral charges in this region [136,138]. This region is commonly referred to as the “anticoagulant site”.

Nonetheless, Stefansson et al. [139] proposed a non-enzymatic mechanism for anticoagulant PLA<sub>2</sub>s. The study demonstrates that a PLA<sub>2</sub> from Black-necked spitting cobra (*Naja nigricollis*) venom that has strong anticoagulant properties, binds to coagulation factor Xa, blocking the further activation of prothrombin. Faure et al. [149] proposed a structural model for the interaction between PLA<sub>2</sub>s and coagulation factor Xa. The authors proposed various bioinformatic approaches and binding studies to propose that specific residues 2, 3, and 7 from helix 1; 16, 18, 19, 23, 24, 31–34 from Ca<sup>2+</sup> binding loop; 53, 59, 60, 69, 70 from helix 3; and 118, 119, 121–124, 129–131, and 133 from β-sheets bind together. Currently accepted knowledge proposes that snake venom PLA<sub>2</sub>s can elicit their anticoagulant activity through both enzymatic and non-enzymatic mechanisms [141,142].

#### *Other biological activities induced by snake venom PLA<sub>2</sub>s*

Venom PLA<sub>2</sub>s can modulate platelet aggregation, either inducing or inhibiting it. These are classified into three distinct classes: A, B, and C [143]. Class A enzymes initiate platelet aggregation [144,145]; class B PLA<sub>2</sub>s cause the inhibition of platelet aggregation [146,147]; and class C PLA<sub>2</sub>s show biphasic effects that induce platelet aggregation at low doses or short incubation times, while they inhibit platelet aggregation at higher concentrations or prolonged incubation [148].

Additionally, these toxins have hypotensive effects. However, the molecular and cellular mechanisms responsible for the reduction of blood pressure are not fully understood [149]. For instance, BthA-I-PLA<sub>2</sub>, isolated from the jararacussu pitviper snake (*Bothrops jararacussu*), reduces blood pressure due to its phospholipase activity. This was supported by the alkylation of His48 with p-bromophenacyl bromide that blocks the enzyme’s catalytic mechanism [150]. On the other hand, the PLA<sub>2</sub> toxins OSC3a and OSC3b isolated from Papuan Taipan (*Oxyuranus scutellatus*), produce hypotensive effects by generating cyclooxygenase metabolites (dilator prostaglandins or prostacyclin) that may be involved in the release of endogenous mediators, such as histamine and bradykinin [151]. However, the mode of action for other enzymes, such as BmooPLA<sub>2</sub>-I, from the Brazilian lancehead (*Bothrops moojeni*), has not been reported [152].

Snake venom PLA<sub>2</sub> has been reported to exhibit cytotoxic, bactericidal, and anti-viral activities. Some toxins elicit these activities in a catalytic-dependent manner, while PLA<sub>2</sub>-homologues have also been reported to have these effects, suggesting that catalytic activity is not fully involved in inducing the mentioned biological effects [153,154]. Further studies are needed to reveal the molecular mechanisms involved in inducing these effects.

## 2.4. Snake venom L-Amino Acid Oxidases (LAAOs)

The L-Amino acid oxidases are widely present in snake venoms, as well as in other organisms [155–157]. These flavoproteins are responsible for the yellow color in snake venoms. They catalyze the stereospecific oxidative deamination of L-amino acids producing the corresponding alpha-keto acid, ammonia, and hydrogen peroxide (H<sub>2</sub>O<sub>2</sub>) (Figure 11). LAAOs are homodimeric proteins and consist of three domains (Table 1). Each monomer has a molecular mass of 57–68 kDa. The enzyme typically makes up 1%–4% of the venom by weight. However, in certain species, such as the Malayan pit viper (*Callosellasma rhodostoma*), the enzyme can represent up to 30% of the dried venom by weight [167]. The presence of LAAOs in snake venoms and their biological activities can enhance the actions of other major toxins and contribute to either prey immobilization or increased toxicity in snakebites.

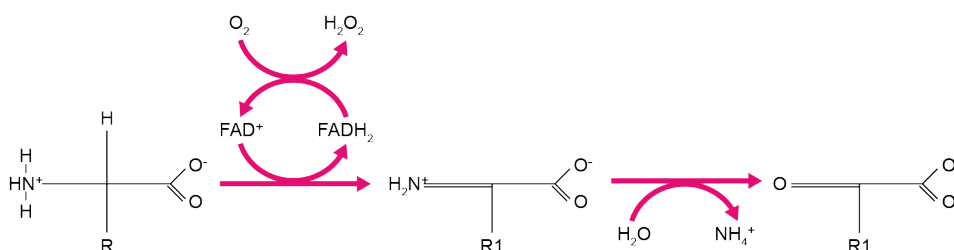


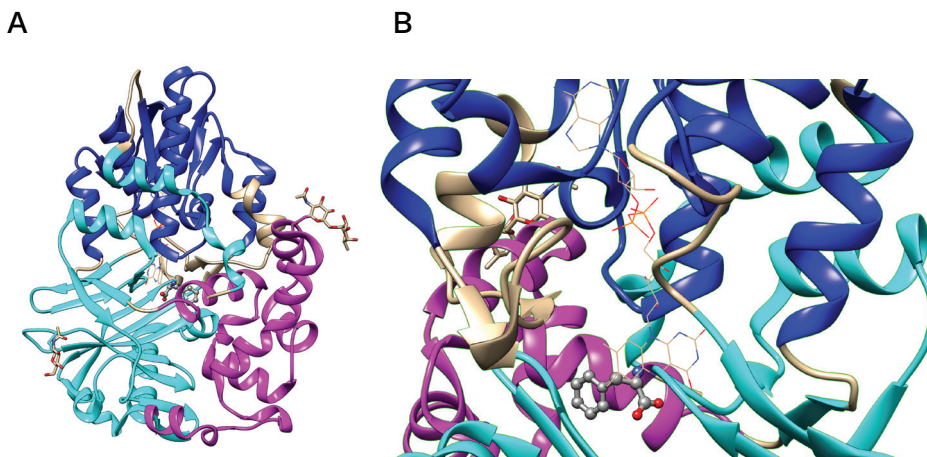
Figure 11. Catalyzed reaction of snake venom LAAOs.

Table 1. Domains of snake venom LAAOs

Domains	Amino acid residues range
FAD-binding domain	35–64, 241–318, 446–471
Substrate-binding domain	5–25,73–129, 232–235,323–420
Helical domain	130–230

The Flavin Adenine Dinucleotide (FAD)-binding domain stabilizes the FAD<sup>+</sup> molecule necessary for catalysis. This domain's secondary structure consists of six β-sheets and five α-helices with the addition of two short β-sheets and one α-helix. Four of the six β-sheets are parallel, and the remaining two are antiparallel. Both short β-sheets are parallel to each other. This domain contains the consensus sequence of glycine residues (G40XG42XXG45) that are involved in access to the negatively charged phosphate group of the coenzyme. Additionally, several salt-bridges stabilize this domain [159,160]. The substrate-binding domain interacts with the amino acid to be oxidized, and it contains six α-helices and eleven β-sheets [159,160]. Finally, the helical domain is the only one with a continuous sequence. The domain's secondary structure consists of six α-helices with one short α-helix, and several loops [159,160] (see Figure 12).

**Figure 12.** Structure of snake venom LAAO. (A) the FAD-binding domain is shown in blue. The substrate-binding domain is displayed in cyan (blue-green), and helical domain is presented in magenta. Glycosilations are depicted as sticks. (B) A phenylalanine residue is shown in balls and sticks in the active site, while FAD is depicted as wire. Figure prepared from PDB code 2IID.



The most important residue for catalysis is His223, which is conserved in all LAAOs found in snake venoms [166,168]. This residue acts as a nucleophile by deprotonating the  $\alpha$ -amino of the substrate (amino acid) [157,159]. Additionally, this amino acid has two conformations, A and B. During catalysis, His223 spends 40% of its time in conformation A and 60% in B. As conformation A, this residue impedes the entry of oxygen; whereas, in conformation B, oxygen can freely enter and participate in the final formation of hydrogen peroxide to recover the FAD<sup>+</sup> [161]. Although LAAOs oxidize all L-amino acids, they prefer aromatic and hydrophobic amino acids, such as phenylalanine and leucine [159,160,162].

It is important to note that these toxins are glycoproteins. In some cases, the removal of carbohydrates is known to reduce the enzymatic and biological effects caused by snake venom LAAOs [163,164]. However, deglycosylation does not affect the enzymatic activities of LAAOs from lancehead pitvipers such as *Bothrops pauloensis*, *B. jararaca*, *B. alternatus*, and *B. moojeni* [165–167]. Therefore, further studies are needed to determine the precise role of glycosylation in snake venom LAAOs and their implications on the biological effects induced by these enzymes. Some LAAOs are known in the venom of medically important Colombian species, including *Crotalus durissus*, *Bothriechis schlegelii*, and *Micrurus mipartitus* [135,168,169]. These enzymes induce several biological effects, which are described below [135,168–170].

### **Biological activities induced by snake venom LAAOs**

The biological effects of LAAOs are attributed to the hydrogen peroxide (H<sub>2</sub>O<sub>2</sub>) generated in the catalytic reaction. The effects are inhibited by H<sub>2</sub>O<sub>2</sub> scavengers such as catalase [171–174]. However, several studies demonstrate that biological effects are not completely recovered by incubation with catalase, suggesting that the effects produced by LAAOs are not solely due to the production of H<sub>2</sub>O<sub>2</sub> [157,175,176].

#### *Hemorrhage*

Some LAAOs found in snake venoms can induce hemorrhage by themselves [165,177–179]. This effect is attributed to the capacity of snake

venom LAAOs to induce apoptosis in endothelial cells. This leads to the rupture of the endothelium and the extravasation of red blood cells. The accumulation of  $H_2O_2$  in blood vessels may be responsible for the apoptotic effect on endothelial cells [177]. Thus, it is suggested that this effect contributes to the hemorrhagic activity provoked by SVMs.

#### *Edema*

Some snake venom LAAOs can induce edema. However, the precise mechanism that produces this effect is not entirely understood. A LAAO from the Japanese snake mamushi (*Gloydius blomhoffii*) is reported to stimulate lymphocytes and monocytes to release proinflammatory cytokines, IL-6, IL-2, and IL-12, which may explain the inflammatory activity of this enzyme [180]. However, Izidoro et al. [171] suggested that edema formation is due to the activation of the inflammatory response by the  $H_2O_2$  generated, as administration of glutathione (an antioxidant) to the mouse paw inhibits the edema-inducing activity of the enzyme [181].

#### *Modulation of platelet aggregation*

The effect of snake venom LAAOs on platelet aggregation is inconclusive. Some enzymes induce platelet aggregation, whereas other toxins produce inhibition of these cells' aggregation [162]. Du and Clemetson [182] proposed that hydrogen peroxide generated in the catalytic reaction of LAAOs is responsible for inducing and inhibiting platelet aggregation. The inhibitory activity may be related to the hydrogen peroxide that impedes the interaction between fibrinogen and its receptor on the surface of the platelet (GPIIb/IIIa) or reduces the binding of ADP to the platelets [183,184]. On the other hand, platelet activation may be a consequence of thromboxane  $A_2$  production elicited by  $H_2O_2$  [172]. Despite this evidence, further systematic studies are required to determine why LAAOs can either elicit or inhibit platelet aggregation.

### **Other biological activities that are not related to snakebite envenoming**

LAAOs induce several activities that make them attractive for searching for therapeutic alternatives for protozoal, viral, bacterial infections, and cancer due to their cytotoxicity (see Chapter 10). Several snake venom LAAOs have antileishmanial activity [171–173,185–187]. This effect is attributed to the  $H_2O_2$  generated by the catalytic cycle of the enzymes.

Likewise, a snake venom LAAO isolated from *Trimeresurus stejnegeri* (Chinese green tree viper) has antiviral activity against HIV-1 [179]. LAAOs have also demonstrated antibacterial activity against both gram-negative and gram-positive bacteria [162,168,181,188]. The mode of action of snake venom LAAOs for inducing this effect is attributed to  $H_2O_2$ . However, the binding of the enzyme to the bacterial surface and further concentration of  $H_2O_2$  seems to be essential for this effect [189]. Several snake venom LAAOs show cytotoxic activity against tumor cell lines [199]. They can induce apoptosis in these cells. This effect involves  $H_2O_2$ , but it is also speculated that glycan moieties are crucial for the interaction with the target cell [191].

## 2.5. Snake venom disintegrins

The term “disintegrin” was first introduced to toxinology in 1987 by Huang et al. [192]. They described the isolation and characterization of Trigamin from the venom of *Craspedocephalus gramineus* (Common bamboo viper). However, today this term is used to define toxins with a length between 40-100 amino acids present in the snake venom of the Viperidae. These toxins are produced by proteolytic processing of P-II and P-III SVMPs. Initially, the Arg-Gly-Asp (RGD) motif was described as an essential structural characteristic for their main activity, which is to inhibit platelet aggregation by blocking  $\beta 1$  and  $\beta 3$  integrins [198].

### Structure of snake venom disintegrins

Snake venom disintegrins can be classified into four groups based on their number of amino acids and disulfide bonds [193,194]. The first group comprises short disintegrins from 41 through 51 residues and four disulfide bonds. The second group consists of medium size disintegrins that contain about 70 amino acids and six disulfide bonds. The third group comprises long peptides with approximately 84 amino acids, and seven cysteine bonds cross-link them. The fourth group incorporates homo and heterodimers. These disintegrins are composed of 67 amino acids and ten cysteine residues, involved in stabilizing the structure by forming intra and interchain disulfide bonds.

The RGD motif is the most common in snake venom disintegrins. Nevertheless, other motifs have also been identified. Table 2 describe the diversity of these motifs and their molecular targets (mainly integrins). Structural studies of short, medium, large size, and dimeric disintegrins revealed a mobile loop that contains the active motif, which protrudes 14–17 Å from the protein core [193,194,195] (see Figure 13).

**Table 2.** Integrins, their function, and snake venom disintegrins that inhibit them.

Integrin	Function	Disintegrins that inhibit it*	References
$\alpha 5\beta 1$	The major fibronectin receptor	RGD, VGD and MDG	
$\alpha 8 \beta 1$	Tenascin receptor	RGD	
$\alpha v\beta 1$	Vitronectin receptor	RGD	
$\alpha v\beta 3$	Vitronectin receptor	RGD, WGD	
$\alpha 11b\beta 3$	Platelet fibrinogen receptor involved in platelet aggregation	RGD, WGD and KGD	
$\alpha 4\beta 1$	Fibronectin and VCAM-1 receptor	MLD	[145,147, 148,193, 197,198]
$\alpha 4\beta 7$	Fibronectin, VCAM-1 and MdcAM receptor	MLD	
$\alpha 3\beta 1$	Laminin receptor	MLD	
$\alpha 6\beta 1$	Laminin receptor	MLD	
$\alpha 7\beta 1$	Laminin receptor	MLD	
$\alpha 9\beta 1$	Tenascin receptor	MLD	
$\alpha 1\beta 1$	Collagen IV receptor	KTS and RTS	

\*Standard Amino Acid 1-letter Code.

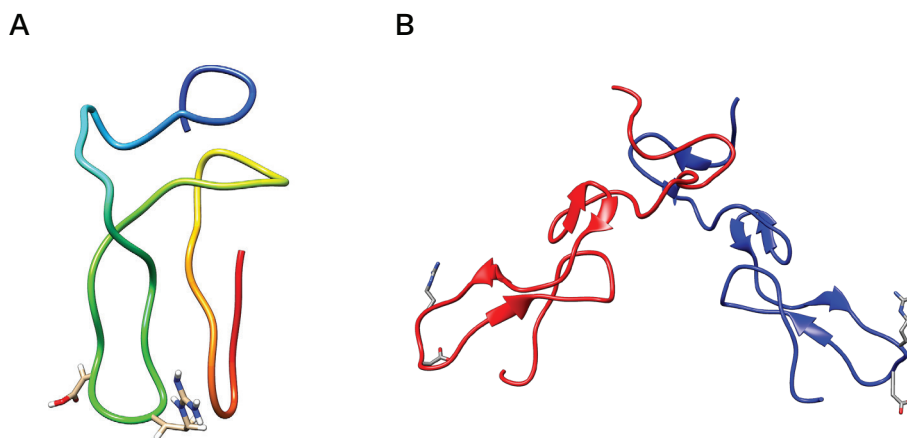


**Figure 13.** Structure of snake venom disintegrins. (A) Monomeric disintegrin; (B) Heterodimeric disintegrin. The blue and red chains represent different subunits. The RGD motif is displayed in the sticks. N-term and C-term represent the N-terminal and C-terminal of each chain, respectively. This image was prepared from PDB structures with codes 2MOP (monomeric) and 1TEJ (heterodimeric).

### **Biological activities induced by snake venom disintegrins**

Due to their capacity to block integrins, the most important activity induced by snake venom disintegrins is the inhibition of platelet aggregation. This can contribute to the hemostatic disorders caused by SVSPs, SVMPs and other toxins in snakebite envenoming [199–203]. In fact, the anti-platelet aggregation activity of disintegrins has made them essential templates for the development of drugs used as antithrombotic agents. For instance, Tirofiban is derived from echistatin found in the venom of *Echis carinatus* (Phoorsa snake) [204] and, Eptifibatide obtained from barbourin present in the venom of *Sistrurus miliarius barbouri* [200,201,205] (see Chapter 10).

Additionally, snake venom disintegrins have shown potential in anti-cancer therapy. Disintegrins can target a wide variety of integrins; and, thus, it is plausible that they have the potential to interfere in essential processes involved in carcinogenesis, tumor growth, invasion, and migration (see Chapter 10). Thus, disintegrins can be used as tools and potential drugs for the treatment of this health problem [197,206–208].

## **2.6. Three-finger toxins (3FTx)**

### **Structure**

The protein family known as three-finger toxins consists of non-enzymatic polypeptides ranging from 60 to 62 amino acid residues (short chain) and between 66 and 74 amino acid residues (long chain). They are typically monomers and contain 4 to 5 highly conserved disulfide bridges. Their folding is characterized by three loops with beta strands that run from a hydrophobic core that is in turn crossed by four disulfide bonds. Venoms from elapids, hydrophids, and colubrids snakes contain these proteins [209].

The primary structure of a protein is determined by its sequence of amino acids that are represented as beads on a necklace. To have a complete and functional structure, specific interactions between amino acids are necessary for proper folding. Figure 14 shows the primary and tertiary

structure of mipartoxin-I, a toxin found in the venom of *Micrurus mipartitus* (Redtail coralsnake).

Although the members of the 3FTx family share conserved structural features that enable them to fold and maintain their integrity, some modifications also occur. These modifications may be related to the diversity of their functions and their affinity for certain molecular targets [210,211]. In addition to the eight cysteine residues present in the central region that favor the formation of disulfide bridges, the aromatic residues of tyrosine or phenylalanine in positions 25 and 27 are also conserved and contribute to the adequate folding and stability of the beta sheet structure in this toxin. The stability of native conformation is also contributed by arginine residues at position 39 and aspartic acid at position 60, as they form salt bridges with any of the terminal ends [209,212]. Table 3 lists the reported variations described for the 3FTx structures, including the main ones.

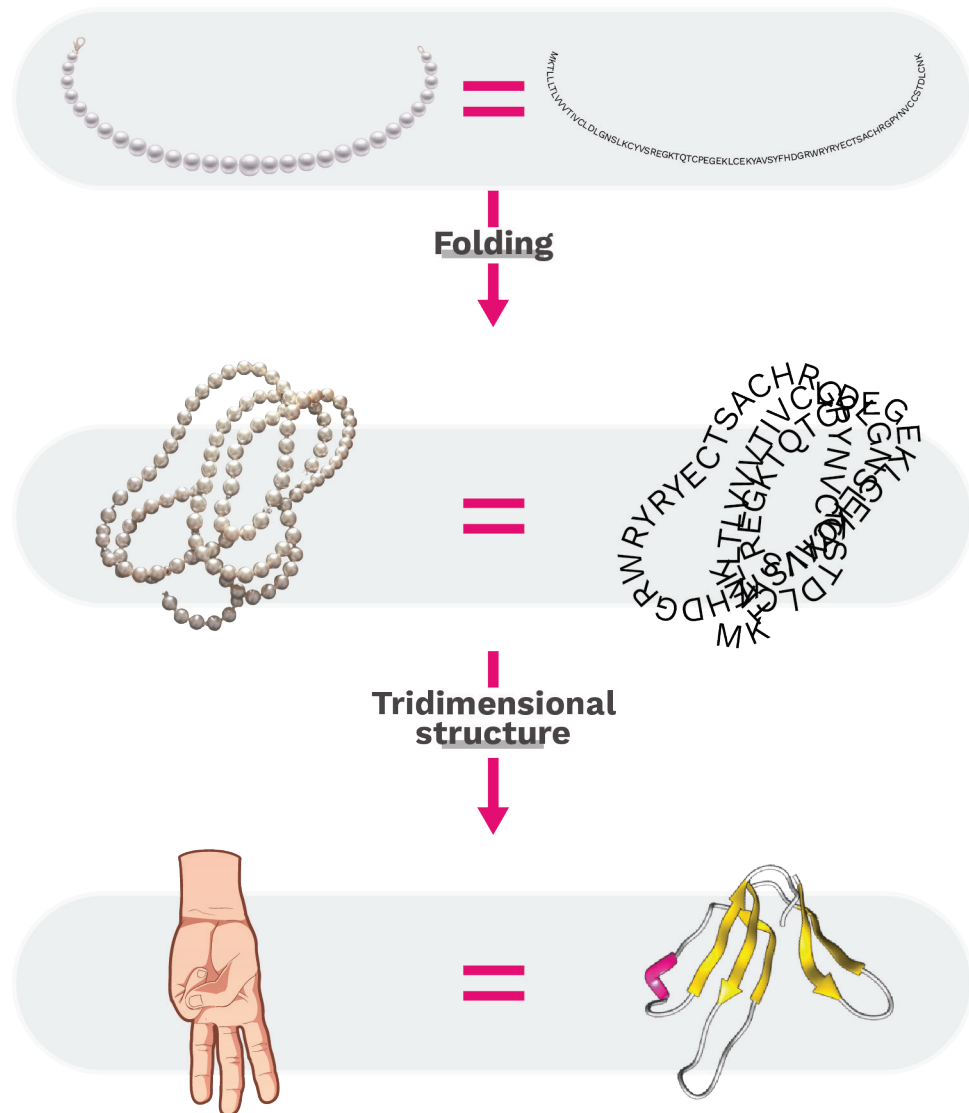
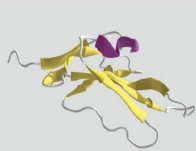


**Figure 14.** Primary structure of mipartoxin-I from the venom of *Micrurus mipartitus* (GenBank code: AVI57319.1) is represented as a long chain. Interactions between amino acid residues facilitate folding at various sites of the chain, contributing to secondary and tertiary structure conformation. Mipartoxin-I, has a tridimensional structure that resembles the three central fingers of a hand. That is why it belongs to the protein family known as three-finger toxins (3FTx) [210].

**Table 3.** Some examples of the structural variations found in the family of three-finger toxins.

Variation / Tridimensional structure	Toxin name	Snake species	Annotations	References
Short chain	Erabutoxin (PDB code 1QKE)	<i>Laticauda semifasciata</i> Chinese sea snake (Elapidae)	62 amino acids	[213]
Long chain	Bungaro-toxin (PDB code 1IKC)	<i>Bungarus multicinctus</i> Krait with many bands from Taiwan (Elapidae)	74 amino acids	[214]
Presence of a fifth disulfide bond in loop I	Recombinant WTX (PDB code 2MJ0)	<i>Naja kaouthia</i> South and Southeast Asian monocol Cobra (Elapidae)	Although it was previously classified as a weak neurotoxin, recent studies show that toxins with a fifth disulfide bond in that position are highly toxic and bind to nicotinic acetylcholine receptors at concentrations in the nanomolar range. These toxins are referred to as “non-conventional 3FTx” due to their differing selectivity and specificity from canonical neurotoxins. An additional example is the BM14 toxin found in the venom of <i>Bungarus multicinctus</i> from Taiwan. This toxin exhibits a higher affinity for the muscarinic receptor of acetylcholine M2 than for M1	[215,216]
Presence of a fifth disulfide bond in loop II	NTX-1 (PDB code 1NTN)	<i>Naja oxiana</i> Central Asian cobra (Elapidae)	The fifth disulfide bond in loop II provides a twist and forms a short helical segment at the tip of the loop. This additional binding plays an important role in specificity on $\alpha 7$ nicotinic acetylcholine receptor blockade. However, toxins such as can-doxin and haditoxin that lack this variation, also bind to this receptor	[217]

### Extensions in N-terminal or C-terminal



Denmotoxin  
(PDB code 2H5F)

*Boiga dendrophila*  
Mangrove snake or the Gold-ringed cat snake from Malaysia (Colubridae)

The protein has an extended N-terminal segment with seven additional residues, which are covered by a pyroglutamic acid. The effect of this structural variation on its function is currently unknown. Typically, long-chain neurotoxins have 2-9 additional residues at the C-terminus

[218]

### Dimers with non-covalent bonds



Haditoxin  
(PDB code 3HH7)

*Ophiophagus hannah*  
King Cobra from India to Southeast Asia (Elapidae)

Most 3FTx are monomers, but some can exist naturally as dimers. Haditoxin is a homodimer, with two short-chain monomers that are non-covalently bonded and oriented in opposite directions. This gives haditoxin the ability to function as an antagonist of muscle (abgd) and neuronal (a7, a3b2 and a4b2) nicotinic acetylcholine receptors

[219]

### Covalently bonded dimers



Irditoxin  
(PDB code 2H7Z)

*Boiga irregularis*  
Brown tree snake of Australia, Papua New Guinea, and islands of northwestern Melanesia (Colubridae)

The heterodimer consists of two non-conventional 3FTx subunits, each containing an extra cysteine that forms an interchain disulfide bond. Additionally, the N-terminal has a seven amino acid residue extension. This results in a potent postsynaptic neurotoxin

[218]

### Synergistic toxins



SynTx  
(PDB code 7C28)

*Dendroaspis jamesoni*  
Congo green mamba (Elapidae)

The molecule is a homodimer connected by an interchain disulfide bond. Dimerization occurs through the loops II and III of the monomers.

Although this group contains molecules with a similar amino acid sequence to other neurotoxins and cytotoxins of the 3FTx family, its toxicity may be low or null. However, its importance lies in the fact that it increases the toxicity of other venom proteins (synergism), such as angusticeps-like toxins, which, in turn, behave as cholinesterase inhibitors.

[5,221,222]

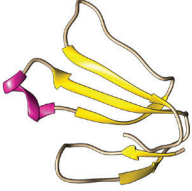
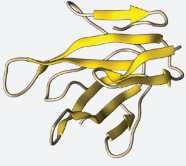
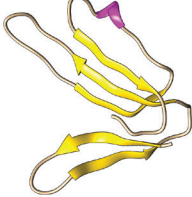
Tridimensional models taken from PDB and prepared in UCSF Chimera v.1.17.3. All these toxins have a 3D model view available in <https://serpientes.ins.gov.co/>

Recently, some authors proposed a guideline to systematically separate and study three-finger toxins due to the high variability between the amino acid sequences of these proteins [223–225]. They assembled a database with selected 3FTx sequences known for *Micrurus* species from Brazil and classified the proteins based on their similarity and structural identity. Accordingly, the authors established parameters for proposing a reclassification based on key functional amino acids, disulfide bridges, charge distribution on the surface, and the phylogenetic relationship of the sequence [223–225]. The functionality of the protein can be attributed to nine groups based on sequence homology. This classification only serves as a reference for the three-finger toxins found in *Micrurus* species from South America.

The models predicted from the primary sequences of Brazilian specimens were based on homologous sequences of Old-World elapids, including *Dendroaspis polylepis*, *Naja atra*, *Bungarus multicinctus*, *B. candidus*, *Ophiophagus hannah*, *Dendroaspis jamesoni* and *Hemachatus haemachatus* (Ring-necked spitting cobra). Only one sequence was built from fuldotoxin of *Micrurus fulvius* venom (PDB code 4RUD). The newly conformed nine groups included representative local specimens such as *Micrurus altirostris*, *Micrurus carvalhoi*, *Micrurus corallinus*, *Micrurus frontalis*, *Micrurus lemniscatus*, *Micrurus paraensis*, *Micrurus spixii*, and *Micrurus surinamensis* [224].

Only a small number of three-finger toxins have been purified and characterized from Colombian *Micrurus* venoms. Currently, only three toxins have three-dimensional models predicted from sequences reported in the literature. Two of these toxins belong to Colombian medically important snake species (*M. mipartitus* and *M. dumerilii*; Table 4) [225]. Moreover, they exemplify the bicolor and monadal pattern groups, respectively [235]. Another species in the monadal pattern group, *M. clarki* has also had 3FTx research conducted on it [227].

**Table 4.** Three finger toxins structures purified from some *Micrurus* venoms in Colombia. Each sequence is assigned to a Uniprot accession number

Three finger toxins name and UniProt accession number	Snake species	Sequence	Predicted 3D model	References
Clarkitoxin-1-Mdum COHLK5	<i>Micrurus dumerilii</i> Capuchin coral snake Elapidae	RICDDSSIPFLRTPQLCPKGQDVCYK- KTPIVKKFKWLQKKGCASSCPKDG- FIKIFKIECCTKDNCI		[226]
Mipartoxin-1 B3EWF8	<i>Micrurus mipartitus</i> Redtailed coral snake	MKTLTLLVVTIVCLDLGNSLKCYWS- REGKTQTCPEGEKLCYAVSYFH- DGRWRYRECTSACHRGPYNVCCST- DLCNK		[226]
Clarkitoxin-1 COHK04	<i>Micrurus clarki</i>	RICDDSSIPFLRTPQLCPKGQDVCYK- KTPIVKKFKWLQKKGCASSCPKNG- FIKIFKIECCTKDNCI		[227]

Sequences used to predict the three-dimensional structures presented using the SWISS MODEL Software [239,240]. Molecules adjusted and prepared in UCSF Chimera v.1.17.3

### **Biological activities**

Although 3FTx family toxins share a structural similarity, they exhibit a wide variety of pathophysiological activities and mechanisms of action, including postsynaptic neurotoxicity, cytotoxicity, cardiotoxicity, anticoagulant, and antiplatelet activities. In addition, they act as L-type  $\text{Ca}^{2+}$  channel antagonists and can synergistically promote hypotension with muscarinic toxins [223]. The 3FTx have a small, compact, and stable structure with multiple interaction sites to achieve various functions that have been evolutionarily optimized [230].

### **Neurotoxins**

Neurotoxicity is possibly the best-known effect of 3FTx due to the drastic effect of flaccid paralysis and respiratory failure in snakebite accidents. Interference with the signal transmission can occur by different routes. In the case of altered cholinergic transmission in the central and peripheral nervous systems, neurotoxicity can occur at various sites in the postsynaptic region, affecting both nicotinic and muscarinic receptors [15] (Figure 15). The following are examples of toxins and their mechanisms of action that lead to neurotoxicity:

*Curare-like toxins or  $\alpha$ -neurotoxins.*— These are similar to the alkaloid curare (from the plant extract from indigenous peoples in Central and South America). They are long and short chain neurotoxins that bind to the muscle acetylcholine receptor  $\alpha 1$  and prevent effective neuromuscular transmission. In contrast, long-chain neurotoxins bind with high affinity to the neuronal acetylcholine receptor  $\alpha 7$ .

*Muscarinic toxins.*— These comprise toxins that act as agonists or antagonists on muscarinic receptors. Muscarinic toxin  $\alpha$  (MT $\alpha$ ) isolated from mamba venom (*Dendroaspis jamesoni*) is a potent  $\alpha 2\text{B}$ -adrenoceptor antagonist [212,223].

*$\alpha$ -neurotoxins.*— These specifically bind to the neuronal nicotinic acetylcholine receptor ( $\alpha 3\beta 4$ ). They resemble long-chain  $\alpha$ -neurotoxins in structure but occur as dimers. They do not recognize  $\alpha 1$  acetylcholine receptor.

Recently, micrurotoxins 1 and 2 (MmTX1 and MmTX2), isolated from the venom of *Micrurus mipartitus* (Redtailed coralsnake), have been described as agonists at the ionotropic GABA<sub>A</sub> receptor that enhances receptor opening and desensitization.

Acetylcholinesterase inhibitors interfere with neuromuscular transmission by inhibiting binding to the peripheral site of the acetylcholinesterase enzyme (AChE) present at the neuromuscular junction. This prevents the AChE from capturing and degrading acetylcholine, leading to muscle twitching due to the accumulation of acetylcholine in the synaptic cleft. These inhibitors are known as fasciculins and have similar structures to short-chain neurotoxins [209,212].

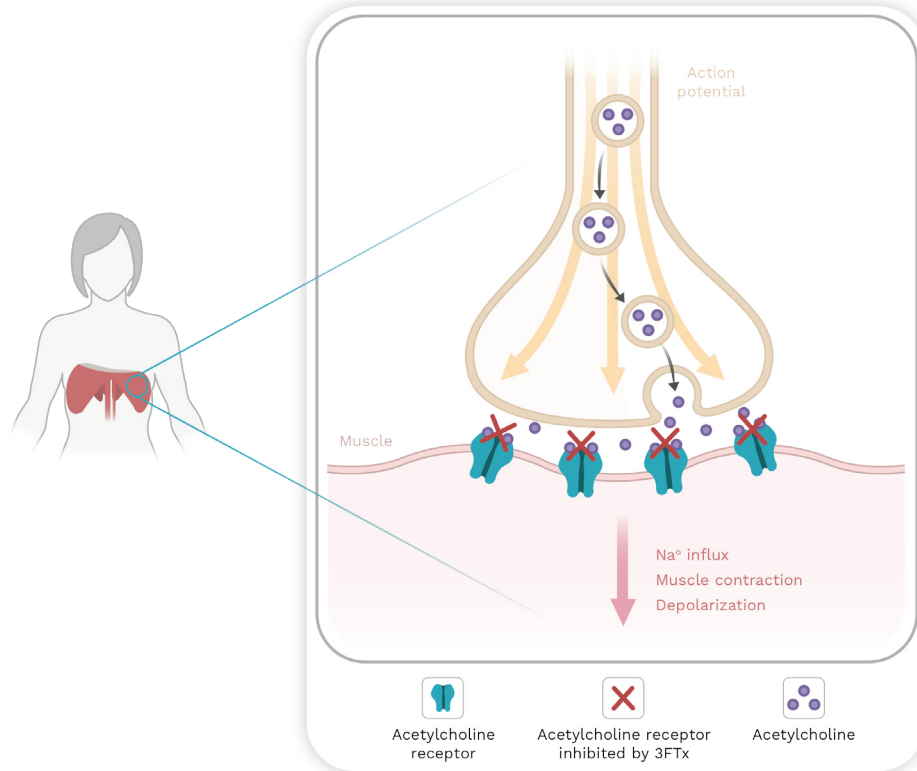


**Figure 15.** Three-finger toxins block acetylcholine receptors on the effector cell in the neuromuscular junction, leading to flaccid paralysis in myocytes, and respiratory failure when diaphragm is affected. Image created with BioRender and edited by Oscar A. Ramirez Ruiz.

### **Cardiotoxins**

Cardiotoxins are a group of toxins that have been found exclusively in cobra venoms, particularly in species of *Naja*. These toxins are similar to short-chain neurotoxins, contain four disulfide bonds, and they represent the second largest group after neurotoxins. They are responsible for increasing the heart rate and can lead to cardiac arrest in a dose-dependent manner. Additionally, many toxins in this group also have cytolytic effects, forming pores in lipid membranes; they are also known as cytolytins. Finally, another subgroup is recognized within this classification, the b-cardiotoxins and related toxins. This subgroup exhibits blocking activity of cardiac  $\beta_1$  and  $\beta_2$  adrenergic receptors [212].

### **L-type calcium channel blockers**

Structurally, these channel blockers are polypeptides similar to short-chain neurotoxins. They bind to the 1,4-dihydropyridine binding site of L-type calcium channels and physically block calcium currents, leading to relaxation of smooth muscle and inhibition of cardiac contractions [212].

### **Hemostasis disorders**

Only a few 3FTx have the amino acid sequence RGD (Arginine-Glycine-Aspartic Acid) in an accessible site for interaction. The RGD tripeptide participates in the adhesive function of several proteins, interfering with the interaction between fibrinogen and its receptor complex for glycoprotein IIb-IIIa ( $\alpha_{IIb}\beta_3$ ) inhibiting platelet aggregation [223].

The KT-6.9, toxin isolated from the venom of the cobra *Naja kaouthia* inhibits platelet aggregation induced by adenosine diphosphate (ADP), thrombin, and arachidonic acid. As a result, it inhibits platelet aggregation (primary hemostasis) in a dose-dependent manner [223]. In secondary hemostasis, the cobra venom of the species *Hemachatus haemachatus* (Ring-necked spitting Cobra) contains ringhalexin and exactin that inhibit the activation of coagulation factor X, causing coagulation alterations [223].

### **Interaction with sodium channels**

Some 3FTxs interact with acid-sensitive ion channels (ASIC) that are normally selective ion channels for Na<sup>+</sup> and are activated by protons. ASICs are widely distributed throughout the peripheral and central nervous system of vertebrates. These channels are involved in synaptic plasticity, neurodegeneration, and pain perception [223].

## **2.7. Snake Venom Serine Proteinase (SVSP)**

### **Structure**

Serine proteinases are glycosylated proteins with enzymatic activity. Their molecular weight ranges between 26 and 67 kDa, depending on the degree of N- or O-glycosylation. The subgroup known as thrombin-like serine proteinases is responsible for degrading fibrinogen and amplifying bleeding conditions during envenomation [244]. In *Bothrops asper* venom (common lancedhead pitviper) serine proteinases are abundant constituents representing between 5%-18% of the proteins, depending on the age of the snake and their geographic region [235]. These proteases, along with hyaluronidases, metalloproteinases, and phospholipases A<sub>2</sub> belong to the group of hemotoxic enzymes that are important to viper venoms [232].

These proteases are characterized by a typical chymotrypsin fold and two barrels of 6-stranded  $\beta$  sheets (Figure 16), their active site is located in the cleft between the latter and includes a canonical catalytic triad of His-Asp-Ser. Although they share between 50%-80% identity in their amino acid sequences, they differ significantly in their substrate specificity, and therefore, in their activity [233]. Several SVSPs have pharmacologic activity (see Chapter 10). For instance, Mambalgins are toxins found in black mamba venom (*Dendroaspis polylepis*). They have analgesic effects by blocking channels with the ASIC1a and ASIC2a subunits in the central nervous system, as well as channels that include the ASIC1b subunit in nociceptors [229].

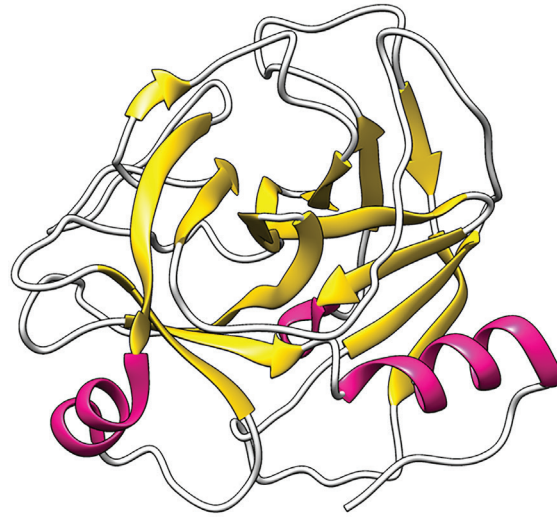


**Figure 16.** AaV-SP-I, a glycosylated serine proteinases found in the snake venom of *Agkistrodon acutus*. Tridimensional model taken from PDB (code 1OP0) and prepared in UCSF Chimera v.1.17.3

## **Biological activities**

### *Hemotoxic and coagulopathic*

The human body can counteract the hemorrhagic effect produced by metalloproteinases. However, the thrombin-like serine proteinases present in the venom of viperids prevent the formation of an effective fibrin plug. Under physiological conditions, endogenous thrombin cleaves specific regions of fibrinogen in the circulation before bleeding. This exposes the site for binding other fibrinogen molecules undergoing the same hydrolysis, forming a fibrin mesh that stabilizes the clot and promotes hemostasis.

Thrombin-like serine proteinases simulate thrombin activity, but they hydrolyze different sites on the fibrinogen molecule. This alters the binding between fibrinogen molecules, resulting in irregular consumption of fibrinogen and unstable fibrin clot formation (Figure 17) [234–237]. While many serine proteinases act on the  $\alpha$  chain of fibrinogen, some purified from *Agkistrodon* species act on both  $\alpha$  and  $\beta$  chains [238]. In addition, this subgroup of enzymes has the ability to activate coagulation factors VIII and XIII, as well as thrombin. They are also responsible for the activation of protein C, platelet aggregation, activation of plasminogen, and factor V. These actions can result in consumptive coagulopathy (Figure 17) [238,239].

Asperase was the first serine proteinases isolated from the venom of *Bothrops asper*. It is a glycosylated enzyme with a molecular mass of 30 kDa. This protein promotes defibrinogenation in murine models and causes behavioral alterations, such as loss of the righting reflex, opisthotonos (spasm of the muscles causing backward arching of the head, neck, and spine), and intermittent rotations along the longitudinal axis of the body. This characteristic is similar to that of Gyroxin, a thrombin-like enzyme found in the venom of *Crotalus durissus* from Brazilian populations [236,240].

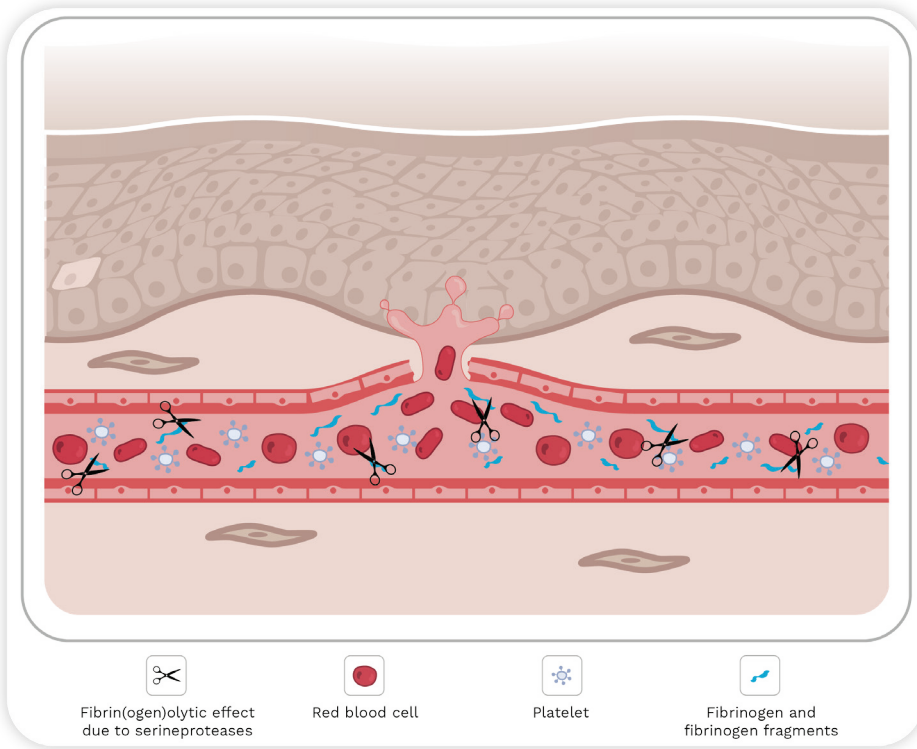


**Figure 17.** Hemostatic alteration model. Circulating fibrinogen molecules (represented in blue) undergo inadequate hydrolysis by thrombin-like serine proteinases, favoring their erratic and excessive consumption and resulting in deficient fibrin clot formation and unsatisfactory hemostasis. Additionally, platelets (structures in white) aggregate inappropriately at sites other than the injury site, leading to inappropriate consumption, uncontained bleeding, and the presence of microthrombi. The image was created with BioRender and edited by Oscar A. Ramirez Ruiz.

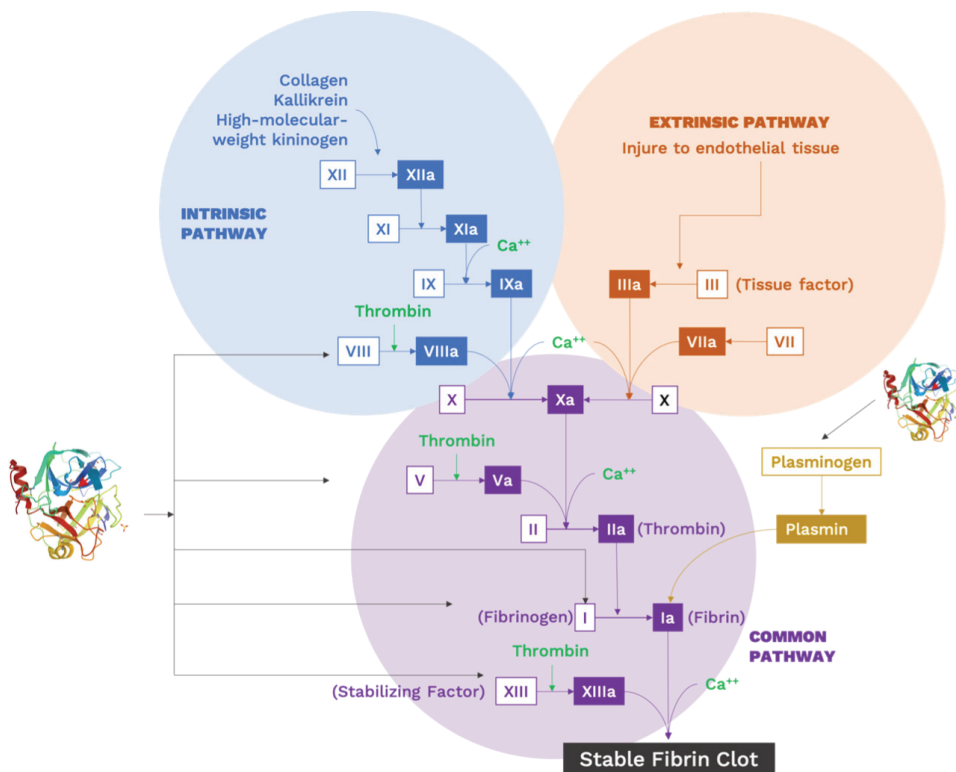


**Figure 18.** Schematic of the blood coagulation cascade pathways under physiological conditions indicating the respective sites of action of snake venom serine proteinases (SVSP). Red arrows indicate activation by SVSPs. The black arrow indicates fibrinogenase activity, causing inadequate consumption of fibrinogen, and the dotted arrow highlights the thrombin-like activity (see more information within the text). Additionally, SVSPs act as platelet activation enzymes, allowing excessive and inappropriate aggregation of platelets. Moreover, SVSPs activate protein C (not shown in the figure) and act as an anticoagulant by irreversibly inactivating factor Va and factor VIIIa. SVSPs can also act as kallikrein-like enzymes, converting kininogen into bradykinin and exacerbating the manifestations associated with hemodynamic disorders.

### *Hypotension*

The production of bradykinin (BK) by kallikrein-like serine proteinases, both with the inhibition of BK degradation by bradykinin potentiating peptides (BPP), results in an overall increase in BK levels. As a result, stimulation of the bradykinin B<sub>2</sub> receptor induces vasodilation, as well as anti-fibrotic and anti-inflammatory effects, through various intracellular mechanisms [149,235].

Some isolated serine proteinases, mainly from viperid venoms but also in elapids such as the sea snake *Hydrophis hardwickii* (Spine-bellied sea snake), exhibit hypotensive activity similar to kallikrein that releases bradykinin and causes vasodilation. These proteases degrade angiotensin I into angiotensin II that is then converted into tetrapeptides that do not have hypertensive activity. Afterwards, fibrinogen levels in the blood decrease, altering blood flow, resulting in the release of BK and Met-Lys-bradykinin from kininogen that act on β<sub>1</sub> and β<sub>2</sub> receptors, causing vasodilation and subsequent hypotension [149].

## **2.8. C-type lectins (CTL) and C-type lectin-like proteins (CLP)**

### **Structure**

Snake venom lectins have properties that are intermediate between the two important families of animal lectins, designated S and C type lectins. They are extracellular and have this name because they require calcium ions for their sugar-interacting activity. S-type lectins owe their name to the fact that they require thiol group-reducing agents for full activity, both intra and extracellular, and exhibit specificity for galactosides [241].

Several C-type lectins and related proteins have been isolated and characterized from snake venoms. These proteins can be broadly classified into two main groups based on their structural and functional properties: true C-type lectins, and a more complex group of proteins structurally related to C-type lectins, but with different functions, called C-type lectin-like proteins (CLP) [242].

The C-type lectins are calcium-dependent. They are carbohydrate-binding proteins with canonical structures like selectins and mannose-binding proteins. They are homodimers (or higher multimers) with sugar binding properties (mainly galactosides; Figure 19A) [242]. The C-type lectins from snake venom (SVgalLs) that bind to galactosides are an example of true C-type lectins. One example of them is known from *Lachesis stenophrys* venom (Central American Bushmaster) but is also present in venoms of vipers such as *Crotalus atrox* (Western diamond-backed rattlesnake) [243].

The carbohydrate recognition domain (CRD) in SVgalLs is generally represented by three amino acid residues, Gln-Pro-Asp, considered determinants in their calcium-mediated affinity for galactose. The specificity for this carbohydrate is related to the interaction of hydroxyl groups 3 and 4, with residues Q96 and D98 through hydrogen bonds [243].

C-type lectin-like proteins have amino acid sequences similar to C-type lectins, but they do not possess carbohydrate-binding properties. Additionally, any association with  $\text{Ca}^{2+}$  does not occur through the classical C-type lectin pathway with the binding loop. They are heterodimers, consisting of closely related  $\alpha$  and  $\beta$  subunits, generally linked by a disulfide bond, and form an integrated structure by exchanging loops. They can also form larger structures through a higher order multimeric association linked by disulfide bonds or by non-covalent interactions [242]. C-type lectin-like proteins (CLP) are named for their high sequence similarity (15%-40%) with the carbohydrate recognition domains of C-type lectins. The  $\alpha$  and  $\beta$  subunits have molecular weights of 14-15 and 13-14 kDa, respectively. Multimerization of these heterodimers can occur through covalent and non-covalent interactions, resulting in  $\alpha\beta$ ,  $(\alpha\beta)_2$ , and  $(\alpha\beta)_4$  structures. CLP  $\alpha\beta$  heterodimers are formed by domain swapping, where a domain from one subunit replaces the corresponding domain of the other (Figure 19B) [244].

CLPs, also known as snakecs, exhibit various activities such as anti-coagulant effects and induction or inhibition of platelet aggregation [260], depending on their structure and function. Pharmacological characterization shows that snakecs can either enhance or inhibit the function of clotting factors, highlighting their potential in drug discovery for blood-related diseases [244].

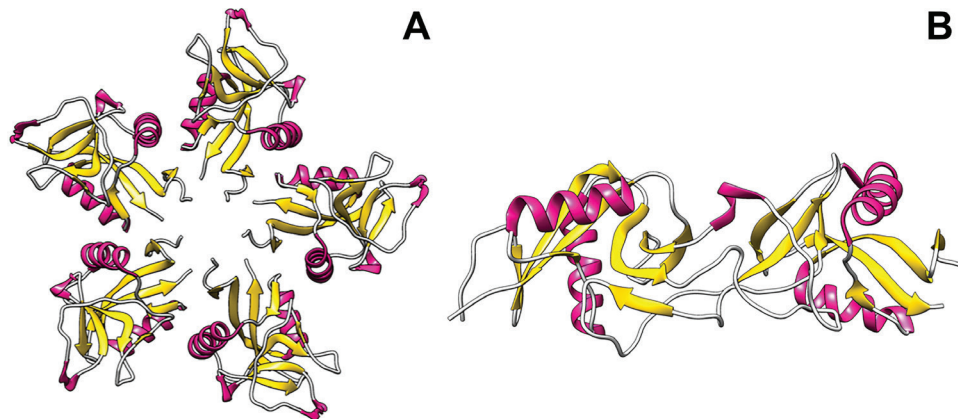


**Figure 19.** (A) Structure of the C-type lectin purified from *Crotalus atrox* snake venom. PDB code 1MUQ. (B) Structure of a C-type lectin-like protein called flavocetin-A, purified from *Trimeresurus flavoviridis* snake venom. PDB code 1C3A. Molecules prepared in UCSF Chimera v.1.17.3

## Biological activities

### Haemostatic disturbances

Platelets are essential for hemostasis, and their aggregation is the first step in the blood coagulation cascade. This process depends on the interaction of many platelet surface receptors, including ADP, collagen, and other factors. Venoms contain components that disrupt this interaction leading to continuous bleeding in the prey (Figure 20).

C-type lectins and related proteins target specific glycoprotein or integrin receptors to inhibit or promote platelet aggregation. Most venom lectins achieve their effects by targeting the platelet surface glycoprotein receptor GPIb, and some also target GPIV that are involved in collagen-platelet interaction. Convulxin, isolated from the venom of *Crotalus durissus* from Brazil-

ian populations, appears to participate in the pathway involving GPIV. Snake venom C-type lectins also bind to integrins, as well as von Willebrand factor (vWF), thrombin, and certain unidentified platelet surface receptors [246].

The effects of snakelects include anticoagulant activity by inhibiting factors Xa and IXa and blocking the interaction between factor Xa and its cofactors in the prothrombinase complex that is dependent on  $Ca^{2+}$  [244,247]. For instance, thrombin inhibition that is dependent on calcium [268], and platelet activation, where C-type lectins such as botrocetin and bitiscetin from *Bothrops jararaca* and *Bitis arietans*, preferentially bind to the von Willebrand factor and enlarge the binding surface with the platelet receptor GPIb, stimulate platelet aggregation [262,267]. In addition, the lectin echicetin found in the venom of *Echis carinatus* has antithrombotic properties, it acts on the platelet receptor GPIb, preventing its aggregation [244].

#### *Inflammatory response*

The role of SVgalL in the inflammatory response has been investigated using different animal models and approaches to evaluate the participation of leukocytes and the recognition of extracellular matrix (ECM) glycoconjugates in the inflammatory response. Lectins from *Bothrops godmani* (BgL) and *Bothrops jararacussu* (BJcuL) have the ability to induce increased vascular permeability in the mouse leg, resulting in moderate acute edema. This relationship may be associated with the ability of lectins to stimulate mast cell degranulation and the release of histamine and serotonin to trigger local inflammatory responses [243].

Other lectin-related inflammatory events have been observed experimentally. For instance, BJcuL increases leukocyte adherence in microvessels of the cremaster muscles of mice. This toxin can bind to fibronectin and vitronectin glycoproteins, suggesting that the migration of peripheral blood leukocytes to the inflammatory site involves cell adhesion to lectin-mediated extracellular matrix (ECM) proteins. BJcuL not only recognizes glycoligands on the surface of the neutrophil cell, but also promotes polarization and migration and improves adhesion to fibronectin and Matrigel that are components of the ECM. This lectin induces functional activation of neutrophils by increasing phagocytosis and superoxide production. Galatrox, a lectin from *Bothrops atrox* venom, promotes acute neutrophil migration and the release of IL-1 $\alpha$  and IL-6 cytokines. In addition, it recognizes neutrophil cell membrane glycoconjugates, interacts with ECM laminin, and induces neutrophil chemotaxis *in vitro* [243].

#### *Effects on kidney function*

In isolated rat kidneys, the lectins BiL (from *Bothrops insularis*), BpirL (from *Bothrops pirajai*), and BmLec (from *Bothrops moojeni*) induced alterations in renal function parameters, including perfusion pressure, vascular resistance, urinary flow, glomerular filtration rate, and ion transport in the tubules. The histological analysis of the kidneys of animals that received BiL suggests a direct lesion of the glomerular and tubular renal cells. The mechanism involves direct cytotoxicity in the glomerular region induced by lectins and the presence of systemic pro-inflammatory mediators such as prostaglandins [242].

# EFFECTS OF SNAKE VENOM ON THE HUMAN BODY

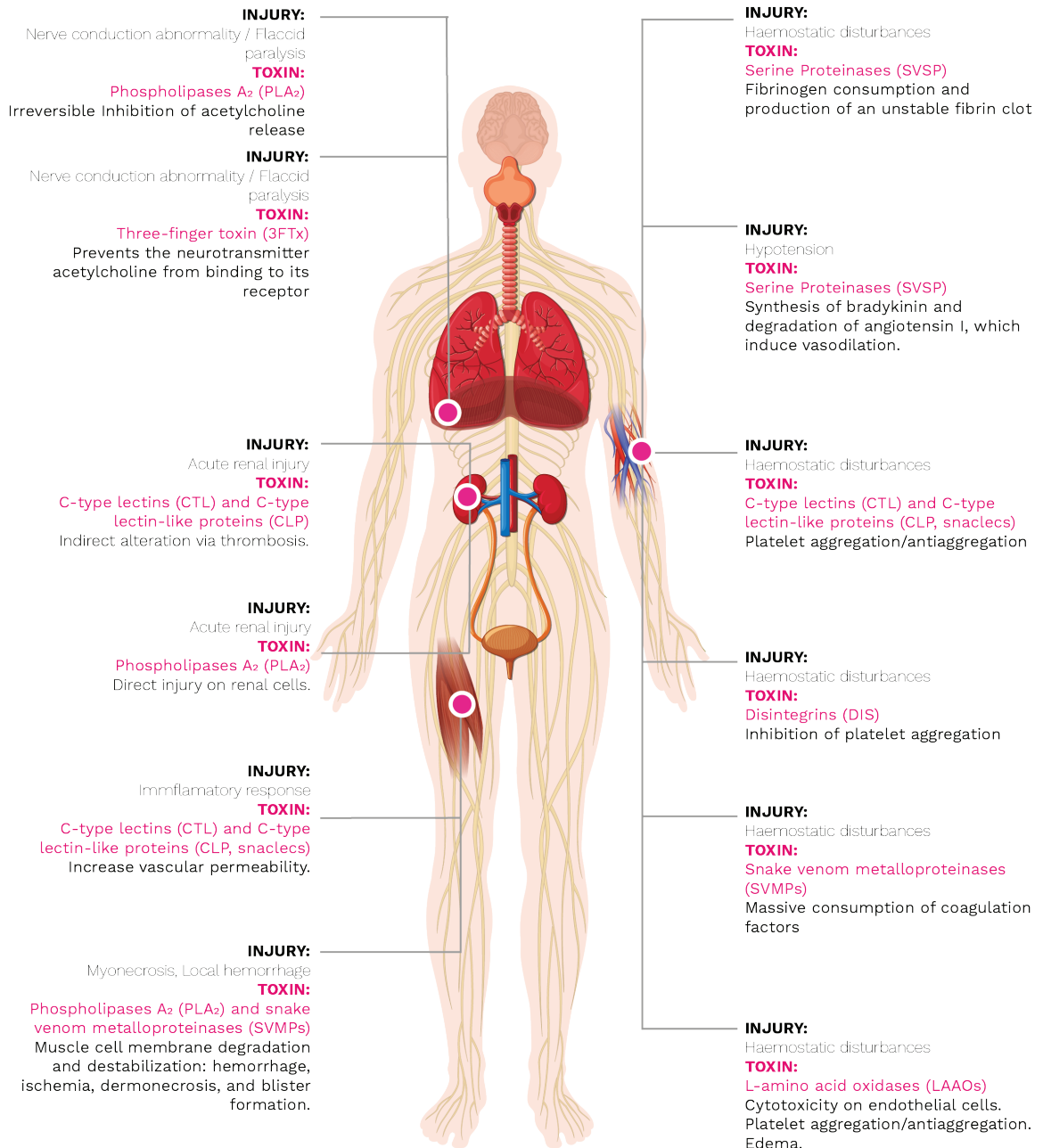


Figure 20. Effects of snake venom on the human body.

## 2.9. Minor proteins and peptides in snake venoms

The omic (proteomic, transcriptomic, and genomic) techniques, along with recent advances in chromatographic methods and bio-guided venom fractionation, have enabled the identification of peptides and proteins that are present in low quantities in snake venom. These substances include enzymes, proteins without enzymatic activity and peptides. The following sections will describe the role of some of these minor toxins in snakebite envenomation, as well as their potential biological activities.

### ***Hyaluronidases***

Hyaluronidases are enzymes found in snake venom that degrade hyaluronan, the principal glycosaminoglycan from the extracellular matrix (ECM) [7,248]. This degradation, combined with the cleavage of other components of ECM such as collagen fibers, laminin, nidogen, and perlecan by SVMPS, promotes the spreading of the other toxins at the bite site. This shows that, for example, a hyaluronidase from *Naja naja* increases the myotoxic activity of a PLA<sub>2</sub> and the hemorrhagic effect of a SVMP [249].

Snake venom hyaluronidase has the potential to generate low molecular mass fragments of hyaluronan that can activate the host's inflammatory response [250,251]. These same fragments may activate matrix metalloproteinases (MMPs) and increase damage to the extracellular matrix (ECM). Studies have shown that these moieties upregulate the expression of MMPs [252].

### ***Acetylcholinesterases***

Acetylcholinesterases are toxins that hydrolyze acetylcholine into choline and acetate. Human enzymes degrade the neurotransmitter in the synapses that is one mechanism for ending the signaling processes. Elapid snake venoms typically contain these enzymes, except for mambas that contain fasciculins, inhibitors of acetylcholinesterases [253,254]. These enzymes could contribute to the neurotoxicity induced by three-finger toxins and PLA<sub>2</sub>s (as discussed earlier in this chapter) by reducing the levels of acetylcholine in synapses and promoting the action of the toxins. However, this hypothesis requires further confirmation through additional research.

### ***Nucleotidases***

Nucleotidases are enzymes that degrade nucleotides into nucleosides. One sub-group of nucleotidases are the 5' nucleotidases that specifically catalyze the hydrolysis of phosphate esterified at carbon 5' of the ribose of the nucleotides. These enzymes have been isolated from snake venoms, and their principal biological activity is the inhibition of platelet aggregation [255–258]. Thus, this activity can contribute to platelet inhibition induced by other toxins, such as disintegrin, C-type lectins, PLA<sub>2</sub>s, and three-finger toxins. Adenosine is probably one of the nucleosides released. It can potentiate other activities, such as prey immobilization by activating neuronal adenosine A<sub>1</sub> receptors, suppressing acetylcholine release from motor neurons and excitatory neurotransmitters from central sites. Adenosine also exacerbates venom-induced hypotension by acti-

vating A<sub>2</sub> receptors in the vasculature. In addition, adenosine activates A<sub>3</sub> receptors on the mast cells that lead to the release of vasoactive substances and increase vascular permeability [259].

### **Phospholipase B (PLB)**

Phospholipase B hydrolyzes glycerophospholipids at the sn-1 and sn-2 positions [260]. These enzymes have been identified in snake venom proteomic studies and venom gland transcriptomic analyses, including from Colombian medically important species such as *Micrurus dumerillii*, *Bothrocophias myersi*, *Porthidium lansbergii*, and *Bothrops asper* [261–264]. The first report of these enzymes in snake venoms indicates that they induce hemolytic activity [265]. The PLBs possibly contribute to the lysis of red blood cells caused by other toxins. However, due to their low quantities in venoms, it has not been possible to identify other biological activities.

### **Cystein-rich secretory proteins (CRISPs)**

Several snake venoms contain cystein-rich secretory proteins that target ion channels such as BKCa channels (large-conductance calcium-activated potassium channels) and cyclic nucleotide-gated (CNG) ion channels [266,267]. In addition, CRISPs increase vascular permeability and inflammatory responses by activating leukocyte and neutrophil infiltration [289]. Therefore, CRISPs contribute to the edema-forming activities of other toxins, mainly PLA<sub>2</sub>s and SVMPs.

### **Growth factors**

Vascular endothelial growth factors (VEGFs) and nerve growth factors (NGFs) have been identified in snake venoms [269,270], but their role in snakebites is yet not fully elucidated. Studies have shown that NGFs and VEGF can induce changes in different cell lines. For instance, a NGF isolated from cobra venom was able to delay the growth of Ehrlich ascites carcinoma [292]. Additionally, another NGF from the cobra *Naja sputatrix* upregulates endogenous expression of NGF in PC12 cells, as well as pro-survival cell surface receptors and ion channels [293]. On the other hand, snake venom VEGFs induce hypotension, vascular permeability, and may lead to endothelial cell differentiation [266,273].

### **Proteinase inhibitors**

Several types of proteinases have been identified in snake venoms, including kazal, Kunitz, and tripeptide inhibitors; but their roles in snakebites have not been fully clarified. Kunitz-type proteinase inhibitors have antibleeding activity by inhibiting plasmin [274,275]. In addition, Kunitz inhibitors have been reported to exhibit antiangiogenic and anti-tumor activities [276]. On the other hand, a kazal-type inhibitor isolated from the venom of *Bothriechis schelegelii* did not display cytotoxic, hemorrhagic, or myotoxic effects. However, it did induce edema in the footpad of mice and inhibited the enzymatic activity of trypsin. This inhibitor may reduce the proteolytic activity while the venom is stored in the venom gland [277]. Some snake venoms contain tripeptide inhibitors that are potent SVMP inhibitors that may attenuate the proteolytic activity of metalloproteinases in the venom gland [278]. Other components identified in snake venoms include phosphodiesterases

[259,279,280], aminopeptidases [281], and Vesprins [282,283], among others. However, their roles in snakebites remain poorly understood.

## 6. Colombian snake proteomes

Venom in snakes facilitates their survival in an exclusive environment. Understanding snake venoms is a challenge due to the complexity of the toxins, their interrelationships, and the pathophysiological consequences of snakebite envenomation. Although venomous snake families share protein groups, each group has related proteins that vary in their amino acid sequence and abundance, contributing to differences in the overall biological activity of individual venoms. For instance, viperid venoms have high enzymatic activity that results in blood coagulation disturbances, while elapid venoms show predominantly neurotoxicity [57].

The biochemical characterization of venoms show that they are essentially mixtures of proteins and peptides that exhibit various biological activities [57]. The understanding of venoms and their properties has become more precise with the advancement of techniques and tools used for their study.

The analysis of venom initially involved chromatographic studies added to one-dimensional polyacrylamide gel electrophoresis, revealing large protein groups. This provided a baseline for more specific studies. With the advent of liquid chromatography associated with mass spectrometry techniques, two-dimensional electrophoresis, and sequencing methods, a global approach was carried out. This allowed for the visualization of the complexity of the venoms and the individual characterization of proteins.

There are effective methods for handling raw venoms. One such involves simplifying the venom prior to conducting mass spectrometry and integrating it with Edman's degradation sequence analysis [32]. Another way to analyze the venom is through direct or shotgun approaches, using liquid chromatography coupled to tandem mass spectrometry. Alternatively, indirect approaches involve analyzing the chromatographic fractions obtained from the crude venom or from the spots resulting from two-dimensional (2-D) electrophoresis.

The method of choice depends on the research question. The total number of unique proteins in the 2-D electrophoresis gel is typically higher than the number determined by direct analysis of the venom through mass spectrometry. Each spot may contain more than one protein. This is related due to the complexity of venoms, the presence of multiple isoforms, and post-translational modifications of proteins, rather than the presence of many different proteins [57].

An example of a methodology for separating venom components is proposed below using crotamine of the venom of *C. d. cumanensis* as a model (Figure 21). In step 1, the venom is separated in each component by using chromatographic methods; then a fraction is selected and taken to enzy-

matic digestion in step 2. Using different techniques like mass spectrometry or Edman sequencing the resulting peptides are overlapping to obtain the primary structure. The study of the resulting peptides can also provide information on different forms (isoforms or proteoforms) of a protein. By using specialized bioinformatics servers, the sequence can be used to predict a tridimensional model of the protein (step 3). Step 4 stands for an alternative way to identify the sequence by selecting the fraction and submitting it to sodium dodecyl sulfate–polyacrylamide gel electrophoresis (SDS-PAGE) to verify its purity. Thus, the band is excised from the gel to be digested enzymatically (step 5), and the identification and modelling are done as previously described in the steps 2 and 3. Step 6 remarks the use of the separated fraction to directly determine molecular mass by mass spectrometry.

An alignment using the Basic Local Alignment Search Tool (BLAST) was performed using the sequences from peptides obtained after enzymatic digestion that allowed for alignment with the crotoamine from *Crotalus durissus terrificus* (Brazilian populations). This sequence was then used to predict the three-dimensional structure using SWISS MODEL Software [228]. Additionally, these techniques have been used to compare venoms, determine genetic, ecological, and geographic variations, and even to build phylogenetic hypothesis of the species that produce specific toxins [57,284,285].

Reverse phase liquid chromatography is the most used technique for intact protein separation. However, it cannot isolate various forms of proteins (proteoforms) due to the variation in their physicochemical properties. Therefore, other separation methods based on hydrophobicity, hydrophilic interaction, charge, size and affinity, are also employed [286]. Even other techniques, such as electrophoresis and isoelectric focusing, have been described as possible alternatives [287].

However, these separation techniques may not always effectively resolve complex proteomes. In contrast, top-down proteomic strategies can be used to identify and characterize proteins by fragmenting intact proteins, rather than measuring peptides produced from proteins through tryptic digestion procedures [198]. Direct analysis of intact proteins provides enriched data, covering nearly the complete protein sequence, and enables identification of proteoforms and the localization of modifications [288]. Currently, this technique is limited to low and medium-size proteins. However, it will probably be used for larger protein complexes in the near future.

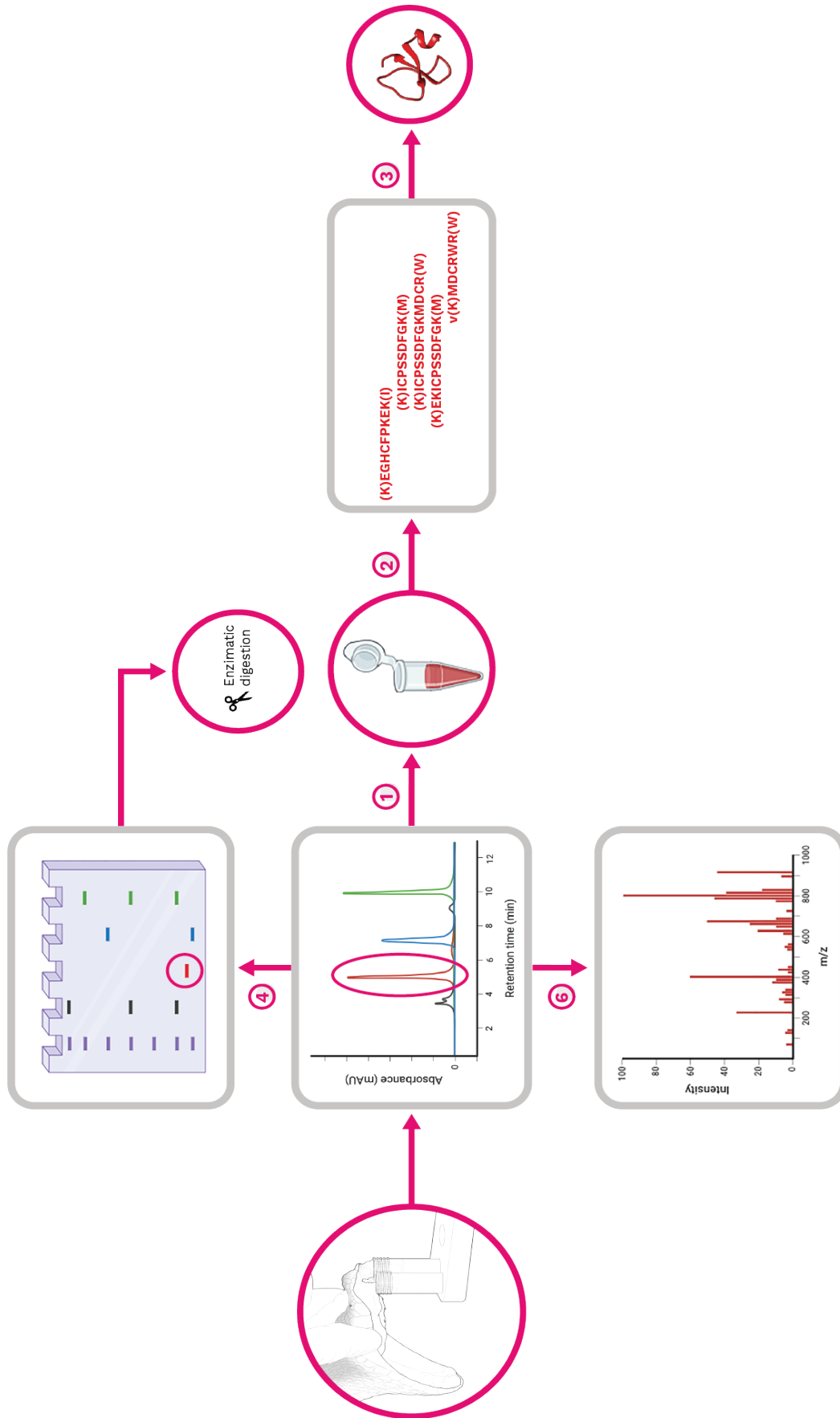


**Figure 21.** Schematic representation of a complete venom approach, using the venom of *Crotalus durissus* (Colombian populations) and its crotamine as an example. The venom initially obtained is separated into fractions using RP-HPLC technique.

Snake venom proteomes are typically represented graphically as pie charts, displaying the abundance percentage of each protein family and its relation to the venom's overall activity (See Chapter 3). In Colombia, the venom of vipers (Figure 22), shows a higher concentration of metalloproteinases in juvenile *Bothrops asper* specimens that tends to decrease in adult individuals. This difference is compensated by a slight increase in the presence of PLA<sub>2</sub>, serine proteinases, and L-amino acid oxidases [289]. In the venom of *Bothrops atrox*, metalloproteinases represent almost 50% of the proteome. While PLA<sub>2</sub> is also present, it is worth noting that the venom contains duplicate amounts of serine proteinases and L-amino acid oxidases compared to its Brazilian counterpart [290].

*Porthidium lansbergii* venom maintains the 2:1 ratio between metalloproteinases and PLA<sub>2</sub>, but it also contains a significant amount of disintegrins and C-type lectins (13% and 7%, respectively) [291]. Although the venom of *P. lansbergii* is rich in these components, studies of their biotechnological applications are still in their early stages [292]. In contrast, the venom of *Bothrocophias myersi* (Equis red snake) is mainly composed of PLA<sub>2</sub> and SVMPs (54% and 21.4%, respectively) [284]. The venoms of other vipers, such as *Bothrocophias campbelli* (Chocoan toadhead pitviper) contain less than 1% disintegrins [198] or the venom from *Crotalus durissus*, which have 1.18% of C-type lectins in its proteome [293].

Particularly, the venom of *C. durissus* is composed of over 60% crotoxin, a neurotoxic PLA<sub>2</sub>, and 6% crotoamine, a low molecular weight myotoxin that is typical of rattlesnakes [293] (Figure 22). In contrast, *Lachesis acrochorda* (Chocoan Bushmaster) has a predominance of serine proteinases, followed by metalloproteinases and vasoactive peptides, including uncommon toxins like bradykinin-potentiating peptides (BPP) and C-type natriuretic peptide (C-NP) [294].

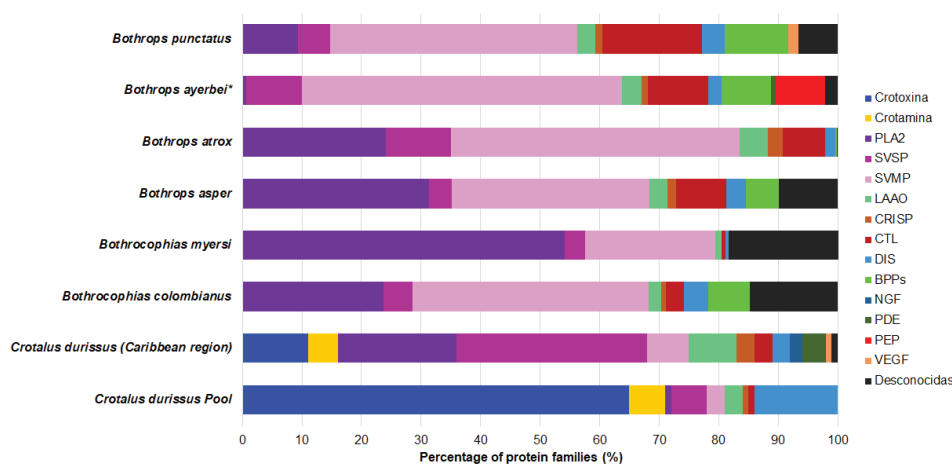
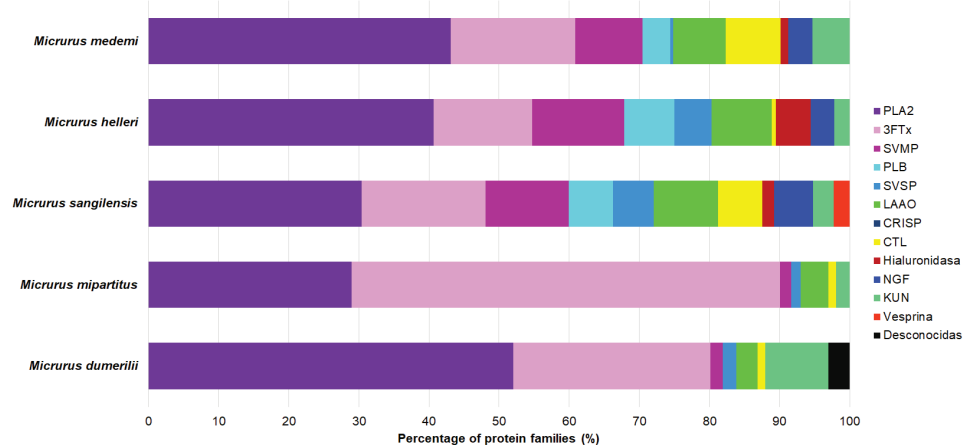


**Figure 22.** Toxin representativeness in the venom proteomes of Colombian pitviper snakes with available data. BPPs: bradykinin-potentiating peptides; PLA<sub>2</sub>: phospholipase A<sub>2</sub>; SVSP: snake venom serine proteinase; SVMP: snake venom metalloproteinase; LAAO: L-amino acid oxidase; CRISP: cysteine-rich secretory protein; CTL: C-type lectins and lectin-like; DIS: disintegrin; NGF: nerve growth factor; VEGF: vascular endothelium growth factor; PEP: other peptides; UNK: unknown; Crotoxin: A crystalline phospholipase A<sub>2</sub> type neurotoxin obtained from rattlesnake venom of the genus *Crotalus*; Crotoamine: A low molecular weight myotoxin from rattlesnake venom of the genus *Crotalus*. Species venom proteomes were retrieved from [81,290,293,295–297].

Only eight species of Colombian elapids have proteomic characterizations available. When considering the dichotomy of 3FTx-PLA<sub>2</sub>, in the venom of *Micrurus mipartitus*, 3FTxs predominate with 61% [285], while for *M.*

*dumerilii*, *M. helleri*, *M. medemi*, and *M. sangilensis* 52%, 41%, 43% and 30% of the proteome is represented by PLA<sub>2</sub>, respectively [264], which includes significant proportions of Kunitz peptides for *M. dumerilii* and metalloproteinases for *M. helleri*, *M. medemi*, and *M. sangilensis* (Figure 23). The venom of the pelagic yellow-bellied sea snake *Hydrophis platurus* from the Costa Rican population contains approximately 50% 3FTx, compared to 33% PLA<sub>2</sub> [297]. However, no Colombian population has been yet characterized.

**Figure 23.** Toxin representativeness in the venom proteomes of Colombian Coral snakes with available data. PLA<sub>2</sub>: phospholipase A<sub>2</sub>; SVSP: snake venom serine proteinases; SVMP: snake venom metalloproteinases; LAAO: L-amino acid oxidase; CRISP: cysteine-rich secretory protein; CTL: C-type lectins and lectin-like; 3FTx: three-finger toxins; KUN: Kunitz peptides. Species venom proteomes were retrieved from [264,285].



Although the characterization of venom proteomes from Colombian snake species has increased, further studies are needed. Due to low encounter rates, cryptic habitats, and high species richness, most venoms from medically important snakes in Colombia lack proteomic characterization, with coral snakes (*Micrurus*) showing the greatest knowledge gap. In this way, identifying the main toxins from the venom of each species will allow us to understand the pathophysiological activities of each component and their potential applications in biotechnology and medicine.

### Potential uses of snake venoms

Snake venoms are complex mixtures containing toxins that target several physiological processes. They have been recognized as sources of bioactive molecules since the discovery and development of captopril (see Chapter 10). There have been successful cases in which drugs have been produced from snake toxins. For instance, Tirofiban is a drug used to inhibit platelet aggregation in acute coronary syndromes. The disintegrin identified in the venom of *Echis carinatus* was modified and formulated to develop this drug [298].

Snake venoms are also useful for studying biological processes. For instance, batroxobin is used for diagnostic purposes in clinical chemistry. Reptilase (Reptilase®, Pentapharm, Basel, Switzerland) is an alternative to thrombin time in samples that contain heparin or to diagnose hypofibrinogenemia [299]. Venoms are important sources of bioactive compounds that have potential as lead compounds for drug development or as molecules for studying some biological processes (see Chapter 10).

## Appendix: Material and Methods

### *Visualization of the Secondary Structure of Toxins in 3D*

In this chapter, the study of toxins is approached from their secondary structure. For accurate visualization, regions with secondary structures are selectively colored: alpha helices (in magenta), beta sheets (in green/yellow), turns, and random structures (in white).

A schematic visualization mode was chosen to showcase the Richardson representation (MolScript). This method resembles the ribbon model but uses arrowheads to indicate the orientation of strands and helices, while segments lacking secondary structure are depicted as cords rather than ribbons [301,302].

In some proteins, or specific regions within them, there are insufficient interactions to distinguish any level of organization beyond the primary structure. In such cases, this is referred to as a random coil conformation.

When the main chain or backbone of a polypeptide folds into a right-handed helical shape, it adopts a conformation known as an alpha helix. Conversely, when the polypeptide's backbone is stretched to its maximum covalent bond length, it assumes a spatial configuration known as a beta structure (beta sheet), typically represented by arrows [302]. Beta sheets can be parallel (when strands run in the same direction) or anti-parallel (when strands run in opposite directions).

Polypeptide chain sequences with alpha or beta structures are often connected by beta turns. These are short sequences with a characteristic conformation that imposes a sharp 180-degree turn on the polypeptide backbone.

The 3D toxin models were obtained from the Protein Data Bank (PDB), downloaded in Wavefront format (.obj), and subsequently optimized using Blender [303,304]. They were then imported into Jmol to generate the schematic-style pattern and exported in 3D VRML format [305]. Finally, the models were imported into the Sketchfab platform to generate the HTML visualization code [306].

## References

1. Kardong, K.; Lavin-Murcio, P. Venom Delivery of Snakes as High-Pressure and Low-Pressure Systems. *Copeia* **1993**, *3*, 644–650, doi:10.2307/1447225
2. Broeckhoven, C.; Du Plessis, A. Has Snake Fang Evolution Lost Its Bite? New Insights from a Structural Mechanics Viewpoint. *Biol Lett* **2017**, *13*, doi:10.1098/rsbl.2017.0293.
3. Vidal, N. Colubroid Systematics: Evidence for an Early Appearance of the Venom Apparatus Followed by Extensive Evolutionary Tinkering. *J Toxicol Toxin Rev* **2002**, *21*, 21–41.
4. Kardong, K. V The Evolution of the Venom Apparatus in Snakes from Colubrids to Viperids & Elapids. *Mem. Inst. Butantan* **1982**, *4*, 106–118.
5. Weinstein, S.A.; Smith, T.L.; Kardong, K. V Reptil Venom Glands: Form, Function, and Future. In *Handbook of venoms and toxins of reptiles*; Mackessy, S.P., Ed.; CRC Press: Boca Raton, **2010**; pp. 65–91 ISBN 978-0-8493-9165-1.
6. Vonk, F.J.; Admiraal, J.F.; Jackson, K.; Reshef, R.; De Bakker, M.A.G.; Vanderschoot, K.; Van Den Berge, I.; Van Atten, M.; Burgerhout, E.; Beck, A.; et al. Evolutionary Origin and Development of Snake Fangs. *Nature* **2008**, *454*, 630–633, doi:10.1038/nature07178.
7. Deufel, A.; Cundall, D. Functional Plasticity of the Venom Delivery System in Snakes with a Focus on the Poststrike Prey Release Behavior. *Zool Anz* **2006**, *245*, 249–267, doi: 10.1016/j.jcz.2006.07.002.
8. Glaudas, X.; Kearney, T.C.; Alexander, G.J. To Hold or Not to Hold? The Effects of Prey Type and Size on the Predatory Strategy of a Venomous Snake. *J Zool* **2017**, *302*, 211–218, doi:10.1111/jzo.12450.
9. Mackessy, S. *Handbook of Venoms and Toxins of Reptiles*; Mackessy, S., Ed.; CRC Press, **2016**; ISBN 9780429186394.
10. Arbuckle, K. Evolutionary Context of Venom in Animals. In *Evolution of Venomous Animals and Their Toxins*; Gopalakrishnakone, P., Malhotra, A., Eds.; Springer: Dordrecht, **2017**; pp. 3–31 ISBN 978-94-007-6458-3.
11. Bock, W.J. The Definition and Recognition of Biological Adaptation. *Am Zool* **1980**, *20*, 217–227.
12. Wexler, P.; Fonger, G.C.; White, J.; Weinstein, S. Toxinology: Taxonomy, Interpretation, and Information Resources. *Sci Technol Libr (New York, NY)* **2015**, *34*, 67–90, doi:10.1080/0194262X.2014.993788.
13. Mebs, D. *Venomous and Poisonous Animals: A Handbook for Biologists, Toxicologists and Toxinologists, Physicians and Pharmacists*; Medpharm Scientific Publ., **2002**; ISBN 9783804750234.
14. Vetter, R.S.; Schmidt, J.O. Semantics of Toxinology. *Toxicon* **2006**, *48*.
15. Casewell, N.R.; Jackson, T.N.W.; Laustsen, A.H.; Sunagar, K. Causes and Consequences of Snake Venom Variation. *Trends Pharmacol Sci* **2020**, *41*.
16. Hiestand, P.C.; Hiestand, R.R. *Dispholidus typus* (Boomslang) Snake Venom: Purification and Properties of the Coagulant Principle. *Toxicon* **1979**, *17*, doi:10.1016/0041-0101(79)90282-4.
17. Lomonte, B.; Cerdas, L.; Solórzano, A.; Martínez, S. El Suero de Neonatos de *Clelia clelia* (Serpentes: Colubridae) Neutraliza La Acción Hemorrágica Del Veneno de *Bothrops asper* (Serpentes: Viperidae). *Revista Biol. Trop.* **1989**, *38*, 325–326.

18. Kazandjian, T.D.; Petras, D.; Robinson, S.D.; van Thiel, J.; Greene, H.W.; Arbuckle, K.; Barlow, A.; Carter, D.A.; Wouters, R.M.; Whiteley, G.; et al. Convergent Evolution of Pain-Inducing Defensive Venom Components in Spitting Cobras. *Science (1979)* **2021**, *371*, 386–390, doi:10.1126/science.abb9303.
19. Amazonas, D.R.; Portes-Junior, J.A.; Nishiyama-Jr, M.Y.; Nicolau, C.A.; Chalkidis, H.M.; Mourão, R.H.V.; Graziotin, F.G.; Rokyta, D.R.; Gibbs, H.L.; Valente, R.H.; et al. Molecular Mechanisms Underlying Intra-specific Variation in Snake Venom. *J Proteomics* **2018**, *181*, 60–72, doi:10.1016/j.jprot.2018.03.032.
20. Chippaux, J.P.; Williams, V.; White, J. Snake Venom Variability: Methods of Study, Results and Interpretation. *Toxicon* **1991**, *29*, 1279–1303.
21. Chippaux, J.P.; Goyffon, M. Venoms, Antivenoms and Immunotherapy. *Toxicon* **1998**, *36*, 823–846, doi:10.1016/S0041-0101(97)00160-8.
22. Lomonte, B.; Rangel, J. Snake Venom Lys49 Myotoxins: From Phospholipases A<sub>2</sub> to Non-Enzymatic Membrane Disruptors. *Toxicon* **2012**, *60*, 520–530, doi: 10.1016/j.toxicon.2012.02.007.
23. Vélez, S.M.; Salazar, M.; Acosta de Patiño, H.; Gómez, L.; Rodríguez, A.; Correa, D.; Saldaña, J.; Navarro, D.; Lomonte, B.; Otero-Patiño, R.; et al. Geographical Variability of the Venoms of Four Populations of *Bothrops asper* from Panama: Toxicological Analysis and Neutralization by a Polyvalent Antivenom. *Toxicon* **2017**, *132*, 55–61, doi: 10.1016/j.toxicon.2017.04.002.
24. Tasoulis, T.; Isbister, G.K. A Review and Database of Snake Venom Proteomes. *Toxins (Basel)* **2017**, doi:10.3390/toxins9090290.
25. Aminoff, M.J.; So, Y.T. Effects of Toxins and Physical Agents on the Nervous System. In *Neurology in Clinical Practice*; Elsevier, **2012**; pp. 1353–1376.
26. Thornton, S.L. Snakes. In *Encyclopedia of Toxicology: Third Edition*; Academic Press, **2014**; pp. 310–312 ISBN 9780123864543.
27. Rolan, T.D. Neurotoxic Snakes of the Americas. *Neurol Clin Pract* **2015**, *5*, 383–388, doi:10.1212/CPJ.0000000000000180.
28. Castro, E.N.; Lomonte, B.; del Carmen Gutiérrez, M.; Alagón, A.; Gutiérrez, J.M. Intraspecific Variation in the Venom of the Rattlesnake *Crotalus Simus* from Mexico: Different Expression of Crotoxin Results in Highly Variable Toxicity in the Venoms of Three Subspecies. *J Proteomics* **2013**, *87*, 103–121, doi:10.1016/j.jprot.2013.05.024.
29. Sunagar, K.; Undheim, E.A.B.; Scheib, H.; Gren, E.C.K.; Cochran, C.; Person, C.E.; Koludarov, I.; Kelln, W.; Hayes, W.K.; King, G.F.; et al. Intraspecific Venom Variation in the Medically Significant Southern Pacific Rattlesnake (*Crotalus oeganus helleri*): Biodiscovery, Clinical and Evolutionary Implications. *J Proteomics* **2014**, *99*, 68–83, doi:10.1016/j.jprot.2014.01.013.
30. Gutiérrez, J.M.; Rucavado, A. Snake Venom Metalloproteinases: Their Role in the Pathogenesis of Local Tissue Damage. *Biochimie* **2000**, *82*, 841–850, doi:10.1016/S0300-9084(00)01163-9.
31. Estêvão-Costa, M.I.; Diniz, C.R.; Magalhães, A.; Markland, F.S.; Sanchez, E.F. Action of Metalloproteinases Mutalysin I and II on Several Components of the Hemostatic and Fibrinolytic Systems. *Thromb Res* **2000**, *99*, 363–376, doi:10.1016/S0049-3848(00)00259-0.

32. Calvete, J.J.; Escolano, J.; Sanz, L. Snake Venomics of *Bitis* Species Reveals Large Intra-genus Venom Toxin Composition Variation: Application to Taxonomy of Congeneric Taxa. *J Proteome Res* **2007**, *6*, 2732–2745, doi:10.1021/pr0701714.
33. Mackessy, S.P. Evolutionary Trends in Venom Composition in the Western Rattlesnakes (*Crotalus viridis* sensu lato): Toxicity vs. Tenderizers. *Toxicon* **2010**, *55*, 1463–1474, doi: 10.1016/j.toxicon.2010.02.028.
34. Salazar, A.M.; Guerrero, B.; Cantu, B.; Cantu, E.; Rodríguez-Acosta, A.; Pérez, J.C.; Galán, J.A.; Tao, A.; Sánchez, E.E. Venom Variation in Hemostasis of the Southern Pacific Rattlesnake (*Crotalus oreganus helleri*): Isolation of Hellerase. *Comparative Biochemistry and Physiology - C Toxicology and Pharmacology* **2009**, *149*, 307–316, doi: 10.1016/j.cbpc.2008.08.007.
35. Lomonte, B.; Escolano, J.; Fernández, J.; Sanz, L.; Angulo, Y.; Gutiérrez, J.M.; Calvete, J.J. Snake Venomics and Antivenomics of the Arboreal Neotropical Pitvipers *Bothriechis lateralis* and *Bothriechis schlegelii*. *J Proteome Res* **2008**, *7*, 2445–2457, doi:10.1021/pr8000139.
36. Boldrini-França, J.; Corrêa-Netto, C.; Silva, M.M.S.; Rodrigues, R.S.; De La Torre, P.; Pérez, A.; Soares, A.M.; Zingali, R.B.; Nogueira, R.A.; Rodrigues, V.M.; et al. Snake Venomics and Antivenomics of *Crotalus durissus* Subspecies from Brazil: Assessment of Geographic Variation and Its Implication on Snakebite Management. *Proteomics* **2010**, *73*, 1758–1776, doi: 10.1016/j.jprot.2010.06.001.
37. Fry, B.G.; Wickramaratna, J.C.; Hodgson, W.C.; Alewood, P.F.; Kini, R.M.; Ho, H.; Wüster, W. Electrospray Liquid Chromatography/Mass Spectrometry Fingerprinting of Acanthophis (Death Adder) Venoms: Taxonomic and Toxinological Implications. *Rapid Communications in Mass Spectrometry* **2002**, *16*, 600–608, doi:10.1002/rcm.613.
38. Daltry, J.C.; Wüster, W.; Thorpe, R.S. Diet and Snake Venom Evolution. *Nature* **1996**, *379*, 537–542, doi:10.1038/379537a0.
39. Sasa, M. Diet and Snake Venom Evolution: Can Local Selection Alone Explain Intraspecific Venom Variation? *Toxicon* **1999**, *37*, 249–252, doi:10.1016/S0041-0101(98)00121-4.
40. Hartmann, P.A.; Hartmann, M.T.; Martins, M. Ecology of a Snake Assemblage in the Atlantic Forest of Southeastern Brazil. *Pap Avulsos Zool* **2009**, *49*, 343–360, doi:10.1590/s0031-10492009002700001.
41. Daltry, J.C.; Ponnudurai, G.; Shin, C.K.; Tan, N.H.; Thorpe, R.S.; Wüster, W. Electrophoretic Profiles and Biological Activities: Intraspecific Variation in the Venom of the Malayan Pit Viper (*Calloselasma rhodostoma*). *Toxicon* **1996**, *34*, 67–79, doi:10.1016/0041-0101(95)00122-0.
42. Calvete, J.J.; Sanz, L.; Pérez, A.; Borges, A.; Vargas, A.M.; Lomonte, B.; Angulo, Y.; Gutiérrez, J.M.; Chalkidis, H.M.; Mourão, R.H.V.; et al. Snake Population Venomics and Antivenomics of *Bothrops atrox*: Paedomorphism along Its Transamazonian Dispersal and Implications of Geographic Venom Variability on Snakebite Management. *J Proteomics* **2011**, *74*, 510–527, doi:10.1016/j.jprot.2011.01.003.
43. Silva, F.M. da; Oliveira, L.S. de; Nascimento, L.R. de S.; Machado, F.A.; Prudente, A.L. da C. Sexual Dimorphism and Ontogenetic Changes of Amazonian Pit Vipers (*Bothrops atrox*). *Zool Anz* **2017**, *271*, 15–24, doi:10.1016/j.jcz.2017.11.001.

44. Gutiérrez, J.; Lomonte, B. Phospholipase A2 Myotoxins from *Bothrops* Snake Venoms. *Toxicon* **1995**, *33*, 1405–1424.
45. López-Lozano, J.L.; de Sousa, M.V.; Ricart, C.A.O.; Chávez-Olortegui, C.; Flores Sanchez, E.; Muniz, E.G.; Bührnheim, P.F.; Morhy, L. Ontogenetic Variation of Metalloproteinases and Plasma Coagulant Activity in Venoms of Wild *Bothrops atrox* Specimens from Amazonian Rain Forest. *Toxicon* **2002**, *40*, 997–1006, doi:10.1016/S0041-0101(02)00096-X.
46. da Silva Aguiar, W.; da Costa Galizio, N.; Sant'Anna, S.S.; Silveira, G.P.M.; de Souza Rodrigues, F.; Grego, K.F.; de Moraes-Zani, K.; Tanaka-Azevedo, A.M. Ontogenetic Study of *Bothrops jararacussu* Venom Composition Reveals Distinct Profiles. *Toxicon* **2020**, *186*, 67–77, doi: 10.1016/j.toxicon.2020.07.030.
47. Antunes, T.C.; Yamashita, K.M.; Barbaro, K.C.; Saiki, M.; Santoro, M.L. Comparative Analysis of Newborn and Adult *Bothrops jararaca* Snake Venoms. *Toxicon* **2010**, *56*, 1443–1458, doi: 10.1016/j.toxicon.2010.08.011.
48. Menezes, M.C.; Furtado, M.F.; Travaglia-Cardoso, S.R.; Camargo, A.C.M.; Serrano, S.M.T. Sex-Based Individual Variation of Snake Venom Proteome among Eighteen *Bothrops jararaca* Siblings. *Toxicon* **2006**, *47*, 304–312, doi:10.1016/j.toxicon.2005.11.007.
49. Chippaux, J.P.; Boche, J.; Courtois, B. Electrophoretic Patterns of the Venoms from a Litter of *Bitis gabonica* Snakes. *Toxicon* **1982**, *20*, 521–522, doi:10.1016/0041-0101(82)90019-8.
50. Williams, V.; White, J.; Schwaner, T.D.; Sparrow, A. Variation in Venom Proteins from Isolated Populations of Tiger Snakes (*Notechis ater niger*, *N. scutatus*) in South Australia. *Toxicon* **1988**, *26*, 1067–1075, doi:10.1016/0041-0101(88)90205-X.
51. Fry, B.G.; Scheib, H.; van der Weerd, L.; Young, B.; McNaughtan, J.; Ryan Ramjan, S.F.; Vidal, N.; Poelmann, R.E.; Norman, J.A. Evolution of an Arsenal: Structural and Functional Diversification of the Venom System in the Advanced Snakes (*Caenophidia*). *Molecular and Cellular Proteomics* **2008**, *7*, 215–246, doi:10.1074/mcp.M700094-MCP200.
52. Gutiérrez, J.M.; Escalante, T.; Rucavado, A.; Herrera, C. Hemorrhage Caused by Snake Venom Metalloproteinases: A Journey of Discovery and Understanding. *Toxins (Basel)* **2016**, *8*, 93, doi:10.3390/toxins8040093.
53. Gutiérrez, J.M.; Rucavado, A.; Escalante, T.; Díaz, C. Hemorrhage Induced by Snake Venom Metalloproteinases: Biochemical and Biophysical Mechanisms Involved in Microvessel Damage. *Toxicon* **2005**, *45*, 997–1011, doi: 10.1016/j.toxicon.2005.02.029.
54. Takeda, S. ADAM and ADAMTS Family Proteins and Snake Venom Metalloproteinases: A Structural Overview. *Toxins (Basel)* **2016**, *8*, doi:10.3390/TOXINS8050155.
55. Gomis-Rüth, F.X. Structural Aspects of the Metzincin Clan of Metalloendopeptidases. *Mol Biotechnol* **2003**, *24*, 157–202, doi:10.1385/MB:24:2:157.
56. Bode, W.; Gomis-Rüth, F.X.; Stöckler, W. Astacins, Serralysins, Snake Venom and Matrix Metalloproteinases Exhibit Identical Zinc-Binding Environments (HEXXHXXGXXH and Met-Turn) and Topologies and Should Be Grouped into a Common Family, the “Metzincins.” *FEBS Lett* **1993**, *331*, 134–140, doi:10.1016/0014-5793(93)80312-i.

57. Fox, J.W.; Serrano, S.M.T. Insights into and Speculations about Snake Venom Metalloproteinase (SVMP) Synthesis, Folding and Disulfide Bond Formation and Their Contribution to Venom Complexity. *FEBS J* **2008**, *275*, 3016–3030, doi:10.1111/j.1742-4658.2008.06466. x.
58. Olaoba, O.T.; Karina Dos Santos, P.; Selistre-de-Araujo, H.S.; Ferreira de Souza, D.H. Snake Venom Metalloproteinases (SVMs): A Structure-Function Update. *Toxicon X* **2020**, *7*, 100052, doi: 10.1016/j.toxcx.2020.100052.
59. Takeda, S.; Takeya, H.; Iwanaga, S. Snake Venom Metalloproteinases: Structure, Function and Relevance to the Mammalian ADAM/ADAMTS Family Proteins. *Biochim Biophys Acta* **2012**, *1824*, 164–176, doi:10.1016/j.bbapap.2011.04.009.
60. Tallant, C.; Marrero, A.; Gomis-Rüth, F.X. Matrix Metalloproteinases: Fold and Function of Their Catalytic Domains. *Biochim Biophys Acta* **2010**, *1803*, 20–28, doi: 10.1016/j.bbamcr.2009.04.003.
61. Coronado, M.A.; de Moraes, F.R.; Ullah, A.; Masood, R.; Santana, V.S.; Mariutti, R.; Brognaro, H.; Georgieva, D.; Murakami, M.T.; Betzel, C.; et al. Three-Dimensional Structures and Mechanisms of Snake Venom Serine Proteinases, Metalloproteinases, and Phospholipase A<sub>2</sub>s. In *Venom Genomics and Proteomics*; Gopalakrishnakone, P., Calvete, J.J., Eds.; Toxinology; Springer Netherlands: Dordrecht, **2016**; pp. 239–267 ISBN 978-94-007-6416-3.
62. Escalante, T.; Rucavado, A.; Pinto, A.F.M.; Terra, R.M.S.; Gutiérrez, J.M.; Fox, J.W. Wound Exudate as a Proteomic Window to Reveal Different Mechanisms of Tissue Damage by Snake Venom Toxins. *J Proteome Res* **2009**, *8*, 5120–5131, doi:10.1021/pr900489m.
63. Escalante, T.; Ortiz, N.; Rucavado, A.; Sanchez, E.F.; Richardson, M.; Fox, J.W.; Gutiérrez, J.M. Role of Collagens and Perlecan in Microvascular Stability: Exploring the Mechanism of Capillary Vessel Damage by Snake Venom Metalloproteinases. *PLoS One* **2011**, *6*, e28017, doi: 10.1371/journal.pone.0028017.
64. Moreira, L.; Borkow, G.; Ovadia, M.; Gutiérrez, J.M. Pathological Changes Induced by BaH1, a Hemorrhagic Proteinase Isolated from *Bothrops asper* (Terciopelo) Snake Venom, on Mouse Capillary Blood Vessels. *Toxicon* **1994**, *32*, 976–987, doi:10.1016/0041-0101(94)90376-x.
65. Ohsaka, A. Hemorrhagic, Necrotizing and Edema-Forming Effects of Snake Venoms. In *Handbook of Experimental Pharmacology*; Springer Verlag: Berlin, Germany, **1979**; Vol. 52, Snake, pp. 480–546.
66. Araki, S. Endothelial Cell Toxicity of Vascular Apoptosis-Inducing Proteins from Hemorrhagic Snake Venom. In *Snake Venoms*; Inagaki, H., Vogel, C.-W., Mukherjee, A.K., Rahmy, T.R., Gopalakrishnakone, P., Eds.; Toxinology; Springer Netherlands: Dordrecht, **2017**; pp. 145–159 ISBN 978-94-007-6410-1.
67. Díaz, C.; Valverde, L.; Brenes, O.; Rucavado, A.; Gutiérrez, J.M. Characterization of Events Associated with Apoptosis/Anoikis Induced by Snake Venom Metalloproteinase BaP<sub>1</sub> on Human Endothelial Cells. *J Cell Biochem* **2005**, *94*, 520–528, doi:10.1002/jcb.20322.
68. Wan, S.-G.; Jin, Y.; Lee, W.-H.; Zhang, Y.A. Snake Venom Metalloproteinase That Inhibited Cell Proliferation and Induced Morphological Changes of ECV304 Cells. *Toxicon* **2006**, *47*, 480–489, doi:10.1016/j.toxicon.2006.01.006.

69. Wang, S.H.; Shen, X.C.; Yang, G.Z.; Wu, X.F. CDNA Cloning and Characterization of Agkistin, a New Metalloproteinase from *Agkistrodon halys*. *Biochem Biophys Res Commun* **2003**, *301*, 298–303, doi:10.1016/S0006-291X(02)03001-2.
70. You, W.-K.; Seo, H.-J.; Chung, K.-H.; Kim, D.-S. A Novel Metalloproteinase from *Gloydius halys* Venom Induces Endothelial Cell Apoptosis through Its Protease and Disintegrin-like Domains. *J Biochem* **2003**, *134*, 739–749, doi:10.1093/jb/mvg202.
71. Rucavado, A.; Núñez, J.; Gutiérrez, J.M. Blister Formation and Skin Damage Induced by BaP1, a Haemorrhagic Metalloproteinase from the Venom of the Snake *Bothrops asper*. *Int J Exp Pathol* **1998**, *79*, 245–254.
72. Moura-da-Silva, A.M.; Marcinkiewicz, C.; Marcinkiewicz, M.; Niewiarowski, S. Selective Recognition of Alpha2beta1 Integrin by Jararhagin, a Metalloproteinase/Disintegrin from *Bothrops jararaca* Venom. *Thromb Res* **2001**, *102*, 153–159, doi:10.1016/S0049-3848(01)00216-x.
73. Baldo, C.; Jamora, C.; Yamanouye, N.; Zorn, T.M.; Moura-da-Silva, A.M. Mechanisms of Vascular Damage by Hemorrhagic Snake Venom Metalloproteinases: Tissue Distribution and in Situ Hydrolysis. *PLoS Negl Trop Dis* **2010**, *4*, e727, doi: 10.1371/journal.pntd.0000727.
74. Herrera, C.; Escalante, T.; Voisin, M.-B.; Rucavado, A.; Morazán, D.; Macêdo, J.K.A.; Calvete, J.J.; Sanz, L.; Nourshargh, S.; Gutiérrez, J.M.; et al. Tissue Localization and Extracellular Matrix Degradation by PI, PII and PIII Snake Venom Metalloproteinases: Clues on the Mechanisms of Venom-Induced Hemorrhage. *PLoS Negl Trop Dis* **2015**, *9*, e0003731, doi: 10.1371/journal.pntd.0003731.
75. Baramova, E.N.; Shannon, J.D.; Bjarnason, J.B.; Gonias, S.L.; Fox, J.W. Interaction of Hemorrhagic Metalloproteinases with Human Alpha 2-Macroglobulin. *Biochemistry* **1990**, *29*, 1069–1074, doi:10.1021/bi00456a032.
76. Camacho, E.; Villalobos, E.; Sanz, L.; Pérez, A.; Escalante, T.; Lomonte, B.; Calvete, J.J.; Gutiérrez, J.M.; Rucavado, A. Understanding Structural and Functional Aspects of PII Snake Venom Metalloproteinases: Characterization of B1atH1, a Hemorrhagic Dimeric Enzyme from the Venom of *Bothriechis lateralis*. *Biochimie* **2014**, *101*, 145–155, doi: 10.1016/j.biochi.2014.01.008.
77. Kamiguti, A.S.; Desmond, H.P.; Theakston, R.D.; Hay, C.R.; Zuzel, M. Ineffectiveness of the Inhibition of the Main Haemorrhagic Metalloproteinase from *Bothrops jararaca* Venom by Its Only Plasma Inhibitor, Alpha 2-Macroglobulin. *Biochim Biophys Acta* **1994**, *1200*, 307–314, doi:10.1016/0304-4165(94)90172-4.
78. Akao, P.K.; Tonoli, C.C.C.; Navarro, M.S.; Cintra, A.C.O.; Neto, J.R.; Arni, R.K.; Murakami, M.T. Structural Studies of BmooMPalpha-I, a Non-Hemorrhagic Metalloproteinase from *Bothrops moojeni* Venom. *Toxicon* **2010**, *55*, 361–368, doi:10.1016/j.toxicon.2009.08.013.
79. Bello, C.A.; Hermogenes, A.L.N.; Magalhaes, A.; Veiga, S.S.; Gremski, L.H.; Richardson, M.; Sanchez, E.F. Isolation and Biochemical Characterization of a Fibrinolytic Proteinase from *Bothrops leucurus* (White-Tailed Jararaca) Snake Venom. *Biochimie* **2006**, *88*, 189–200, doi:10.1016/j.biochi.2005.07.008.

80. Gutiérrez, J.M.; Romero, M.; Núñez, J.; Chaves, F.; Borkow, G.; Ovadia, M. Skeletal Muscle Necrosis and Regeneration after Injection of BaH1, a Hemorrhagic Metalloproteinase Isolated from the Venom of the Snake *Bothrops asper* (Terciopelo). *Exp Mol Pathol* **1995**, *62*, 28–41, doi:10.1006/exmp.1995.1004.
81. Patiño, A.C.; Pereañez, J.A.; Núñez, V.; Benjumea, D.M.; Fernandez, M.; Rucavado, A.; Sanz, L.; Calvete, J.J. Isolation and Biological Characterization of Batx-I, a Weak Hemorrhagic and Fibrinogenolytic PI Metalloproteinase from Colombian *Bothrops atrox* Venom. *Toxicon* **2010**, *56*, 936–943, doi:10.1016/j.toxicon.2010.06.016.
82. Wallnoefer, H.G.; Lingott, T.; Gutiérrez, J.M.; Merfort, I.; Liedl, K.R. Backbone Flexibility Controls the Activity and Specificity of a Protein-Protein Interface: Specificity in Snake Venom Metalloproteases. *J Am Chem Soc* **2010**, *132*, 10330–10337, doi:10.1021/ja909908y.
83. de Souza, R.A.; Díaz, N.; Nagem, R.A.P.; Ferreira, R.S.; Suárez, D. Unraveling the Distinctive Features of Hemorrhagic and Non-Hemorrhagic Snake Venom Metalloproteinases Using Molecular Simulations. *J Comput Aided Mol Des* **2016**, *30*, 69–83, doi:10.1007/s10822-015-9889-5.
84. Preciado, L.M.; Pereañez, J.A.; Singam, E.R.A.; Comer, J. Interactions between Triterpenes and a P-I Type Snake Venom Metalloproteinase: Molecular Simulations and Experiments. *Toxins (Basel)* **2018**, *10*, 1–20, doi:10.3390/toxins10100397.
85. Gutiérrez, J.M.; Escalante, T.; Hernández, R.; Gastaldello, S.; Saravia-Otten, P.; Rucavado, A. Why Is Skeletal Muscle Regeneration Impaired after Myonecrosis Induced by Viperid Snake Venoms? *Toxins (Basel)* **2018**, *10*, E182, doi:10.3390/toxins10050182.
86. Tidball, J.G. Regulation of Muscle Growth and Regeneration by the Immune System. *Nat Rev Immunol* **2017**, *17*, 165–178, doi:10.1038/nri.2016.150.
87. Queiroz, L.S.; Santo Neto, H.; Assakura, M.T.; Reichl, A.P.; Mandelbaum, F.R. Pathological Changes in Muscle Caused by Haemorrhagic and Proteolytic Factors from *Bothrops jararaca* Snake Venom. *Toxicon* **1985**, *23*, 341–345, doi:10.1016/0041-0101(85)90158-8.
88. Homma, M.; Tu, A.T. Morphology of Local Tissue Damage in Experimental Snake Envenomation. *Br J Exp Pathol* **1971**, *52*, 538–542.
89. Jiménez, N.; Escalante, T.; Gutiérrez, J.M.; Rucavado, A. Skin Pathology Induced by Snake Venom Metalloproteinase: Acute Damage, Re-vascularization, and Re-Epithelization in a Mouse Ear Model. *J Invest Dermatol* **2008**, *128*, 2421–2428, doi:10.1038/jid.2008.118.
90. Macêdo, J.K.A.; Joseph, J.K.; Menon, J.; Escalante, T.; Rucavado, A.; Gutiérrez, J.M.; Fox, J.W. Proteomic Analysis of Human Blister Fluids Following Envenomation by Three Snake Species in India: Differential Markers for Venom Mechanisms of Action. *Toxins (Basel)* **2019**, *11*, E246, doi:10.3390/toxins11050246.
91. Laing, G.D.; Clissa, P.B.; Theakston, R.D.G.; Moura-da-Silva, A.M.; Taylor, M.J. Inflammatory Pathogenesis of Snake Venom Metalloproteinase-Induced Skin Necrosis. *Eur J Immunol* **2003**, *33*, 3458–3463, doi:10.1002/eji.200324475.
92. Fernandes, C.M.; Zamuner, S.R.; Zuliani, J.P.; Rucavado, A.; Gutiérrez, J.M.; Teixeira, C. de F.P. Inflammatory Effects of BaP1 a Metallopro-

- teinase Isolated from *Bothrops asper* Snake Venom: Leukocyte Recruitment and Release of Cytokines. *Toxicon* **2006**, *47*, 549–559, doi: 10.1016/j.toxicon.2006.01.009.
93. Teixeira, C. de F.P.; Fernandes, C.M.; Zuliani, J.P.; Zamuner, S.F. Inflammatory Effects of Snake Venom Metalloproteinases. *Mem Inst Oswaldo Cruz* **2005**, *100 Suppl*, 181–184, doi:10.1590/s0074-02762005000900031.
94. Clissa, P.B.; Laing, G.D.; Theakston, R.D.; Mota, I.; Taylor, M.J.; Moura-da-Silva, A.M. The Effect of Jararhagin, a Metalloproteinase from *Bothrops jararaca* Venom, on pro-Inflammatory Cytokines Released by Murine Peritoneal Adherent Cells. *Toxicon* **2001**, *39*, 1567–1573, doi:10.1016/s0041-0101(01)00131-3.
95. Schaloske, R.H.; Dennis, E.A. The Phospholipase A<sub>2</sub> Superfamily and Its Group Numbering System. *Biochim Biophys Acta* **2006**, *1761*, 1246–1259, doi: 10.1016/j.bbali.2006.07.011.
96. Filkin, S.Y.; Lipkin, A. V.; Fedorov, A.N. Phospholipase Superfamily: Structure, Functions, and Biotechnological Applications. *Biochemistry (Mosc)* **2020**, *85*, S177–S195, doi:10.1134/S0006297920140096.
97. Kini, R.M. Excitement Ahead: Structure, Function and Mechanism of Snake Venom Phospholipase A<sub>2</sub> Enzymes. *Toxicon* **2003**, *42*, 827–840, doi: 10.1016/j.toxicon.2003.11.002.
98. Días, E.H.V.; Dos Santos Paschoal, T.; da Silva, A.P.; da Cunha Pereira, D.F.; de Sousa Simamoto, B.B.; Matias, M.S.; Santiago, F.M.; Rosa, J.C.; Soares, A.; Santos-Filho, N.A.; et al. BaltPLA2: A New Phospholipase A<sub>2</sub> from *Bothrops alternatus* Snake Venom with Antiplatelet Aggregation Activity. *Protein Pept Lett* **2018**, *25*, 943–952, doi:10.2174/0929866525666181004101622.
99. Nunes, E.; Frihling, B.; Barros, E.; de Oliveira, C.; Verbisck, N.; Flores, T.; de Freitas Júnior, A.; Franco, O.; de Macedo, M.; Migliolo, L.; et al. Antibiofilm Activity of Acidic Phospholipase Isoform Isolated from *Bothrops erythromelas* Snake Venom. *Toxins (Basel)* **2020**, *12*, E606, doi:10.3390/toxins12090606.
100. Jiménez-Charris, E.; Montealegre-Sánchez, L.; Solano-Redondo, L.; Castro-Herrera, F.; Fierro-Pérez, L.; Lomonte, B. Divergent Functional Profiles of Acidic and Basic Phospholipases A<sub>2</sub> in the Venom of the Snake *Porthidium lansbergii lansbergii*. *Toxicon* **2016**, *119*, 289–298, doi: 10.1016/j.toxicon.2016.07.006.
101. Posada Arias, S.; Rey-Suárez, P.; Pereáñez J, A.; Acosta, C.; Rojas, M.; Delazari Dos Santos, L.; Ferreira, R.S.; Núñez, V. Isolation and Functional Characterization of an Acidic Myotoxic Phospholipase A<sub>2</sub> from Colombian *Bothrops asper* Venom. *Toxins (Basel)* **2017**, *9*, E342, doi:10.3390/toxins9110342.
102. Vargas, L.J.; Londoño, M.; Quintana, J.C.; Rua, C.; Segura, C.; Lomonte, B.; Núñez, V. An Acidic Phospholipase A<sub>2</sub> with Antibacterial Activity from *Porthidium nasutum* Snake Venom. *Comp Biochem Physiol B Biochem Mol Biol* **2012**, *161*, 341–347, doi: 10.1016/j.cbpb.2011.12.010.
103. Kini, R.M.; Evans, H.J. A Model to Explain the Pharmacological Effects of Snake Venom Phospholipases A<sub>2</sub>. *Toxicon* **1989**, *27*, 613–635, doi:10.1016/0041-0101(89)90013-5.
104. Scott, D. Phospholipase A<sub>2</sub>: Structure and Catalytic Properties. In

- Venom phospholipase A<sub>2</sub> enzymes: structure, function and mechanism*; Kini, R., Ed.; John Wiley & Sons: Chichester, **1997**; pp. 97–128.
105. Berg, O.G.; Gelb, M.H.; Tsai, M.D.; Jain, M.K. Interfacial Enzymology: The Secreted Phospholipase A<sub>2</sub>-Paradigm. *Chem Rev* **2001**, *101*, 2613–2654, doi:10.1021/cr990139w.
  106. Maraganore, J.M.; Merutka, G.; Cho, W.; Welches, W.; Kézdy, F.J.; Henrikson, R.L. A New Class of Phospholipases A<sub>2</sub> with Lysine in Place of Aspartate 49. Functional Consequences for Calcium and Substrate Binding. *J Biol Chem* **1984**, *259*, 13839–13843.
  107. Gutiérrez, J.M.; León, G.; Lomonte, B. Pharmacokinetic-Pharmacodynamic Relationships of Immunoglobulin Therapy for Envenomation. *Clin Pharmacokinet* **2003**, *42*, 721–741, doi:10.2165/00003088-200342080-00002.
  108. Lambeau, G.; Schmid-Alliana, A.; Lazdunski, M.; Barhanin, J. Identification and Purification of a Very High Affinity Binding Protein for Toxic Phospholipases A<sub>2</sub> in Skeletal Muscle. *Journal of Biological Chemistry* **1990**, *265*, 9526–9532, doi:10.1016/s0021-9258(19)38881-7.
  109. Massimino, M.L.; Simonato, M.; Spolaore, B.; Franchin, C.; Arrigoni, G.; Marin, O.; Monturiol-Gross, L.; Fernández, J.; Lomonte, B.; Tonello, F. Cell Surface Nucleolin Interacts with and Internalizes *Bothrops asper* Lys49 Phospholipase A<sub>2</sub> and Mediates Its Toxic Activity. *Sci Rep* **2018**, *8*, 10619, doi:10.1038/s41598-018-28846-4.
  110. Fernandes, C.A.H.; Borges, R.J.; Lomonte, B.; Fontes, M.R.M. A Structure-Based Proposal for a Comprehensive Myotoxic Mechanism of Phospholipase A<sub>2</sub>-like Proteins from Viperid Snake Venoms. *Biochim Biophys Acta Proteins Proteom* **2014**, *1844*, 2265–2276, doi: 10.1016/j.bbapap.2014.09.015.
  111. Gutiérrez, J.M.; Ownby, C.L. Skeletal Muscle Degeneration Induced by Venom Phospholipases A<sub>2</sub>: Insights into the Mechanisms of Local and Systemic Myotoxicity. *Toxicon* **2003**, *42*, 915–931, doi: 10.1016/j.toxicon.2003.11.005.
  112. Montecucco, C.; Gutiérrez, J.M.; Lomonte, B. Cellular Pathology Induced by Snake Venom Phospholipase A<sub>2</sub> Myotoxins and Neurotoxins: Common Aspects of Their Mechanisms of Action. *Cell Mol Life Sci* **2008**, *65*, 2897–2912, doi:10.1007/s00018-008-8113-3.
  113. Otero-Patiño, R. Snake Bites in Colombia. In *Clinical Toxinology: Clinical Toxinology*; Gopalakrishnakone, P., Faiz, S.M.A., Gnanathanan, C.A., Habib, A.G., Fernando, R., Yang, C.-C., Eds.; Springer Netherlands: Dordrecht, **2013**; pp. 1–42 ISBN 978-94-007-6288-6.
  114. Sarkar, S.; Sinha, R.; Chaudhury, A.R.; Maduwage, K.; Abeyagunawardena, A.; Bose, N.; Pradhan, S.; Bresolin, N.L.; Garcia, B.A.; McCulloch, M. Snake Bite Associated with Acute Kidney Injury. *Pediatr Nephrol* **2020**, *36*, 3829–3840, doi:10.1007/s00467-020-04911-x.
  115. Sitprija, V. Animal Toxins and the Kidney. *Nat Clin Pract Nephrol* **2008**, *4*, 616–627, doi:10.1038/ncpneph0941.
  116. Teixeira, C.F.P.; Landucci, E.C.T.; Antunes, E.; Chacur, M.; Cury, Y. Inflammatory Effects of Snake Venom Myotoxic Phospholipases A<sub>2</sub>. *Toxicon* **2003**, *42*, 947–962, doi: 10.1016/j.toxicon.2003.11.006.
  117. Costa, S.K.P.; Camargo, E.A.; Antunes, E. Inflammatory Action of Secretory Phospholipases A<sub>2</sub> from Snake Venoms. In *Toxins and Drug*

- Discovery*; Cruz, L.J., Luo, S., Gopalakrishnakone, P., Eds.; Toxinology; Springer Netherlands: Dordrecht, **2017**; pp. 35–52 ISBN 978-94-007-6452-1.
118. Pungerčar, J.; Križaj, I. Understanding the Molecular Mechanism Underlying the Presynaptic Toxicity of Secreted Phospholipases A<sub>2</sub>. *Toxicon* **2007**, *50*, 871–892, doi: 10.1016/j.toxicon.2007.07.025.
  119. Montecucco, C.; Rossetto, O. How Do Presynaptic PLA<sub>2</sub> Neurotoxins Block Nerve Terminals? *Trends Biochem Sci* **2000**, *25*, 266–270, doi:10.1016/s0968-0004(00)01556-5.
  120. Tonello, F.; Rigoni, M. Cellular Mechanisms of Action of Snake Phospholipase A<sub>2</sub> Toxins. In *Snake Venoms*; Inagaki, H., Vogel, C.-W., Mukherjee, A.K., Rahmy, T.R., Gopalakrishnakone, P., Eds.; Toxinology; Springer Netherlands: Dordrecht, **2017**; pp. 49–65 ISBN 978-94-007-6410-1.
  121. Lambeau, G.; Barhanin, J.; Schweitz, H.; Qar, J.; Lazdunski, M. Identification and Properties of Very High Affinity Brain Membrane-Binding Sites for a Neurotoxic Phospholipase from the Taipan Venom. *Journal of Biological Chemistry* **1989**, *264*, 11503–11510, doi:10.1016/s0021-9258(18)60492-2.
  122. Paoli, M.; Rigoni, M.; Koster, G.; Rossetto, O.; Montecucco, C.; Postle, A.D. Mass Spectrometry Analysis of the Phospholipase A<sub>2</sub> Activity of Snake Pre-Synaptic Neurotoxins in Cultured Neurons. *J Neurochem* **2009**, *111*, 737–744, doi:10.1111/j.1471-4159.2009.06365.x.
  123. Rigoni, M.; Caccin, P.; Gschmeissner, S.; Koster, G.; Postle, A.D.; Rossetto, O.; Schiavo, G.; Montecucco, C. Equivalent Effects of Snake PLA<sub>2</sub> Neurotoxins and Lysophospholipid-Fatty Acid Mixtures. *Science* **2005**, *310*, 1678–1680, doi:10.1126/science.1120640.
  124. Nicotera, P.; Bellomo, G.; Orrenius, S. Calcium-Mediated Mechanisms in Chemically Induced Cell Death. *Annu Rev Pharmacol Toxicol* **1992**, *32*, 449–470, doi:10.1146/annurev.pa.32.040192.002313.
  125. Montecucco, C.; Rossetto, O.; Caccin, P.; Rigoni, M.; Carli, L.; Morbiato, L.; Muraro, L.; Paoli, M. Different Mechanisms of Inhibition of Nerve Terminals by Botulinum and Snake Presynaptic Neurotoxins. *Toxicon* **2009**, *54*, 561–564, doi: 10.1016/j.toxicon.2008.12.012.
  126. Kovacic, L.; Novinec, M.; Petan, T.; Krizaj, I. Structural Basis of the Significant Calmodulin-Induced Increase in the Enzymatic Activity of Secreted Phospholipases A<sub>2</sub>. *Protein Eng Des Sel* **2010**, *23*, 479–487, doi:10.1093/protein/gzq019.
  127. Mattiazzi, M.; Sun, Y.; Wolinski, H.; Bavdek, A.; Petan, T.; Anderluh, G.; Kohlwein, S.D.; Drubin, D.G.; Križaj, I.; Petrovič, U. A Neurotoxic Phospholipase A<sub>2</sub> Impairs Yeast Amphiphysin Activity and Reduces Endocytosis. *PLoS One* **2012**, *7*, e40931, doi: 10.1371/journal.pone.0040931.
  128. Šribar, J.; Oberčkal, J.; Križaj, I. Understanding the Molecular Mechanism Underlying the Presynaptic Toxicity of Secreted Phospholipases A<sub>2</sub>: An Update. *Toxicon* **2014**, *89*, 9–16, doi: 10.1016/j.toxicon.2014.06.019.
  129. Kordiš, D.; Križaj, I. Secreted Phospholipases A<sub>2</sub> with β-Neurotoxic Activity. In *Snake Venoms*; Inagaki, H., Vogel, C.-W., Mukherjee, A.K., Rahmy, T.R., Gopalakrishnakone, P., Eds.; Toxinology; Springer Netherlands: Dordrecht, **2017**; pp. 67–86 ISBN 978-94-007-6410-1.
  130. Pereañez, J.A.; Núñez, V.; Huancahuire-Vega, S.; Marangoni, S.; Ponce-Soto, L.A. Biochemical and Biological Characterization of a PLA<sub>2</sub> from

- Crotoxin Complex of *Crotalus durissus cumanensis*. *Toxicon* **2009**, *53*, 534–542, doi: 10.1016/j.toxicon.2009.01.021.
131. Hendon, R.A.; Fraenkel-Conrat, H. Biological Roles of the Two Components of Crotoxin. *Proc Natl Acad Sci USA* **1971**, *68*, 1560–1563, doi:10.1073/pnas.68.7.1560.
  132. Habermann, E.; Breithaupt, H. Mini-Review. The Crotoxin Complexan Example of Biochemical and Pharmacological Protein Complementa-tion. *Toxicon* **1978**, *16*, 19–30, doi:10.1016/0041-0101(78)90056-9.
  133. Canziani, G.; Seki, C.; Vidal, J.C. The Mechanism of Inhibition of Phos-pholipase Activity of Crotoxin B by Crotoxin A. *Toxicon* **1983**, *21*, 663–674, doi:10.1016/0041-0101(83)90272-6.
  134. Pereañez, J.A.; Gómez, I.D.; Patiño, A.C. Relationship between the Structure and the Enzymatic Activity of Crotoxin Complex and Its Phospholipase A<sub>2</sub> Subunit: An in-Silico Approach. *J Mol Graph Model* **2012**, *35*, 36–42, doi: 10.1016/j.jmgm.2012.01.004.
  135. Rey-Suárez, P.; Núñez, V.; Saldarriaga-Cordoba, M.; Lomonte, B. Primary Structures and Partial Toxicological Characterization of Two Phospho-lipases A<sub>2</sub> from *Micrurus mipartitus* and *Micrurus dumerilii* Coral Snake Venoms. *Biochimie* **2017**, *137*, 88–98, doi: 10.1016/j.biochi.2017.03.008.
  136. Kini, R.M. Structure-Function Relationships and Mechanism of Anti-coagulant Phospholipase A<sub>2</sub> Enzymes from Snake Venoms. *Toxicon* **2005**, *45*, 1147–1161, doi: 10.1016/j.toxicon.2005.02.018.
  137. Verheij, H.M.; Boffa, M.C.; Rothen, C.; Bryckaert, M.C.; Verger, R.; de Haas, G.H. Correlation of Enzymatic Activity and Anticoagulant Properties of Phospholipase A<sub>2</sub>. *Eur J Biochem* **1980**, *112*, 25–32, doi:10.1111/j.1432-1033.1980.tb04982. x.
  138. Kini, R.M.; Evans, H.J. Structure-Function Relationships of Phospho-lipases. The Anticoagulant Region of Phospholipases A<sub>2</sub>. *J Biol Chem* **1987**, *262*, 14402–14407.
  139. Stefansson, S.; Kini, R.M.; Evans, H.J. The Basic Phospholipase A<sub>2</sub> from *Naja nigricollis* Venom Inhibits the Prothrombinase Complex by a Novel Nonenzymatic Mechanism. *Biochemistry* **1990**, *29*, 7742–7746, doi:10.1021/bi00485a024.
  140. Faure, G.; Gowda, V.T.; Maroun, R.C. Characterization of a Human Co-agulation Factor Xa-Binding Site on Viperidae Snake Venom Phospho-lipases A<sub>2</sub> by Affinity Binding Studies and Molecular Bioinformatics. *BMC Struct Biol* **2007**, *7*, 82, doi:10.1186/1472-6807-7-82.
  141. Faure, G.; Xu, H.; Saul, F. Anticoagulant Phospholipases A<sub>2</sub> Which Bind to the Specific Soluble Receptor Coagulation Factor Xa. In *Toxins and Hemostasis: From Bench to Bedside*; Kini, R.M., Clemetson, K.J., Mark-land, F.S., McLane, M.A., Morita, T., Eds.; Springer Netherlands: Dor-drecht, **2010**; pp. 201–217 ISBN 978-90-481-9295-3.
  142. Saikia, D.; Mukherjee, A.K. Anticoagulant and Membrane Damaging Properties of Snake Venom Phospholipase A<sub>2</sub> Enzymes. In *Snake Ven-oms*; Gopalakrishnakone, P., Inagaki, H., Mukherjee, A.K., Rahmy, T.R., Vogel, C.-W., Eds.; Toxinology; Springer Netherlands: Dordrecht, **2015**; pp. 1–14 ISBN 978-94-007-6648-8.
  143. Kini, R.M.; Evans, H.J. Effects of Phospholipase Enzymes on Platelet Aggregation. In *Venom Phospholipase A<sub>2</sub> Enzymes: Structure, Function and Mechanism*; John Wiley: Chichester, England, **1997**; pp. 369–387.

144. Ouyang, C.; Teng, C.M. The Action Mechanism of the Purified Platelet Aggregation Principle of *Trimeresurus mucrosquamatus* Venom. *Thromb Haemost* **1979**, *41*, 475–490.
145. Landucci, E.C.; Condino-Neto, A.; Perez, A.C.; Hyslop, S.; Corrado, A.P.; Novello, J.C.; Marangoni, S.; Oliveira, B.; Antunes, E.; de Nucci, G. Crotoxin Induces Aggregation of Human Washed Platelets. *Toxicon* **1994**, *32*, 217–226, doi:10.1016/0041-0101(94)90111-2.
146. Ouyang, C.; Yeh, H.I.; Huang, T.F. A Potent Platelet Aggregation Inhibitor Purified from *Agkistrodon halys* (Mamushi) Snake Venom. *Toxicon* **1983**, *21*, 797–804, doi:10.1016/0041-0101(83)90068-5.
147. Li, Y.S.; Liu, K.F.; Wang, Q.C.; Ran, Y.L.; Tu, G.C. A Platelet Function Inhibitor Purified from *Vipera russelli siamensis* (Smith) Snake Venom. *Toxicon* **1985**, *23*, 895–903, doi:10.1016/0041-0101(85)90381-2.
148. Ouyang, C.; Huang, T.F. Effect of the Purified Phospholipases A<sub>2</sub> from Snake and Bee Venoms on Rabbit Platelet Function. *Toxicon* **1984**, *22*, 705–718, doi:10.1016/0041-0101(84)90154-5.
149. Péterfi, O.; Boda, F.; Szabó, Z.; Ferencz, E.; Bába, L. Hypotensive Snake Venom Components-A Mini-Review. *Molecules* **2019**, *24*, 1–16, doi:10.3390/molecules24152778.
150. Andrião-Escarso, S.H.; Soares, A.M.; Fontes, M.R.M.; Fuly, A.L.; Corrêa, F.M.A.; Rosa, J.C.; Greene, L.J.; Giglio, J.R. Structural and Functional Characterization of an Acidic Platelet Aggregation Inhibitor and Hypotensive Phospholipase A<sub>2</sub> from *Bothrops jararacussu* Snake Venom. *Biochem Pharmacol* **2002**, *64*, 723–732, doi:10.1016/s0006-2952(02)01210-8.
151. Chaisakul, J.; Isbister, G.K.; Tare, M.; Parkington, H.C.; Hodgson, W.C. Hypotensive and Vascular Relaxant Effects of Phospholipase A<sub>2</sub> Toxins from Papuan Taipan (*Oxyuranus scutellatus*) Venom. *Eur J Pharmacol* **2014**, *723*, 227–233, doi: 10.1016/j.ejphar.2013.11.028.
152. Silveira, L.B.; Marchi-Salvador, D.P.; Santos-Filho, N.A.; Silva, F.P.; Marcussi, S.; Fuly, A.L.; Nomizo, A.; da Silva, S.L.; Stábeli, R.G.; Arantes, E.C.; et al. Isolation and Expression of a Hypotensive and Anti-Platelet Acidic Phospholipase A<sub>2</sub> from *Bothrops moojeni* Snake Venom. *J Pharm Biomed Anal* **2013**, *73*, 35–43, doi: 10.1016/j.jpba.2012.04.008.
153. Almeida, J.R.; Palacios, A.L. V.; Patiño, R.S.P.; Mendes, B.; Teixeira, C.A.S.; Gomes, P.; da Silva, S.L. Harnessing Snake Venom Phospholipases A<sub>2</sub> to Novel Approaches for Overcoming Antibiotic Resistance. *Drug Dev Res* **2019**, *80*, 68–85, doi:10.1002/ddr.21456.
154. Hiu, J.J.; Yap, M.K.K. Cytotoxicity of Snake Venom Enzymatic Toxins: Phospholipase A<sub>2</sub> and L-Amino Acid Oxidase. *Biochem Soc Trans* **2020**, *48*, 719–731, doi:10.1042/BST20200110.
155. Asano, Y.; Yasukawa, K. Identification and Development of Amino Acid Oxidases. *Curr Opin Chem Biol* **2019**, *49*, 76–83, doi: 10.1016/j.cbpa.2018.10.020.
156. Hossain, G.S.; Li, J.; Shin, H.D.; Du, G.; Liu, L.; Chen, J. L-Amino Acid Oxidases from Microbial Sources: Types, Properties, Functions, and Applications. *Appl Microbiol Biotechnol* **2014**, *98*, 1507–1515, doi:10.1007/s00253-013-5444-2.
157. Paloschi, M. V.; Pontes, A.S.; Soares, A.M.; Zuliani, J.P. An Update on Potential Molecular Mechanisms Underlying the Actions of Snake

- Venom L-Amino Acid Oxidases (LAAOs). *Curr Med Chem* **2018**, *25*, 2520–2530, doi:10.2174/0929867324666171109114125.
158. Tan, N.H. L-Amino Acid Oxidases and Lactate Deshydrogenases. In *Enzymes from snake venom*; Bailey, G.S., Ed.; Alaken: Fort Collins, **1998**; pp. 579–598.
159. Ullah, A. Structure–Function Studies and Mechanism of Action of Snake Venom L-Amino Acid Oxidases. *Front Pharmacol* **2020**, *11*, 110, doi:10.3389/fphar.2020.00110.
160. Izidoro, L.F.M.; Sobrinho, J.C.; Mendes, M.M.; Costa, T.R.; Grabner, A.N.; Rodrigues, V.M.; Da Silva, S.L.; Zanchi, F.B.; Zuliani, J.P.; Fernandes, C.F.C.; et al. Snake Venom L-Amino Acid Oxidases: Trends in Pharmacology and Biochemistry. *Biomed Res Int* **2014**, *2014*, doi:10.1155/2014/196754.
161. Moustafa, I.M.; Foster, S.; Lyubimov, A.Y.; Vrieling, A. Crystal Structure of LAAO from *Calloselasma rhodostoma* with an L-Phenylalanine Substrate: Insights into Structure and Mechanism. *J Mol Biol* **2006**, *364*, 991–1002, doi: 10.1016/j.jmb.2006.09.032.
162. Guo, C.; Liu, S.; Yao, Y.; Zhang, Q.; Sun, M.Z. Past Decade Study of Snake Venom L-Amino Acid Oxidase. *Toxicon* **2012**, *60*, 302–311.
163. Liu, J.W.; Chai, M.Q.; Du, X.Y.; Song, J.G.; Zhou, Y.C. [Purification and characterization of L-amino acid oxidase from *Agkistrodon halys pallas* venom]. *Sheng Wu Hua Xue Yu Sheng Wu Wu Li Xue Bao (Shanghai)* **2002**, *34*, 305–310.
164. Torii, S.; Yamane, K.; Mashima, T.; Haga, N.; Yamamoto, K.; Fox, J.W.; Naito, M.; Tsuruo, T. Molecular Cloning and Functional Analysis of Apoxin I, a Snake Venom- Derived Apoptosis-Inducing Factor with L-Amino Acid Oxidase Activity. *Biochemistry* **2000**, *39*, 3197–3205, doi:10.1021/bi992416z.
165. Stábeli, R.G.; Marcussi, S.; Carlos, G.B.; Pietro, R.C.L.R.; Selistre-De-Araújo, H.S.; Giglio, J.R.; Oliveira, E.B.; Soares, A.M. Platelet Aggregation and Antibacterial Effects of an L-Amino Acid Oxidase Purified from *Bothrops alternatus* Snake Venom. *Bioorg Med Chem* **2004**, *12*, 2881–2886, doi: 10.1016/j.bmc.2004.03.049.
166. Rodrigues, R.S.; da Silva, J.F.; Boldrini França, J.; Fonseca, F.P.P.; Otaviano, A.R.; Henrique Silva, F.; Hamaguchi, A.; Magro, A.J.; Braz, A.S.K.; dos Santos, J.I.; et al. Structural and Functional Properties of Bp-LAAO, a new L-Amino Acid Oxidase Isolated from *Bothrops pauloensis* Snake Venom. *Biochimie* **2009**, *91*, 490–501, doi: 10.1016/j.biochi.2008.12.004.
167. Ciscotto, P.; Machado de Avila, R.A.; Coelho, E.A.F.; Oliveira, J.; Diniz, C.G.; Fariás, L.M.; de Carvalho, M.A.R.; Maria, W.S.; Sanchez, E.F.; Borges, A.; et al. Antigenic, Microbicidal and Antiparasitic Properties of an L-Amino Acid Oxidase Isolated from *Bothrops jararaca* Snake Venom. *Toxicon* **2009**, *53*, 330–341, doi: 10.1016/j.toxicon.2008.12.004.
168. Vargas, L.J.; Quintana, J.C.; Pereañez, J.A.; Núñez, V.; Sanz, L.; Calvete, J. Cloning and Characterization of an Antibacterial L-Amino Acid Oxidase from *Crotalus durissus cumanensis* Venom. *Toxicon* **2013**, *64*, 1–11, doi: 10.1016/j.toxicon.2012.11.027.
169. Vargas Muñoz, L.J.; Estrada-Gomez, S.; Núñez, V.; Sanz, L.; Calvete, J.J. Characterization and CDNA Sequence of *Bothriechis schlegelii* L-

- Amino Acid Oxidase with Antibacterial Activity. *Int J Biol Macromol* **2014**, *69*, 200–207, doi: 10.1016/j.ijbiomac.2014.05.039.
170. Bedoya-Medina, J.; Mendivil-Perez, M.; Rey-Suarez, P.; Jimenez-Del-Rio, M.; Núñez, V.; Velez-Pardo, C. L-Amino Acid Oxidase Isolated from *Micrurus mipartitus* Snake Venom (MipLAAO) Specifically Induces Apoptosis in Acute Lymphoblastic Leukemia Cells Mostly via Oxidative Stress-Dependent Signaling Mechanism. *Int J Biol Macromol* **2019**, *134*, 1052–1062, doi: 10.1016/j.ijbiomac.2019.05.174.
171. Izidoro, L.F.M.; Ribeiro, M.C.; Souza, G.R.L.; Sant'Ana, C.D.; Hamaguchi, A.; Homsí-Brandeburgo, M.I.; Goulart, L.R.; Belebóni, R.O.; Nomizo, A.; Sampaio, S. V; et al. Biochemical and Functional Characterization of an L-Amino Acid Oxidase Isolated from *Bothrops pirajai* Snake Venom. *Bioorg Med Chem* **2006**, *14*, 7034–7043, doi: 10.1016/j.bmc.2006.06.025.
172. Toyama, M.H.; Toyama, D. de O.; Passero, L.F.D.; Laurenti, M.D.; Corbett, C.E.; Tomokane, T.Y.; Fonseca, F. V; Antunes, E.; Joazeiro, P.P.; Beriam, L.O.S.; et al. Isolation of a New L-Amino Acid Oxidase from *Crotalus durissus cascavella* Venom. *Toxicon* **2006**, *47*, 47–57, doi: 10.1016/j.toxicon.2005.09.008.
173. Soares, T.G.; Santos, J.L. Dos; Alvarenga, V.G. de; Santos, J.S.C.; Leclercq, S.Y.; Faria, C.D.; Oliveira, M.A.A.; Bemquerer, M.P.; Sanchez, E.O.F.; de Lima, M.E.; et al. Biochemical and Functional Properties of a New L-Amino Acid Oxidase (LAAO) from *Micrurus lemniscatus* Snake Venom. *Int J Biol Macromol* **2020**, *154*, 1517–1527, doi: 10.1016/j.ijbiomac.2019.11.033.
174. Samel, M.; Vija, H.; Rönholm, G.; Siigur, J.; Kalkkinen, N.; Siigur, E. Isolation and Characterization of an Apoptotic and Platelet Aggregation Inhibiting L-Amino Acid Oxidase from *Vipera berus berus* (Common Viper) Venom. *Biochim Biophys Acta* **2006**, *1764*, 707–714, doi: 10.1016/j.bbapap.2006.01.021.
175. Suhr, S.M.; Kim, D.S. Comparison of the Apoptotic Pathways Induced by L-Amino Acid Oxidase and Hydrogen Peroxide. *J Biochem* **1999**, *125*, 305–309, doi: 10.1093/oxfordjournals.jbchem.a022287.
176. Ande, S.R.; Kommoju, P.R.; Draxl, S.; Murkovic, M.; Macheroux, P.; Ghisla, S.; Ferrando-May, E. Mechanisms of Cell Death Induction by L-Amino Acid Oxidase, a Major Component of Ophidian Venom. *Apoptosis* **2006**, *11*, 1439–1451, doi:10.1007/s10495-006-7959-9.
177. Souza, D.H.; Eugenio, L.M.; Fletcher, J.E.; Jiang, M.S.; Garratt, R.C.; Oliva, G.; Selistre-de-Araujo, H.S. Isolation and Structural Characterization of a Cytotoxic L-Amino Acid Oxidase from *Agkistrodon contortrix laticinctus* Snake Venom: Preliminary Crystallographic Data. *Arch Biochem Biophys* **1999**, *368*, 285–290, doi:10.1006/abbi.1999.1287.
178. Alves, R.M.; Antonucci, G.A.; Paiva, H.H.; Cintra, A.C.O.; Franco, J.J.; Mendonça-Franqueiro, E.P.; Dorta, D.J.; Giglio, J.R.; Rosa, J.C.; Fuly, A.L.; et al. Evidence of Caspase-Mediated Apoptosis Induced by L-Amino Acid Oxidase Isolated from *Bothrops atrox* Snake Venom. *Comparative biochemistry and physiology. Part A, Molecular & integrative physiology* **2008**, *151*, 542–550, doi: 10.1016/j.cbpa.2008.07.007.
179. Zhang, H.; Yang, Q.; Sun, M.; Teng, M.; Niu, L. Hydrogen Peroxide Produced by Two Amino Acid Oxidases Mediates Antibacterial Actions. *J Microbiol* **2004**, *42*, 336–339.

180. Wei, X.-L.; Wei, J.-F.; Li, T.; Qiao, L.-Y.; Liu, Y.-L.; Huang, T.; He, S.-H. Purification, Characterization and Potent Lung Lesion Activity of an L-Amino Acid Oxidase from *Agkistrodon blomhoffii ussurensis* Snake Venom. *Toxicon* **2007**, *50*, 1126–1139, doi: 10.1016/j.toxicon.2007.07.022.
181. Izidoro, L.F.M.; Alves, L.M.; Rodrigues, V.M.; Silva, D.A.O.; Mineo, J.R. Bothrops Pirajai Snake Venom L-Amino Acid Oxidase: In Vitro Effects on Infection of *Toxoplasma gondii* in Human Foreskin Fibroblasts. *Revista Brasileira de Farmacognosia* **2011**, *21*, 477–485, doi:10.1590/S0102-695X2011005000108.
182. Du, X.-Y.; Clemetson, K.J. Snake Venom L-Amino Acid Oxidases. *Toxicon* **2002**, *40*, 659–665, doi:10.1016/s0041-0101(02)00102-2.
183. Belisario, M.A.; Tafuri, S.; Di Domenico, C.; Squillacioti, C.; Della Morte, R.; Lucisano, A.; Staiano, N. H<sub>2</sub>O<sub>2</sub> Activity on Platelet Adhesion to Fibrinogen and Protein Tyrosine Phosphorylation. *Biochim Biophys Acta Mol Cell Res* **2000**, *1495*, 183–193, doi:10.1016/S0167-4889(99)00160-3.
184. Pignatelli, P.; Pulcinelli, F.M.; Lenti, L.; Gazzaniga, P.P.; Violi, F. Hydrogen Peroxide Is Involved in Collagen-Induced Platelet Activation. *Blood* **1998**, *91*, 484–490.
185. Bregge-Silva, C.; Nonato, M.C.; de Albuquerque, S.; Ho, P.L.; Junqueira de Azevedo, I.L.M.; Vasconcelos Diniz, M.R.; Lomonte, B.; Rucavado, A.; Díaz, C.; Gutiérrez, J.M.; et al. Isolation and Biochemical, Functional and Structural Characterization of a Novel L-Amino Acid Oxidase from *Lachesis muta* Snake Venom. *Toxicon* **2012**, *60*, 1263–1276, doi: 10.1016/j.toxicon.2012.08.008.
186. Izidoro, L.F.M.; Sobrinho, J.C.; Mendes, M.M.; Costa, T.R.; Grabner, A.N.; Rodrigues, V.M.; da Silva, S.L.; Zanchi, F.B.; Zuliani, J.P.; Fernandes, C.F.C.; et al. Snake Venom L-Amino Acid Oxidases: Trends in Pharmacology and Biochemistry. *Biomed Res Int* **2014**, *2014*, 196754, doi:10.1155/2014/196754.
187. Wiesel, G.A.; Rustiguel, J.K.; Morgenstern, D.; Zoccal, K.F.; Faccioli, L.H.; Nonato, M.C.; Ueberheide, B.; Arantes, E.C. Insights into the Structure, Function and Stability of Bordonein-L, the First L-Amino Acid Oxidase from *Crotalus durissus terrificus* Snake Venom. *Biochimie* **2019**, *163*, 33–49, doi: 10.1016/j.biochi.2019.05.009.
188. Rey-Suárez, P.; Acosta, C.; Torres, U.; Saldarriaga-Cordoba, M.; Lomonte, B.; Núñez, V. MipLAAO, a New L-Amino Acid Oxidase from the Redtail Coral Snake *Micrurus mipartitus*. *PeerJ* **2018**, *2018*, e4924, doi:10.7717/peerj.4924.
189. Zhang, L.; Wei, L.-J. ACTX-8, a Cytotoxic L-Amino Acid Oxidase Isolated from *Agkistrodon acutus* Snake Venom, Induces Apoptosis in Hela Cervical Cancer Cells. *Life Sci* **2007**, *80*, 1189–1197, doi: 10.1016/j.lfs.2006.12.024.
190. Tan, K.K.; Bay, B.H.; Gopalakrishnakone, P. L-Amino Acid Oxidase from Snake Venom and Its Anticancer Potential. *Toxicon* **2018**, *144*, 7–13.
191. Bhattacharjee, P.; Mitra, J.; Bhattacharyya, D. L-Amino Acid Oxidase from Venoms BT - Toxins and Drug Discovery. In; Cruz, L.J., Luo, S., Gopalakrishnakone, P., Eds.; Springer Netherlands: Dordrecht, **2017**; pp. 295–320 ISBN 978-94-007-6452-1.
192. Huang, T.F.; Holt, J.C.; Lukasiewicz, H.; Niewiarowski, S. Trigramin. A Low Molecular Weight Peptide Inhibiting Fibrinogen Interaction with

- Platelet Receptors Expressed on Glycoprotein IIb-IIIa Complex. *J Biol Chem* **1987**, *262*, 16157–16163.
193. Calvete, J.J. The Continuing Saga of Snake Venom Disintegrins. *Toxicon* **2013**, *62*, 40–49, doi: 10.1016/j.toxicon.2012.09.005.
194. Calvete, J.J.; Moreno-Murciano, M.P.; Theakston, R.D.G.; Kisiel, D.G.; Marcinkiewicz, C. Snake Venom Disintegrins: Novel Dimeric Disintegrins and Structural Diversification by Disulphide Bond Engineering. *Biochemical Journal* **2003**, *372*, 725–734, doi:10.1042/BJ20021739.
195. Bilgrami, S.; Tomar, S.; Yadav, S.; Kaur, P.; Kumar, J.; Jabeen, T.; Sharma, S.; Singh, T.P. Crystal Structure of Schistatin, a Disintegrin Homodimer from Saw-Scaled Viper (*Echis carinatus*) at 2.5 Å Resolution. *J Mol Biol* **2004**, *341*, 829–837, doi: 10.1016/j.jmb.2004.06.048.
196. Carbajo, R.J.; Sanz, L.; Perez, A.; Calvete, J.J. NMR Structure of Bitistatin – a Missing Piece in the Evolutionary Pathway of Snake Venom Disintegrins. *FEBS J* **2015**, *282*, 341–360, doi:10.1111/FEBS.13138.
197. Arruda Macedo, J.; Fox, J.; Souza Castro, M. Disintegrins from Snake Venoms and Their Applications in Cancer Research and Therapy. *Curr Protein Pept Sci* **2015**, *16*, 532–548, doi:10.2174/1389203716666150515125002.
198. Calvete, J.; Juárez, P.; Sanz, L. Snake Venomics. Strategy and Applications. *Journal of Mass Spectrometry* **2007**, *42*, 1405–1414, doi:10.1002/jms.1242.
199. Jang, Y.J.; Jeon, O.H.; Kim, D.S. Saxatilin, a Snake Venom Disintegrin, Regulates Platelet Activation Associated with Human Vascular Endothelial Cell Migration and Invasion. *J Vasc Res* **2007**, *44*, 129–137, doi:10.1159/000098519.
200. Kuo, Y.J.; Chung, C.H.; Huang, T.F. From Discovery of Snake Venom Disintegrins to A Safer Therapeutic Antithrombotic Agent. *Toxins (Basel)* **2019**, *11*, doi:10.3390/TOXINS11070372.
201. Lazarovici, P.; Marcinkiewicz, C.; Lelkes, P.I. From Snake Venom's Disintegrins and C-Type Lectins to Anti-Platelet Drugs. *Toxins* **2019**, *Vol. 11*, Page 303 **2019**, *11*, 303, doi:10.3390/TOXINS11050303.
202. Sánchez, E.E.; Galán, J.A.; Russell, W.K.; Soto, J.G.; Russell, D.H.; Pérez, J.C. Isolation and Characterization of Two Disintegrins Inhibiting ADP-Induced Human Platelet Aggregation from the Venom of *Crotalus scutulatus scutulatus* (Mohave Rattlesnake). *Toxicol Appl Pharmacol* **2006**, *212*, 59–68, doi: 10.1016/j.taap.2005.07.004.
203. Sánchez, E.E.; Rodríguez-Acosta, A.; Palomar, R.; Lucena, S.E.; Bashir, S.; Soto, J.G.; Pérez, J.C. Colombistatin: A Disintegrin Isolated from the Venom of the South American Snake (*Bothrops colombiensis*) That Effectively Inhibits Platelet Aggregation and SK-Mel-28 Cell Adhesion. *Arch Toxicol* **2009**, *83*, 271–279, doi:10.1007/s00204-008-0358-y.
204. Gan, Z.R.; Gould, R.J.; Jacobs, J.W.; Friedman, P.A.; Polokoff, M.A. Echistatin. A Potent Platelet Aggregation Inhibitor from the Venom of the Viper, *Echis carinatus*. *Journal of Biological Chemistry* **1988**, *263*, 19827–19832, doi:10.1016/s0021-9258(19)77710-2.
205. Scarborough, R.M.; Rose, J.W.; Hsu, M.A.; Phillips, D.R.; Fried, V.A.; Campbell, A.M.; Nannizzi, L.; Charo, I.F. Barbourin: A GPIIb-IIIa-Specific Integrin Antagonist from the Venom of *Sistrurus M. Barbouri*. *Journal of Biological Chemistry* **1991**, *266*, 9359–9362, doi:10.1016/s0021-9258(18)92826-7.

206. Selistre-de-Araujo, H.S.; Pontes, C.L.S.; Montenegro, C.F.; Martin, A.C.B.M. Snake Venom Disintegrins and Cell Migration. *Toxins* **2010**, *2*, 2606–2621, doi:10.3390/toxins2112606.
207. Swenson, S.; Ramu, S.; Markland, F. Anti-Angiogenesis and RGD-Containing Snake Venom Disintegrins. *Curr Pharm Des* **2007**, *13*, 2860–2871, doi:10.2174/138161207782023793.
208. Uzair, B.; Atlas, N.; Malik, S.B.; Jamil, N.; Ojuolape, S.T.; Rehman, M.U.; Khan, B.A. Snake Venom as an Effective Tool Against Colorectal Cancer. *Protein Pept Lett* **2018**, *25*, 626–632, doi:10.2174/0929866525666180614112935.
209. Kini, R.M.; Doley, R. Structure, Function and Evolution of Three-Finger Toxins: Mini Proteins with Multiple Targets. *Toxicon* **2010**, *56*, 855–867, doi: 10.1016/j.toxicon.2010.07.010.
210. Rey-Suárez, P.; Floriano, R.S.; Rostelato-Ferreira, S.; Saldarriaga-Cordoba, M.; Núñez, V.; Rodrigues-Simioni, L.; Lomonte, B. Mipartoxin-I, a Novel Three-Finger Toxin, Is the Major Neurotoxic Component in the Venom of the Redtail Coral Snake *Micrurus mipartitus* (Elapidae). *Toxicon* **2012**, *60*, 851–863.
211. Kessler, P.; Marchot, P.; Silva, M.; Servent, D. The Three-Finger Toxin Fold: A Multifunctional Structural Scaffold Able to Modulate Cholinergic Functions. *J Neurochem* **2017**, *142*, 7–18, doi:10.1111/jnc.13975.
212. Aird, S.D.; da Silva, N.J. Chemistry of Coralsnake Venoms. In *Advances in Coralsnake Biology: With an Emphasis on South America*; Eagle Mountain Publishing, L.C., **2021**; pp. 399–484 ISBN 9780972015462.
213. Nastopoulos, V. Structure of Dimeric and Monomeric Erabutoxin a Refined at 1.5 Å Resolution. *Acta Crystallogr D Biol Crystallogr* **1998**, *54*, 964–974, doi:10.1107/S0907444998005125.
214. Scarselli, M.; Spiga, O.; Ciutti, A.; Bernini, A.; Bracci, L.; Lelli, B.; Lozzi, L.; Calamandrei, D.; Maro, D. Di; Klein, S.; et al. NMR Structure of R-Bungarotoxin Free and Bound to a Mimotope of the Nicotinic Receptor. *Methods* **2002**, 1457–1463.
215. Chung, C.; Wu, B.N.; Yang, C.C.; Chang, L.S. Muscarinic Toxin-Like Proteins from Taiwan Banded Krait (*Bungarus multicinctus*) Venom: Purification, Characterization and Gene Organization. *Journal of Biological Chemistry* **2002**, *383*, 1397–1406, doi:10.1023/A:1019760401692.
216. Lukyanova, E.N.; Shenkarev, Z.O.; Shulepko, M.A.; Paramonov, A.S.; Chugunov, A.O.; Janickova, H.; Dolejsi, E.; Dolezal, V.; Utkin, Y.N.; Tsetlin, V.I.; et al. Structural Insight into Specificity of Interactions between Nonconventional Three-Finger Weak Toxin from *Naja kaouthia* (WTX) and Muscarinic Acetylcholine Receptors. *Journal of Biological Chemistry* **2015**, *290*, 23616–23630, doi:10.1074/jbc.M115.656595.
217. Nickitenko, A. V.; Michailov, A.M.; Betzel, C.; Wilson, K.S. Three-Dimensional Structure of Neurotoxin-1 from *Naja naja oxiana* Venom at 1.9 Å Resolution. *FEBS Lett* **1993**, *320*, 111–117, doi:10.1016/0014-5793(93)80073-4.
218. Pawlak, J.; Mackessy, S.P.; Fry, B.G.; Bhatia, M.; Mourier, G.; Fruchart-Gaillard, C.; Servent, D.; Ménez, R.; Stura, E.; Ménez, A.; et al. Denmotoxin, a Three-Finger Toxin from the Colubrid Snake *Boiga dendrophalia* (Mangrove Catsnake) with Bird-Specific Activity. *Journal of Biological Chemistry* **2006**, *281*, 29030–29041, doi:10.1074/jbc.M605850200.

219. Roy, A.; Zhou, X.; Chong, M.Z.; D'Hoedt, D.; Foo, C.S.; Rajagopalan, N.; Nirthanan, S.; Bertrand, D.; Sivaraman, J.; Manjunatha Kini, R. Structural and Functional Characterization of a Novel Homodimeric Three-Finger Neurotoxin from the Venom of *Ophiophaga hannah* (King Cobra). *Journal of Biological Chemistry* **2010**, *285*, 8302–8315, doi:10.1074/jbc.M109.074161.
220. Pawlak, J.; Mackessy, S.P.; Sixberry, N.M.; Stura, E.A.; Le Du, M.H.; Ménez, R.; Foo, C.S.; Ménez, A.; Nirthanan, S.; Kini, R.M. Irditoxin, a Novel Covalently Linked Heterodimeric Three-Finger Toxin with High Taxon-Specific Neurotoxicity. *The FASEB Journal* **2009**, *23*, 534–545, doi: <https://doi.org/10.1096/fj.08-113555>.
221. Aoki-Shioi, N.; Jobichen, C.; Sivaraman, J.; Kini, R.M. Unusual Quaternary Structure of a Homodimeric Synergistic-Type Toxin from Mamba Snake Venom Defines Its Molecular Evolution. *Biochemical Journal* **2020**, *477*, 3951–3962, doi:10.1042/BCJ20200529.
222. Anadón, A.; Martínez-Larrañaga, M.R.; Valerio, L.G. Onchidal and Fasciculins. In *Handbook of Toxicology of Chemical Warfare Agents: Second Edition*; Elsevier Inc., **2015**; pp. 411–420 ISBN 9780128001592.
223. Utkin, Y. Last Decade Update for Three-Finger Toxins: Newly Emerging Structures and Biological Activities. *World J Biol Chem* **2019**, *10*, 17–27.
224. Kleiz-Ferreira, J.M.; Cirauqui, N.; Trajano, E.A.; Almeida, M. da S.; Zingali, R.B. Three-Finger Toxins from Brazilian Coral Snakes: From Molecular Framework to Insights in Biological Function. *Toxins (Basel)* **2021**, *13*, 1–19, doi:10.3390/toxins13050328.
225. Castillo-Beltrán, M.C.; Hurtado-Gómez, J.P.; Corredor-Espinel, V.; Ruiz-Gómez, F.J. A Polyvalent Coral Snake Antivenom with Broad Neutralization Capacity. *PLoS Negl Trop Dis* **2018**, *13*, 1–14, doi: 10.1371/journal.pntd.0007250.
226. Rey-Suárez, P.; Saldarriaga, M.; Torres, U.; Marin-villa, M.; Lomonte, B.; Núñez, V. Novel three-finger toxins from *Micrurus dumerilii* and *Micrurus mipartitus* coral snake venoms: Phylogenetic relationships and characterization of Clarkitoxin-I-Mdum. *Toxicon* **2019**, *170*, 85–93.
227. Lomonte, B.; Sasa, M.; Rey-Suárez, P.; Bryan, W.; Gutiérrez, J.M. Venom of the Coral Snake *Micrurus Clarki*: Proteomic Profile, Toxicity, Immunological Cross-Neutralization, and Characterization of a Three-Finger Toxin. *Toxins (Basel)* **2016**, *8*, doi:10.3390/toxins8050138.
228. Bertoni, M.; Kiefer, F.; Biasini, M.; Bordoli, L.; Schwede, T. Modeling Protein Quaternary Structure of Homo- and Hetero-Oligomers beyond Binary Interactions by Homology. *Sci Rep* **2017**, *7*, 10480, doi:10.1038/s41598-017-09654-8.
229. Utkin, Y.N. Three-Finger Toxins, a Deadly Weapon of Elapid Venom - Milestones of Discovery. *Toxicon* **2013**, *62*, 50–55, doi: 10.1016/j.toxicon.2012.09.007.
230. Kini, R.M.; Koh, C.Y. Snake Venom Three-Finger Toxins and Their Potential in Drug Development Targeting Cardiovascular Diseases. *Biochem Pharmacol* **2020**, *181*, 114105, doi: 10.1016/j.bcp.2020.114105.
231. Zaqueo, K.D.; Kayano, A.M.; Domingos, T.F.S.; Moura, L.A.; Fuly, A.L.; da Silva, S.L.; Acosta, G.; Oliveira, E.; Albericio, F.; Zanchi, F.B.; et al. BbrzSP-32, the First Serine Protease Isolated from Bothrops Brazilii

- Venom: Purification and Characterization. *Comp Biochem Physiol A Mol Integr Physiol* **2016**, *195*, 15–25, doi: 10.1016/j.cbpa.2016.01.021.
232. Roldán-Padrón, O.; Castro-Guillén, J.; García-Arredondo, J.; Cruz-Pérez, M.; Díaz-Peña, L.; Saldaña, C.; Blanco-Labra, A.; García-Gasca, T. Snake Venom Hemotoxic Enzymes : Biochemical Comparison between *Crotalus* Species from Central Mexico. *Molecules* **2019**, *24*, 1–16.
233. Latinović, Z.; Leonardi, A.; Koh, C.Y.; Kini, R.M.; Bakija, A.T.; Pungertar, J.; Križaj, I. The Procoagulant Snake Venom Serine Protease Potentially Having a Dual, Blood Coagulation Factor v and X-Activating Activity. *Toxins* **2020**, *12*, 1–15, doi:10.3390/toxins12060358.
234. Stefanelli, V.L.; Barker, T.H. The Evolution of Fibrin-Specific Targeting Strategies. *J Mater Chem B* **2015**, *3*, 1177–1186, doi:10.1039/c4tb01769b.
235. Mackessy, S. Venom Composition in Rattlesnakes: Trends and Biological Significance. In *The Biology of Rattlesnakes*; Hayes, W.K., Beaman, K.R., Cardwell, M.D., Bush, S.P., Eds.; Loma Linda University Press: Loma Linda, CA, **2008**; pp. 495–510.
236. Angulo, Y.; Lomonte, B. Biochemistry and Toxicology of Toxins Purified from the Venom of the Snake *Bothrops asper*. *Toxicon* **2009**, *54*, 949–957.
237. Gutiérrez, J.M.; Calvete, J.; Habib, A.; Harrison, R.; Williams, D.; Warrell, D. Snakebite Envenoming. *Nat Rev Dis Primers* **2017**, *3*, 1–20.
238. Serrano, S.M.T.; Maroun, R.C. Snake Venom Serine Proteinases: Sequence Homology vs. Substrate Specificity, a Paradox to Be Solved. *Toxicon* **2005**, *45*, 1115–1132, doi: 10.1016/j.toxicon.2005.02.020.
239. Serrano, S.M.T. The Long Road of Research on Snake Venom Serine Proteinases. *Toxicon* **2013**, *62*, 19–26, doi: 10.1016/j.toxicon.2012.09.003.
240. Yonamine, C.M.; Kondo, M.Y.; Nering, M.B.; Gouvêa, I.E.; Okamoto, D.; Andrade, D.; Alberto da Silva, J.A.; Prieto da Silva, Á.R.; Yamane, T.; Juliano, M.A.; et al. Enzyme Specificity and Effects of Gyroxin, a Serine Protease from the Venom of the South American Rattlesnake *Crotalus durissus terrificus*, on Protease-Activated Receptors. *Toxicon* **2014**, *79*, 64–71.
241. Carvalho, D.D.; Marangoni, S.; Oliveira, B.; Novello, J.C. Isolation and Characterization of a New Lectin From the Venom of the Snake *Bothrops jararacussu*. *Biochem Mol Biol Int* **1998**, *44*, 933–938.
242. Clemetson, K.; Morita, T.; Manjunatha Kini, R. Classification and Nomenclature of Snake Venom C-Type Lectins and Related Proteins. *Toxicon* **2009**, *54*, 83.
243. Sartim, M.A.; Sampaio, S. V Snake Venom Galactoside-Binding Lectins: A Structural and Functional Overview. *Journal of Venomous Animals and Toxins including Tropical Diseases* **2015**, *21*, 1–11, doi:10.1186/s40409-015-0038-3.
244. Arlinghaus, F.T.; Eble, J.A. C-Type Lectin-like Proteins from Snake Venoms. *Toxicon* **2012**, *60*, 512–519.
245. Vonk, F.J.; Jackson, K.; Doley, R.; Madaras, F.; Mirtschin, P.J.; Vidal, N. Snake Venom: From Fieldwork to the Clinic: Recent Insights into Snake Biology, Together with New Technology Allowing High-Throughput Screening of Venom, Bring New Hope for Drug Discovery. *BioEssays* **2011**, *33*, 269–279.
246. Chakrabarty, D.; Sarkar, A. Cytotoxic Effects of Snake Venoms. **2017**, *111*, 1–7.

247. Thakur, R.; Mukherjee, A.K. Pathophysiological Significance and Therapeutic Applications of Snake Venom Protease Inhibitors. *Toxicon* **2017**, *131*, 37–47.
248. Girish, K.S.; Jagadeesha, D.K.; Rajeev, K.B.; Kemparaju, K. Snake Venom Hyaluronidase: An Evidence for Isoforms and Extracellular Matrix Degradation. *Mol Cell Biochem* **2002**, *240*, 105–110, doi:10.1023/A:1020651607164.
249. Girish, K.S.; Shashidharamurthy, R.; Nagaraju, S.; Gowda, T. V.; Kemparaju, K. Isolation and Characterization of Hyaluronidase a “Spreading Factor” from Indian Cobra (*Naja naja*) Venom. *Biochimie* **2004**, *86*, 193–202, doi: 10.1016/j.biochi.2004.02.004.
250. Jiang, D.; Liang, J.; Noble, P.W. Hyaluronan as an Immune Regulator in Human Diseases. *Physiol Rev* **2011**, *91*, 221–264, doi:10.1152/physrev.00052.2009.
251. Noble, P.W. Hyaluronan and Its Catabolic Products in Tissue Injury and Repair. *Matrix Biology* **2002**, *21*, 25–29, doi:10.1016/S0945-053X(01)00184-6.
252. Ohno, S.; Im, H.J.; Knudson, C.B.; Knudson, W. Hyaluronan Oligosaccharides Induce Matrix Metalloproteinase 13 via Transcriptional Activation of NFκB and P38 MAP Kinase in Articular Chondrocytes. *Journal of Biological Chemistry* **2006**, *281*, 17952–17960, doi:10.1074/jbc.M602750200.
253. Frobert, Y.; Créminon, C.; Cousin, X.; Rémy, M.H.; Chatel, J.M.; Bon, S.; Bon, C.; Grassi, J. Acetylcholinesterases from *Elapidae* Snake Venoms: Biochemical, Immunological and Enzymatic Characterization. *Biochimica et Biophysica Acta - Protein Structure and Molecular Enzymology* **1997**, *1339*, 253–267, doi:10.1016/S0167-4838(97)00009-5.
254. Karlsson, E.; Mbugua, P.M.; Rodriguez-Ithurralde, D. Fasciculins, Anticholinesterase Toxins from the Venom of the Green Mamba *Dendroaspis angusticeps*. *J Physiol (Paris)* **1984**, *79*, 232–240.
255. Bin Asad, M.H.H.; Iqbal, M.; Akram, M.R.; Khawaja, N.R.; Muneer, S.; Shabbir, M.Z.; Khan, M.S.; Murtaza, G.; Hussain, I. 5'-Nucleotidases of *Naja naja* Karachiensis Snake Venom: Their Determination, Toxicities and Remedial Approach by Natural Inhibitors (Medicinal Plants). *Acta Poloniae Pharmaceutica - Drug Research* **2016**, *73*, 667–673.
256. Ouyang, C.; Huang, T.F. Inhibition of Platelet Aggregation by 5'-Nucleotidase Purified from *Trimeresurus gramineus* Snake Venom. *Toxicon* **1983**, *21*, 491–501, doi:10.1016/0041-0101(83)90127-7.
257. Ouyang, C.; Huang, T.F. Platelet Aggregation Inhibitors from *Agkistrodon acutus* Snake Venom. *Toxicon* **1986**, *24*, 1099–1106, doi:10.1016/0041-0101(86)90136-4.
258. Trummal, K.; Samel, M.; Aaspõllu, A.; Tõnismägi, K.; Titma, T.; Subbi, J.; Siigur, J.; Siigur, E. 5'-Nucleotidase from *Vipera lebetina* Venom. *Toxicon* **2015**, *93*, 155–163, doi: 10.1016/j.toxicon.2014.11.234.
259. Aird, S.D. Ophidian Envenomation Strategies and the Role of Purines. *Toxicon* **2002**, *40*, 335–393, doi:10.1016/S0041-0101(01)00232-X.
260. Aloulou, A.; Rahier, R.; Arhab, Y.; Noiriél, A.; Abousalham, A. Phospholipases: An Overview. In *Methods in Molecular Biology*; Methods Mol Biol, **2018**; Vol. 1835, pp. 69–105.
261. Jiménez-Charris, E.; Montealegre-Sanchez, L.; Solano-Redondo, L.; Mora-Obando, D.; Camacho, E.; Castro-Herrera, F.; Fierro-Pérez, L.;

- Lomonte, B. Proteomic and Functional Analyses of the Venom of *Porthidium lansbergii lansbergii* (Lansberg's Hognose Viper) from the Atlantic Department of Colombia. *J Proteomics* **2015**, *114*, 287–299, doi: 10.1016/j.jprot.2014.11.016.
262. Mora-Obando, D.; Salazar-Valenzuela, D.; Pla, D.; Lomonte, B.; Guerrero-Vargas, J.A.; Ayerbe, S.; Gibbs, H.L.; Calvete, J.J. Venom Variation in Bothrops Asper Lineages from North-Western South America. *J Proteomics* **2020**, *229*, doi: 10.1016/j.jprot.2020.103945.
263. Pereañez, J.A.; Preciado, L.M.; Fernández, J.; Camacho, E.; Lomonte, B.; Castro, F.; Cañas, C.A.; Galvis, C.; Castaño, S. Snake Venomics, Experimental Toxic Activities and Clinical Characteristics of Human Envenomation by *Bothrocophias myersi* (Serpentes: Viperidae) from Colombia. *J Proteomics* **2020**, *220*, doi: 10.1016/j.jprot.2020.103758.
264. Rey-Suárez, P.; Núñez, V.; Fernández, J.; Lomonte, B. Integrative Characterization of the Venom of the Coral Snake *Micrurus dumerilii* (Elapidae) from Colombia: Proteome, Toxicity, and Cross-Neutralization by Antivenom. *J Proteomics* **2016**, *136*, 262–273, doi: 10.1016/j.jprot.2016.02.006.
265. Bernheimer, A.W.; Linder, R.; Weinstein, S.A.; Kim, K.S. Isolation and Characterization of a Phospholipase B from Venom of Collett's Snake, *Pseudechis colleti*. *Toxicon* **1987**, *25*, 547–554, doi:10.1016/0041-0101(87)90290-x.
266. Yamazaki, Y.; Koike, H.; Sugiyama, Y.; Motoyoshi, K.; Wada, T.; Hishinuma, S.; Mita, M.; Morita, T. Cloning and Characterization of Novel Snake Venom Proteins That Block Smooth Muscle Contraction. *Eur J Biochem* **2002**, *269*, 2708–2715, doi:10.1046/j.1432-1033.2002.02940.x.
267. Brown, R.L.; Lynch, L.L.; Haley, T.L.; Arsanjani, R. Pseudechetoxin Binds to the Pore Turret of Cyclic Nucleotide-Gated Ion Channels. *Journal of General Physiology* **2003**, *122*, 749–760, doi:10.1085/jgp.200308823.
268. Lodovicho, M.E.; Costa, T.R.; Bernardes, C.P.; Menaldo, D.L.; Zoccal, K.F.; Carone, S.E.; Rosa, J.C.; Pucca, M.B.; Cerni, F.A.; Arantes, E.C.; et al. Investigating Possible Biological Targets of Bj-CRP, the First Cysteine-Rich Secretory Protein (CRISP) Isolated from *Bothrops jararaca* Snake Venom. *Toxicol Lett* **2017**, *265*, 156–169, doi: 10.1016/j.toxlet.2016.12.003.
269. Kostiza, T.; Meier, J. Nerve Growth Factors from Snake Venoms: Chemical Properties, Mode of Action and Biological Significance. *Toxicon* **1996**, *34*, 787–806, doi:10.1016/0041-0101(96)00023-2.
270. Yamazaki, Y.; Matsunaga, Y.; Tokunaga, Y.; Obayashi, S.; Saito, M.; Morita, T. Snake Venom Vascular Endothelial Growth Factors (VEGF-Fs) Exclusively Vary Their Structures and Functions among Species. *Journal of Biological Chemistry* **2009**, *284*, 9885–9891, doi:10.1074/jbc.M809071200.
271. Osipov, A. V.; Terpinskaya, T.I.; Kryukova, E. V.; Ulaschik, V.S.; Paulovets, L. V.; Petrova, E.A.; Blagun, E. V.; Starkov, V.G.; Utkin, Y.N. Nerve Growth Factor from Cobra Venom Inhibits the Growth of Ehrlich Tumor in Mice. *Toxins (Basel)* **2014**, *6*, 784–795, doi:10.3390/toxins6030784.
272. Koh, D.C.I.; Armugam, A.; Jeyaseelan, K. Sputa Nerve Growth Factor Forms a Preferable Substitute to Mouse 7S- $\beta$  Nerve Growth Factor. *Biochemical Journal* **2004**, *383*, 149–158, doi:10.1042/BJ20040569.

273. Takahashi, H.; Hattori, S.; Iwamatsu, A.; Takizawa, H.; Shibuya, M. A Novel Snake Venom Vascular Endothelial Growth Factor (VEGF) Predominantly Induces Vascular Permeability through Preferential Signaling via VEGF Receptor-1. *Journal of Biological Chemistry* **2004**, *279*, 46304–46314, doi:10.1074/jbc.M403687200.
274. Flight, S.M.; Johnson, L.A.; Du, Q.S.; Warner, R.L.; Trabi, M.; Gaffney, P.J.; Lavin, M.F.; De Jersey, J.; Masci, P.P. Textilinin-1, an Alternative Anti-Bleeding Agent to Aprotinin: Importance of Plasmin Inhibition in Controlling Blood Loss. *Br J Haematol* **2009**, *145*, 207–211, doi:10.1111/j.1365-2141.2009.07605.x.
275. Masci, P.P.; Whitaker, A.N.; Sparrow, L.G.; De Jersey, J.; Winzor, D.J.; Watters, D.J.; Lavin, M.F.; Gaffney, P.J. Textilins from *Pseudonaja textilis textilis*. Characterization of Two Plasmin Inhibitors That Reduce Bleeding in an Animal Model. *Blood Coagulation and Fibrinolysis* **2000**, *11*, 385–393, doi:10.1097/00001721-200006000-00011.
276. Morjen, M.; Kallech-ziri, O.; Bazaa, A.; Othman, H.; Mabrouk, K.; Zouari-kessentini, R.; Sanz, L.; Calvete, J.J.; Srairi-Abid, N.; El Ayeb, M.; et al. PIVL, a New Serine Protease Inhibitor from *Macrovipera lebetina* Transmediterranea Venom, Impairs Motility of Human Glioblastoma Cells. *Matrix Biology* **2013**, *32*, 52–62, doi: 10.1016/j.matbio.2012.11.015.
277. Fernández, J.; Gutiérrez, J.M.; Calvete, J.J.; Sanz, L.; Lomonte, B. Characterization of a Novel Snake Venom Component: Kazal-Type Inhibitor-like Protein from the Arboreal Pitviper *Bothriechis schlegelii*. *Biochimie* **2016**, *125*, 83–90, doi: 10.1016/j.biochi.2016.03.004.
278. Wagstaff, S.C.; Favreau, P.; Cheneval, O.; Laing, G.D.; Wilkinson, M.C.; Miller, R.L.; Stöcklin, R.; Harrison, R.A. Molecular Characterisation of Endogenous Snake Venom Metalloproteinase Inhibitors. *Biochem Biophys Res Commun* **2008**, *365*, 650–656, doi: 10.1016/j.bbrc.2007.11.027.
279. Ullah, A.; Ullah, K.; Ali, H.; Betzel, C.; Rehman, S.U. The Sequence and a Three-Dimensional Structural Analysis Reveal Substrate Specificity among Snake Venom Phosphodiesterases. *Toxins (Basel)* **2019**, *11*, doi:10.3390/toxins11110625.
280. Uzair, B.; Khan, B.A.; Sharif, N.; Shabbir, F.; Menaa, F. Phosphodiesterases (PDEs) from Snake Venoms: Therapeutic Applications. *Protein Pept Lett* **2018**, *25*, 612–618, doi:10.2174/0929866525666180628160616.
281. Gao, J.F.; Qu, Y.F.; Zhang, X.Q.; He, Y.; Ji, X. Neonate-to-Adult Transition of Snake Venomics in the Short-Tailed Pit Viper, *Gloydus brevicaudus*. *J Proteomics* **2013**, *84*, 148–157, doi: 10.1016/j.jprot.2013.04.003.
282. Yuh, F.P.; Wong, P.T.H.; Kumar, P.P.; Hodgson, W.C.; Kini, R.M. Ohanin, a Novel Protein from King Cobra Venom, Induces Hypolocomotion and Hyperalgesia in Mice. *Journal of Biological Chemistry* **2005**, *280*, 13137–13147, doi:10.1074/jbc.M414137200.
283. Vejjayan, J.; Khoon, T.L.; Ibrahim, H. Comparative Analysis of the Venom Proteome of Four Important Malaysian Snake Species. *Journal of Venomous Animals and Toxins Including Tropical Diseases* **2014**, *20*, doi:10.1186/1678-9199-20-6.
284. Tan, C.H.; Tan, K.Y.; Tan, N.H. A Protein Decomplexation Strategy in Snake Venom Proteomics. *Methods Mol Biol* **2019**, *1871*, 83–92, doi:10.1007/978-1-4939-8814-3\_5.

285. Rey-Suárez, P.; Núñez, V.; Gutiérrez, J.M.; Lomonte, B. Proteomic and Biological Characterization of the Venom of the Redtail Coral Snake, *Micrurus mipartitus* (Elapidae), from Colombia and Costa Rica. *J Proteomics* **2011**, *75*, 655–667, doi: 10.1016/J.JPROT.2011.09.003.
286. Lomonte, B.; Rey-Suárez, P.; Fernández, J.; Sasa, M.; Pla, D.; Vargas, N.; Bénard-Valle, M.; Sanz, L.; Corrêa-Netto, C.; Núñez, V.; et al. Venoms of *Micrurus* Coral Snakes: Evolutionary Trends in Compositional Patterns Emerging from Proteomic Analyses. *Toxicon* **2016**, *122*, 7–25, doi: 10.1016/J.TOXICON.2016.09.008.
287. Fox, J.W.; Serrano, S.M.T. Exploring Snake Venom Proteomes: Multifaceted Analyses for Complex Toxin Mixtures. *Proteomics* **2008**, *8*, 909–920, doi:10.1002/PMIC.200700777.
288. Ghezellou, P.; Garikapati, V.; Kazemi, S.M.; Strupat, K.; Ghassempour, A.; Spengler, B. A Perspective View of Top-down Proteomics in Snake Venom Research. *Rapid Communications in Mass Spectrometry* **2019**, *33*, 20–27, doi:10.1002/rcm.8255.
289. Alape-Girón, A.; Sanz, L.; Escolano, J.; Flores-Díaz, M.; Madrigal, M.; Sasa, M.; Calvete, J.J. Snake Venomics of the Lancehead Pitviper *Bothrops asper*: Geographic, Individual, and Ontogenetic Variations. *J Proteome Res* **2008**, *7*, 3556–3571, doi:10.1021/PR800332P.
290. Núñez, V.; Cid, P.; Sanz, L.; de La Torre, P.; Angulo, Y.; Lomonte, B.; Gutiérrez, J.M.; Calvete, J.J. Snake Venomics and Antivenomics of *Bothrops atrox* Venoms from Colombia and the Amazon Regions of Brazil, Perú and Ecuador Suggest the Occurrence of Geographic Variation of Venom Phenotype by a Trend towards Paedomorphism. *J Proteomics* **2009**, *73*, 57–78, doi: 10.1016/j.jprot.2009.07.013.
291. Jiménez-Charris, E.; Montealegre-Sanchez, L.; Solano-Redondo, L.; Mora-Obando, D.; Camacho, E.; Castro-Herrera, F.; Fierro-Pérez, L.; Lomonte, B. Proteomic and Functional Analyses of the Venom of *Porthidium lansbergii lansbergii* (Lansberg's Hognose Viper) from the Atlantic Department of Colombia. *J Proteomics* **2015**, *114*, 287–299, doi: 10.1016/j.jprot.2014.11.016.
292. Salazar-Valenzuela, D.; Mora-Obando, D.; Fernández, M.L.; Loaiza-Lange, A.; Gibbs, H.L.; Lomonte, B. Proteomic and Toxicological Profiling of the Venom of *Bothrocophias campbelli*, a Pitviper Species from Ecuador and Colombia. *Toxicon* **2014**, *90*, 15–25, doi:10.1016/j.toxicon.2014.07.012.
293. Quintana-Castillo, J.C.; Johana vargas, L.; Segura, C.; Estrada-Gómez, S.; Bueno-Sánchez, J.C.; Alarcón, J.C. Characterization of the Venom of C. d. Cumanesis of Colombia: Proteomic Analysis and Antivenomic Study. *Toxins (Basel)* **2018**, *10*, doi:10.3390/toxins10020085.
294. Madrigal, M.; Sanz, L.; Flores-Díaz, M.; Sasa, M.; Núñez, V.; Alape-Girón, A.; Calvete, J.J. Snake Venomics across Genus *Lachesis*. Ontogenetic Changes in the Venom Composition of *Lachesis stenophrys* and Comparative Proteomics of the Venoms of Adult *Lachesis melanocephala* and *Lachesis acrochorda*. *J Proteomics* **2012**, *77*, 280–297, doi: 10.1016/j.jprot.2012.09.003.
295. Céspedes, N.; Castro, F.; Jiménez, E.; Montealegre, L.; Castellanos, A.; Cañas, C.; Arévalo-Herrera, M.; Herrera, S. Biochemical Comparison of Venoms from Young Colombian *Crotalus durissus cumanensis*

- and Their Parents. *Journal of Venomous Animals and Toxins including Tropical Diseases* **2010**, *16*, 268–284.
296. Culma, M.F.; Pereañez, J.A.; Rangel, V.Ñ.; Lomonte, B. Snake Venomics of *Bothrops punctatus*, a Semiarboreal Pitviper Species from Antioquia, Colombia. *PeerJ* **2014**, *2*, 1–16, doi:10.7717/PEERJ.246.
297. Lomonte, B.; Pla, D.; Sasa, M.; Tsai, W.C.; Solórzano, A.; Ureña-Díaz, J.M.; Fernández-Montes, M.L.; Mora-Obando, D.; Sanz, L.; Gutiérrez, J.M.; et al. Two Color Morphs of the Pelagic Yellow-Bellied Sea Snake, *Pelamis platurus*, from Different Locations of Costa Rica: Snake Venomics, Toxicity, and Neutralization by Antivenom. *J Proteomics* **2014**, *103*, 137–152, doi: 10.1016/j.jprot.2014.03.034.
298. Lazarovici, P.; Marcinkiewicz, C.; Lelkes, P.I. From Snake Venom's Disintegrins and C-Type Lectins to Anti-Platelet Drugs. *Toxins (Basel)* **2019**, *11*, 1–15, doi:10.3390/toxins11050303.
299. Karapetian, H. Reptilase Time (RT). *Methods Mol Biol* **2013**, *992*, 273–277, doi:10.1007/978-1-62703-339-8\_20.
300. Rodríguez-Vargas, A.; Franco-Vásquez, A.; Bolívar-Barbosa, J.; Vega, N.; Reyes-Montaño, E.; Arreguín-Espinosa, R.; Carbajal-Saucedo, A.; Angarita-Sierra, T.; Ruíz-Gómez, F. Unveiling the Venom composition of the Coral Venom Snakes *Micrurus helleri*, *M. medemi*, and *M. sangilensis*. *Toxins* **2023**, *15*, doi:10.3390/toxins15110622.
301. Garrido Garrido, M.B.; Herráez, A. *Guía de Jmol*. Available online: <https://biomodel.uah.es/Jmol/jmolguia/otrasopciones.html> (accessed on 12/04/2023).
302. González Mañas, J.M. *Curso de Biomoléculas*. Universidad del País Vasco. Available online: <https://www.ehu.eus/biomoleculas/index.htm> (accessed on 12/04/2023).
303. Protein Data Bank (PDB). Available online: <https://www.rcsb.org/> (accessed on 12/04/2023).
304. Blender. Available online: <https://www.blender.org/> (accessed on 12/04/2024).
305. Jmol: An Open-Source Java Viewer for Chemical Structures in 3D. Available online: <http://jmol.sourceforge.net/> (accessed on 12/04/2023).
306. Sketchfab. Website for Visualizing and Sharing 3D Content Online. Available online: <https://sketchfab.com/> (accessed on 12/04/2023).

